Université d'Ottawa · University of Ottawa

Cloning *msx* and *dlx* Homeobox-Containing Genes from the Mexican Axolotl (*Ambystoma mexicanum*)

Thesis submitted to the School of Graduate Studies and Research
University of Ottawa
in partial fulfillment of the requirements for the
M.Sc. degree in the

Ottawa-Carleton Institute of Biology

Thèse soumise à
l'École des études supérieures et de la recherche
Université d'Ottawa
en vue de l'obtention de la maîtrise ès sciences à

L'Institut de biologie d'Ottawa-Carleton

Dedication

I would like to dedicate this thesis to the living memory of my brother Thomas who died at the young age of seventeen one rainy evening in a motorcycle accident. He died alone at a quiet Oak Bay intersection in Victoria B.C., on Sunday, December 3rd, 1983.

Acknowledgements

One of my biggest thank you's is for John Armstrong who without his willingness to support me and simultaneously satisfy my desire to do a molecular biology project with the axolotl, none of this work would have been possible. I feel particularly indebited to you, John, because you supported me but saw little of me in your laboratory since I spent all of my time over at the LOEB institute. This situation must have been particularly trying, and I want to sincerely thank you for having faith in me that I was working hard.

I am equally indebited to Marc Ekker who on two very 'crucial' occassions acted immediately to help me continue and succeed in my project. First, I thank you for moving quickly to write to Carl Sequin for his library, and second, I thank you for helping me during my financial crisis by inquiring and immediately obtaining support from the LOEB institute for the last three months of my project. In addition, I would like to thank you for putting up with me in your laboratory during the past two years, and allowing me to come into you laboratory and drive everybody crazy.

To both Lucille Joly and Ted Zerucha I have the greatest amount of admiration and compassion. Both of you supported me emotionally when times were tough. You listened to me patiently and offered moral support when I was disillusioned with my lack of forward progress. Without you two special people in my life I don't think I would have made it this far.

I would also like to thank Cris Martin. In particular, I would like to thank him for his suggestion that I try PCR on aliquots taken directly from my cDNA library in order to amplify homeoboxes. This suggestion worked and, for me, it was a turning point in my project.

Abstract

The lateral line system is an unique sensory system found in fishes and amphibians. It is composed of two types of sensory organs: electroreceptors (ampullary organs) and mechanoreceptors (neuromasts). These organs are arranged in lines throughout the surface of the head and the body, and allow the animal to detect weak electric field and to sense motion in the immediate surroundings.

We are interested in studying the genes involved in regulating the development of the hair cells of the neuromast organ because these hair cells are considered to be homologous to the hair cells of the vertebrate inner ear. When damaged by noise trauma, birds are capable of regenerating the hair cells of the inner ear whereas other vertebrates, such as humans, become permanently deaf. Since axolotl neuromasts are readily accessible to experimental manipulation and are capable of regeneration, they are an excellent model for studying the genes involved in the development and regeneration of hair cells.

Two gene families that play extensive roles in pattern formation during embryonic development are the *msx* and *dlx* homeobox-containing genes. Members from both families are expressed in the developing hair cells of the zebrafish inner ear, and therefore are excellent candidates for regulating the development of the neuromast organs in axolotls. As a first step towards examining the expression of members of these two families in the axolotl, we have cloned the cDNA sequences of *msx-1*, *msx-2*, *dlx-3*, *dlx-5*, and *dlx-7*. In addition, we have cloned the homeobox portions of the axolotl *dlx-1* and *dlx-6* genes. We also provide evidence of two different transcripts for the axolotl *dlx-3* gene suggesting the existance of two copies of this gene in the axolotl genome.

Resumé

La ligne latérale est un système sensoriel unique chez les poissons et les amphibiens comprenant deux types d'organes sensoriels: les électrorécepteurs ("organe ampullary") et les mécanorécepteurs ("neuromastes"). Ces organes sont allignés sur la surface de la tête et du corps et permettent à l'animal de détecter les champs électriques faibles ainsi que le mouvement produit dans son entourage.

Nous voulons étudier les genes impliqués dans la régulation du développement des cellules ciliées du neuromaste car ces cellules sont considérées comme étant homologues aux cellules ciliées de l'oreille interne des vertébrés. Lorsque ces cellules sont endommagées par le bruit, les oiseaux peuvent les regénérer alors que les autres vertébrés, comme les humains, deviennent sourds. Les neuromastes des axolotls sont d'excellents modèles pour étudier les gènes impliqués dans le développement et la regénération des cellules ciliées car ils sont faciles à manipuler et sont capables de se regénérer.

Les genes *msx* et *dlx* que sont des gènes a boîtehoméo constituent deux familles de gènes, jouant un rôle important durant la morphogenèse. Certains gènes appaitenant aux deux familles sont exprimés durant les développement des cellules cilieés de l'oreille interne du poisson zèbre, par consèquent, ils sont d'excellents candidats dans la régulation du développement des neuromastes chez les axolotls. En premier lieu, l'expression de certains membres des deux familles chez l'axolotl ont été examinés. Nous avons cloné les sequences d'ADNc des gènes *msx-1*, *msx-2*, *dlx-3*, *dlx-5*, et *dlx-7* ainsi que les séquences a boîtehoméo des gènes *dlx-1* et *dlx-6* de l'axolotl. Nous avons trouvé des évidences nous permettant d'affirmer que les deux transcripts de gène *dlx-3* provient des deux copies de gène présents dans le génome de l'axolotl.

Table of Contents

List of Figures

List of Tables

Chapter 1: Introduction

1.1 The Need to Develop a Model to Study the Hair Cells of the Inner Ear

Over a third of the world's population will suffer from hearing loss by old age (Corey and Breakefield, 1994). In more than half of these cases, the gradual loss of hearing has a hereditary basis (Friedman and Ryan, 1992). In addition, congenital deafness due to inherited genetic disorders is common. For example, in the United States, 1 in 2000 people are born deaf (Gibson *et al.*, 1995). In the majority of these cases the hair cells that line the organ of Corti are abnormal, reduced, or destroyed. Therefore it would be immensely beneficial to determine what regulates the patterning and differentiation of these hair cells because we could manipulate these factors to regenerate lost or damaged hair cells.

Currently the proposal of treating deafness by regenerating auditory hair cells is not feasible because many of the genetic factors involved in the development of these hair cells are unknown. Although it is believed that hair cell replacement does not occur in the organ of Corti of mature mammals (Roberson and Rubel, 1994), it has been demonstrated that birds regenerated their hair cells after these cells are destroyed by severe noise trama (Corwin and Cotanche, 1988; Ryals and Rubel, 1988). Furthermore, there have been reports of hair cell regeneration in mammalian cultures (Forge *et al.*, 1993; Warchol *et al.*, 1993), and of the different factors that stimulate hair cell regeneration *in vitro* (Ard *et al.*, 1985; Sokolowski *et al.*, 1993; Yamashita and Oesterle, 1995; Leon *et al.*, 1995; Navaratnam *et al.*, 1996). Unfortunately, most of these cultures are derived from the organs used in balance and head orientation because the hair cells in cochlear cultures degenerate. Consequently, the reports of regenerated hair cells *in vitro* describe hair cell regeneration in utricular cultures which contain hair cells that are morphologically different, and therefore functionally different, than auditory hair cells (Sokolowski *et al.*, 1993).

Perhaps the problem with these experiments is that the main focus is on mitogenic factors such as growth factors and oncogenes. If we were to study the genetic factors that normally regulate the patterning and differentiation of the hair cell, then possibly we can duplicate the genetic conditions that will lead to regeneration of auditory hair cells. In order to achieve this goal, we would first need to develop a suitable model.

The ideal model for hair cells development should have three desirable characteristics. The hair cells should be readily accessible so that they can be manipulated *in vivo*. There should be the possibility of developing a 'hair cell' organ culture so that different substances can be tested in the absence of surrounding tissue influences, and it would be useful if the organ could intrinsically regenerate its hair cells. This latter criteria would allow us to see if the genes that initially control the development of the hair cell are re-expressed in the same temporal and spatial pattern.

Naturally the immediate choice for an organism to study hair cell development would be the mouse, however it suffers several drawbacks as a modeling system. Its greatest disadvantage is that its hair cells are located deep within the auditory system. To examine these cells, it is necessary to sacrifice the animal. In addition, like other mammals, its is not capable of regenerating the hair cells of the auditory epithelium. So already two of the criteria for a hair cell model can not be satisfied by using a mammalian animal.

Consequently, it would be advantageous if we could examine a system in which the hair cells are exposed directly to the environment. Such a possibility exist with the hair cells found in the neuromast organs that make up the lateral line system of fishes and amphibians. These neuromast hair cells are considered to be homologous to the hair cells of the inner ear because of their similar structure and function (Fritzsch and Wahnschaffe, 1987; Collazo *et al.*, 1994).

Currently, there exist three readily available organisms that each have a lateral line system composed of neuromast organs. These are the zebrafish (*Brachydanio rerio*), the African clawed frog (*Xenopus laevis*), and the Mexican axolotl (*Ambystoma mexicanum*). Of these three possibilities, we would like to examine the genetic development of the hair cells of the neuromast organ in the Mexican axolotl because the neuromast organs that make up its lateral line system are large, epidermally located, and capable of regenerating a new organ when it has been excised. Moreover, the lateral line system, in both axolotl and fishes, has been extensively studied (reviewed by Lannoo and Smith, 1989). We hope to demonstrate that there exist genetic similarities between the hair cells of the urodele neuromast and the hair cells of the vertebrate inner ear with respect to the genes that are involved in their genesis. Our argument for using the hair cells of the axolotl neuromast organs is not a new one since other researchers, such as Jones

and Corwin (1993), have used the neuromast organs of salamanders to model inner ear hair cell replacement.

Before we can introduce the Mexican axolotl and its lateral line system, it is necessary to discuss the vertebrate ear, specifically the inner ear, its development, and the genetic factors that may play a role in the differentiation and patterning of its hair cells.

1.2 The Ear: Its Origins, Structure, and Function

The development of the vertebrate ear has been studied for almost one hundred years. In 1903 Harrison published the first of three papers that specifically dealt with the early development of the salamander inner ear (1903, 1924, and 1935) with Stone making further contributions in 1931. Since these early papers, there has been a bewildering amount of publications on the tissue and cellular interactions that mediate ear development. Most of the research has focused on describing the inductive events, and recently the genes, involved in the early stages of ear development. Considering the amount of time that has been spent on researching ear development, we are only beginning to understand the patterning events of the ear at the cellular level (Leon *et al.*, 1995). As for the identity of the actual genes that control its development, numerous genes have been described but their specific function during ear development remains to be established.

Out of all the vertebrates, the mammalian ear is the most complex, and arguably, the most evolved. It can be subdivided into three distinct regions comprising the outer, middle, and inner ear (figure 1-1A). The outer ear consists of structures for channeling sound waves towards the sensory cells located within the inner ear. It is composed of the pinna, the ear canal or external acoustic meatus, and the tympanic membrane which is otherwise known as the eardrum. The tympanic membrane transmits sound to the inner ear through three auditory ossicles. These three small bones; the malleus, incus, and stapes, make up the functional parts of the middle ear. The stapes is connected to the inner ear via the oval window. The major feature of the inner ear is a complex structure known appropriately as 'the labyrinth'[1]. This labyrinth contains the

[1] Technically, there are two labyrinths: the osseous and the membranous. The membranous labyrinth is housed within the osseous labyrinth, and is filled with endolymph and consists of the semicircular ducts (utricule and saccule) and cochlear duct. The osseous labyrinth is filled with perilymph and contains the semicircular canals, vestibule, and cochlea.

Figure 1-1. Cross-sections of the human (A), bird (B), and frog (C) ear. In all three examples, the cochlea/lagena, which is where the auditory hair cells are located, has been darkly shaded. Notice how tiny the lagena of the frog ear is in comparison to the bird and human cochlea. In the human ear the stapes (St) communicate with the inner ear through its connection to the oval window (which is not illustrated). Legend: EC, outer ear canal; ET, eustachian tube; In, incus; Ma, malleus; OW, oval window; Pi, pinna; SC, semicircular canals; St, stapes; and Ut, utriculus (Adapted from Mitchell *et al.*, 1988).

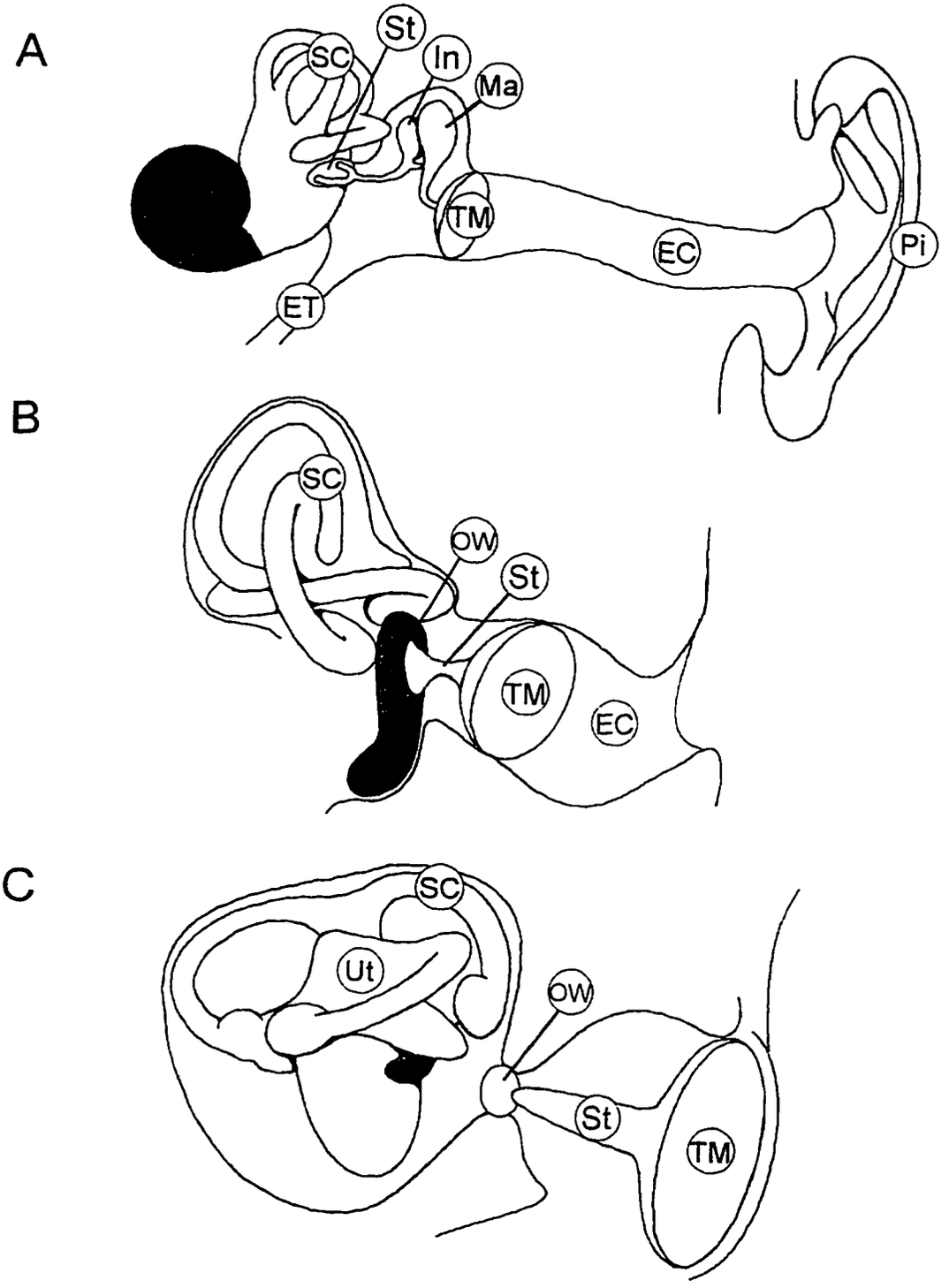
A
St
SC
In
Ma
TM
EC
Pi
ET
B
SC
OW
St
TM
EC
C
SC
Ut
OW
St
TM

semicircular canals, the vestibule, and the cochlea. Within the cochlear duct, the sound waves travel through a spiraling tunnel that contains the organ of Corti. The basilar membrane of this organ is lined with numerous arrays of hair cells. These hair cells translate the mechanical energy of the sound wave into nervous impulse which are then passed onto the brain via the cochlear nerve (reviewed by Pickles and Corey, 1992).

In other vertebrates, such as birds and amphibians, many of these structures are reduced (figure 1-1B and 1-1C respectively). In particular, the part of the inner ear concerned with hearing is very reduced in amphibians and reptiles and is known as the lagena (figure 1-1C). In birds, the lagena is more elongated and considered to be a cochlea (figure 1-1B). The cochlea is very well developed in mammals, and consequently, we have the ability to resolve differences in sound frequencies that span a hugh range from greater than 32 kHz to less than 500 Hz (Mitchell *et al.*, 1988). In comparison, the reduced ears of amphibians are generally restricted to a range between 5 kHz and 20 Hz (Roth *et al.*, 1992).

1.3 Embryological Development of the Ear

The embryonic origin of most of the ear's major structures has been known for quite some time, although active research continues to further elucidate tissue involvement and interdependence in the formation of these structures. For example, Mallo and Gridley (1996) recently demonstrated that the formation of the tympanic ring is necessary to regulate the formation and growth of the external acoutic meatus.

The development of the inner ear first starts with the appearance of an ectodermal thickening known as the otic placode (figure 1-2A). One placode develops on each side of the head, and is positionned next to the developing hindbrain where rhombomeres 5 and 6 will form (Lumsden and Keynes, 1989). Each placode sinks into the head of embryo to form an otic pit (figure 1-2C), which subsequently pinches off from the surface to form an otic vesicle or otocyst (figure 1-2D and E)(reviewed in Kalthoff, 1996). The otic vesicle then undergoes a series of complex morphological rearrangements to form the various structures of the inner ear. The floor of the spiraling cochlea differentiates into the organ of Corti, where the auditory hair cells are located (figure 1-2H).

Figure 1-2. Development of the vertebrate inner ear. The appearance of the inner ear first begins with an ectodermal placode located next to the portion of the neural tube that will develop into rhombomeres 5 and 6. Panel (A) is a transverse cross-section of a vertebrate embryo showing the neural tube and the formation of the otic placode, one on each side of the body. Panel (B) is a enlargement of (A) showning the placode as a thickening of the ectodermal cells. In panel (C) the placode has started to invaginate and in the next panel, (D), the otic vesicle begins to form. As the placode moves away from the surface it further differentiates into several layers (E). In panel (F), there are three major layers with the greater epithelial ridge (GER) and the lesser epithelial ridge (LER) contributing to the development of the cochlea. Around this stage, cells will leave part of the otic vesicle to form the acoustic ganglion (not shown). As the otic vesicle begins to stretch and twist into the various structures of the inner ear (G), the auditory epithelium becomes clearly visible (boxed). Panel (H) is an enlargement of the box in panel (G) at several later stages when the inner ear hair cells (shaded dark gray) have developed beneath the tectorial membrane (TM)(Adapted from Corey and Breakefield, 1994).

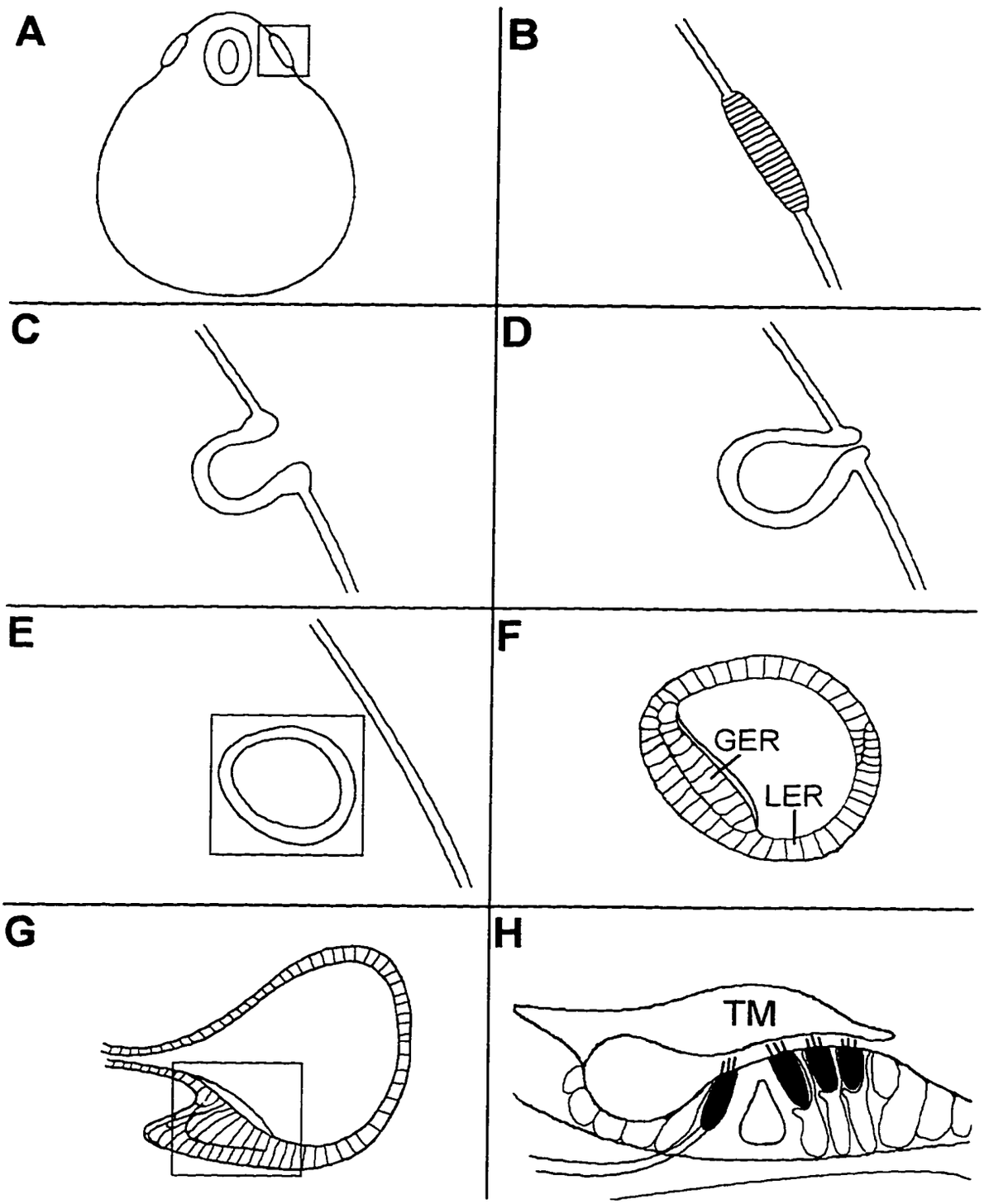
A
B
C
D
E
F
GER
LER
G
H
TM

Further differentiation of each otic vesicle into the complex labyrinth structure of the inner ear requires poorly understood interactions between the vesicle and the surrounding mesoderm and hindbrain. However, as suggested by Waddington (1937), the steps leading from the formation of the otic placode to the otocyst probably involve a two-step induction process with the first induction signal originating from the chordamesoderm and specifying the area of ectoderm that will become the otic placode. Later, a second induction signal, coming from the rhombencephalic neural tube, induces the formation of the otic vesicle (Alvarez and Navascues, 1990). So far, the actual identities of the inducer(s) have not be established, however, as we will see, there are some possible candidates.

As the otic vesicle starts its complex differentiation into inner ear structures, the first elements of the middle and outer ear begin to form. The canal of the outer ear is created by the inward growth of a solid cylinder of ectodermal cells, called the meatal plug which is derived from the first pharyngeal cleft (Moore and Persaud, 1993). The actual canal forms when cells in the center of the plug undergo apoptosis, leaving a hollow cylinder lined with epithelial cells (Moore and Persaud, 1993). Meanwhile, the adjacent middle ear cavity is formed when the endodermal layer of the first pharyngeal pouch expands and elongates to form the eustachian tube and part of the tympanic membrane (Moore and Persaud, 1993). The malleus and incus bones of the middle ear are derived from the first pharyngeal arch while the stapes is derived from the second pharyngeal arch (Moore and Persaud, 1993). The tympanic membrane, which delinates the boundaries of the outer and middle ear, is made up of three separately derived cell layers. The outer layer is the epithelial lining of the external acoutic meatus, the middle layer is derived from cells that come from both the first and second pharyngeal arch, and the inner layer is the lining of the middle ear cavity. These three layers fuse together to form the eardrum. The tympanic ring which supports the tympanic membrane but is not necessary for its formation (Mallo and Gridley, 1996) is derived from the first pharyngeal arch.

1.4 Molecular Genetics of Inner Ear Development

In less than a decade there has been an explosion of papers implicating various genes involved in ear development. The reason for this extraordinary increase in identifying possible molecules regulating ear development is three-fold. Foremost, the technique of *in situ*

hybridization has had the greatest impact because it implicates various genes in the development of the ear when it demonstrates their expression in these regions. When this information is used to target specific genes for disruption, the resulting loss-of-function mutations can provide information regarding the role of these genes during ear development. In addition, there has been rapid advancements in uncovering the genes involved in abnormal ear development in various mouse mutants.

So far, many of the genes that have been described to play a role in ear development are transcription factors. These transcription factors can be crudely categorized into two groups: the non-homeobox-containing group and the homeobox-containing group. Prominent among the transcription factors that do not have a homeobox yet play a role in ear development are the nuclear receptors for retinoic acid (RA) and thyroid hormones, both of which are members of the steroid/thyroid hormone receptor superfamily and have zinc-finger DNA binding domains (Corey and Breakefield, 1994).

RA has been demonstrated to be involved in pattern formation during limb development (Thaller and Eichele, 1987), hindbrain segmentation (Durston *et al.*, 1989; Ruiz I Altaba and Jessell, 1991), and limb regeneration (Tickle *et al.*, 1982). Feeding RA to pregnant mice results in embryos with skeletal transformations and abnormal ear development (Kessel, 1992). In the case of the skeletal transformations, the addition of RA to the developing embryos alters the *Hox* code responsible for controlling the identities of each skeletal element (Kessel, 1992). Whereas the effects of RA on disturbing ear development could be caused by two different processes. First, the anteriorly expressed *Hox* genes may also be involved in ear development, and therefore, altering their expression results in disrupting ear differentiation. Or, second, the addition of RA to endogenous levels present in the developing ear may over-stimulate or prematurely bind the RA receptors which have been detected in the sensory epithelium of the inner ear (Dollé *et al.*, 1990; Ruberte *et al.*, 1992) to trigger a development pathway which is normally turned on at later stages. The possible role of RA and its receptor in the inner ear may be to signal differentiation of the presumptive hair cells. When RA is added to embryonic otic vesicle cultures, it induces further differentiation of the sensory epithelium (Represa *et al.*, 1990) and increases the number of hair cells (Kelley *et al.*, 1993; Lefebvre *et al.*, 1993).

Similarly, thyroid receptors (TRs) have been detected in the ventral region of otic vesicle which will become the cochlea (Bradley *et al.*, 1994). As the otic vesicle further develops, these receptors become restricted to the cochlea and are only found in the region that will form the sensory epithelium (Bradley *et al.*, 1994). The role of the TRs might be to determine which part of the developing organ of Corti will become the sensory epithelium. Experiments in which pregnant rats were fed propylthiouracil, an iodine analog which blocks thyroid synthesis, resulted in pups with abnormal organ of Corti (Uziel *et al.*, 1981). This result was not particularly surprising since diseases that result in impaired thyroid synthesis or iodine deficiency, such as Pendred syndrome or congenital hypothyroidism, result in hearing loss (Corey and Breakefield, 1994).

Some research has been done on examining the effects that growth factors play on the development of the ear (Represa *et al.*, 1991; Mansour *et al.*, 1993; Yamashita and Oesterle, 1995). Most of these growth factors have been tested for their ability to induce hair cell proliferation *in vitro*. Both transforming growth factor-β (TGF-β), and epidermal growth factor (EGF) together with insulin, have the ability to stimulate hair cell proliferation whereas EGF alone did not (Yamashita and Oesterle, 1995).

In particular, fibroblast growth factor-3 (*FGF-3*) has received much attention because early research suggested that it might be one of the possible inducers for otic vesicle formation (Represa *et al.*, 1991). Its expression was detected in rhomobomeres 5 and 6 at a time when the otic placode began to invaginated, and hence it was suggested that it determines where the inner ear develops (Wilkinson *et al.*, 1988). Represa and co-workers (1991) set up experiments to test this proposal. When they added antisense *FGF-3* oligonucleotides or used antibodies directed against the protein, the otic vesicle failed to form. Therefore, they concluded that *FGF-3* was required to induce the otic placode to invaginate and form an otic vesicle.

However, when the *FGF-3* gene was inactivated in mice, the embryos were able to form otic vesicles but the resulting inner ear structures were abnormal (Mansour *et al.*, 1993). Several possible reasons were offered by Mansour and co-workers (1993) of why the results were contradictory to the experiments of Represa *et al.* (1991). Perhaps the most convincing explanation for this contradiction was that Represa and his co-worker used human *FGF-3* antisense mRNA to block its chicken ortholog because, at the time, the chick *FGF-3* had not yet

been cloned. Consequently they may have blocked something related to *FGF-3* but not the chicken *FGF-3* itself. However, in spite of these contradictions, *FGF-3* clearly plays a role in inner ear development by possibly inducing part of the otic vesicle to form the endolymphatic duct (Mansour *et al.*, 1993). Similar abnormalities were seen in experiments in which the endolymphatic ducts were removed from developing chick ears (Hendriks and Toerien, 1973).

In addition to creating transgenetic mice with ear defects, there are several mouse mutations that result in hearing loss. Three of these mutations; *Splotch* (*Sp*), *kreisler* (*kr*), and *shaker* (*sh*), all display varying degrees of abnormal inner ear development.

In the *Sp* mutation, homozygous mice have severe neural tube defect, abnormal inner ear development, and die several days after birth. The defects of the inner ear include irregular coiling of the cochlear duct, under development of the vestibular region, and an abnormal endolymphatic duct (Deol, 1966). It seems that all of these defects are the result of a partial deletion of the homeobox of the *Pax-3* gene (Epstein *et al.*, 1991). A similar defect has been reported in humans afflicated with Waardenburg syndrome type 1, and consequently, the *Sp* mouse has been suggested to be the mouse homologue of this disorder (Foy et al., 1990).

The *kr* mice mutation was created and described by Hertwig who named it 'kreisler' (German for 'circler') because the mutant mice ran around in circles (Cordes and Barsh, 1994). In addition to this abnormal behavior, the mice were also deaf. Histological examination of these mice revealed the absence of rhombomere 5 and an abnormal displaced otic vesicle which failed to develop any inner ear structures (Deol, 1964). In the absence of rhombomere 5, rhombomeres 4 and 6 appeared as one large bulge (Deol, 1964; Cordes and Barsh, 1994). The affected gene was found to be a leucine zipper transcription factor which in the wild-type embryo is initially expressed throughout the hindbrain, but later becomes restricted to the area of the hindbrain that forms rhombomeres 5 and 6 (Cordes and Barsh, 1994). Therefore, based on its normal pattern of expression, the *kr* gene is believed to be important in hindbrain segmentation. Without proper hindbrain segmentation, the proper placement and subsequent development of the otic vesicle is affected (Cordes and Barsh, 1994).

Another mouse mutation that results in deafness, as a result of inner ear defect, is the *sh* mutation. In 1995, Gibson and co-workers cloned the murine *shaker-1* (*sh1*) gene. *sh1* homozygotes progressively lose their hearing and develop difficulty with balance. They found

that the *sh1* gene encoded a defective myosin molecule of the type VII family. Normally, myosin VII is involved in the mechanotransduction of the sound waves by forming the 'tip link' of the stereocilia of the hair cells (Pickles and Corey, 1992). If this 'tip link' is defective then the hair cell undergoes apoptosis. Consequently in *shaker-1* mice, the organ of Corti degenerates and the mice become deaf (Gibson *et al.*, 1995).

So far we have not discussed any genes that might determine the patterning of the hair cells, or, with the exception of RA, regulate the differentiation of the pre-hair cells. Arguably, this patterning and differentiation could be controlled by homeobox-containing genes which play crucial roles in patterning other structures such as the limb and axial skeleton during development.

1.5 An Introduction to Homeobox Genes

One of the most intriguing aspects of developmental biology is how the embryo is able to impart positional identity to its cells so that specific groups of cells develop into the appropriate structure during the course of organogenesis (McGinnis and Krumlauf, 1992). This patterning process has to start from a single-celled zygote. As seen in the fly, the future anterior-posterior axis is initially set up by the unequal distribution of transcription factors which are deposited into the egg during oogenesis (Akam, 1987). These 'maternal effect' genes represent the beginning of a chain of regulatory genes that will ultimately involve homeotic genes in determining the anterior-posterior body plan of the developing fly (Akam, 1987).

In the developing *Drosophila* larvae, homeotic genes have been demonstrated to specify the identity of each body segment (Lewis, 1978). This ability was discovered when the mutation of these genes lead to homeotic transformations. For instance, *Ultrabithorax* (*Ubx*) is normally expressed in the third thoracic segment of the fly where wing balancers (i.e., halteres) form. When *Ubx* is deleted, the third thoracic segment becomes transformed into another second thoracic segment thereby forming wings, and thus a four-winged fly is created (Lewis, 1978)

The proteins of these homeotic genes are structurally related because they each contain a highly conserved 60 amino acid motif known as the homeodomain which is encoded by a 180 bp genetic element called the homeobox (McGinnis and Krumlauf, 1992). Nuclear magnetic resonance (NMR) spectroscopy of the *Antennapedia* homeodomain revealed that it contains four

α helices, with the second and third helices forming a helix-turn-helix motif that is very similar to the DNA binding region of prokaryotic repressors (Qian *et al.*, 1989). Additional NMR spectroscopy and x-ray crystallography studies demonstrated that the helix-turn-helix motif of the *Antennapedia* homeobox gene binds to the major groove of DNA, thereby supporting the view that homeotic genes function as transcriptional regulators (Otting *et al.*, 1990).

Depending upon the amount of conservation within the homeodomain of each homeotic gene, they can be placed into one of several classes. Therefore, homeotic genes with a homeodomain that is most similar to that of the *Antennapedia* (*Antp*) homeodomain were grouped together. In *Drosophila*, it was discovered that genes belonging to the *Antp* class mapped to two complexes, the *Antennapedia* (*ANT-C*) and *Bithorax* (*BX-C*) complexes (figure 1-3)(Lewis, 1978). Together these two complexes were referred to as the homeotic complex, or *HOM-C* (McGinnnis and Krumlauf, 1992).

As more work was done on the homeotic genes of the *HOM-C* complex, several surprising discoveries were made. First of all, the genes that made up the *HOM-C* cluster mapped in the same order as they were expressed along the anterioposterior axis of the fly (McGinnis and Krumlauf, 1992). Therefore, the most 3' gene of the complex, *lab*, was expressed at the most anterior portion of the fly while the most 5' gene of the complex, *Abd-B*, was found to be expressed in the most posterior elements of the fly (figure 1-3). What was even more startling was the discovery that these homeotic genes existed in vertebrates (McGinnis and Krumlauf, 1992).

The vertebrate *Hox* genes have been thoroughly examined in both the mouse and the human. Unlike the single cluster in the fly, there appears to have been two duplications of the ancestral *HOM-C* cluster resulting in four complexes in vertebrates (Kappen *et al.*, 1989). These four complexes exist on separate chromosomes and are now labelled A, B, C, and D to distinguish amongst them (figure 1-3)(Scott, 1992). Each complex contains approximately thirteen genes with each gene having a 'paralog' on another complex (i.e.: the paralogs of *Hoxa-4* are *Hoxb-4*, *Hoxc-4*, and *Hoxd-4*)(figure 1-3).

The most dramatic discovery of these *Hox* genes and their fly counterparts is the amount of conservation of not only the sequences, but the maintainence of the same order on the

Figure 1-3. Comparison of the *Drosophila HOM* complex against the vertebrate *Hox* complex. (Adapted from Kalthoff, 1996). For the purpose of illustration, the *Hox* expression in the vertebrate embryo is an over-simplification (please refer to Kalthoff, 1996; Hunt *et al.*, 1991; or McGinnis and Krumlauf, 1992, for further detail). Notice that the expression of the *Hox* genes starts at the midbrain-hindbrain border and travels posteriorly. In the fly, the *HOM* complex is split onto two chromosome into two complexes: the *ANT*-complex, and the *BX*-complex. Together, the genes of the *HOM* complex are *lab* (*labial*), *pb* (*proboscipedia*), *Dfd* (*Deformed*), *Scr* (*Sex-combs reduced*), *Antp* (*Antennapedia*), *Ubx* (*Ultrabithorax*), *abd-A* (*abdominal-A*), and *Abd-B* (*Abdominal-B*). In vertebrates, the *Hox* genes are organized into four clusters, each located on a separate chromosome. These four clusters are designated by the letters A, B, C, and D; and can contain from nine to eleven genes. *Hox* genes that are most similar to their fly counterparts are presented directly below their corresponding fly homolog.

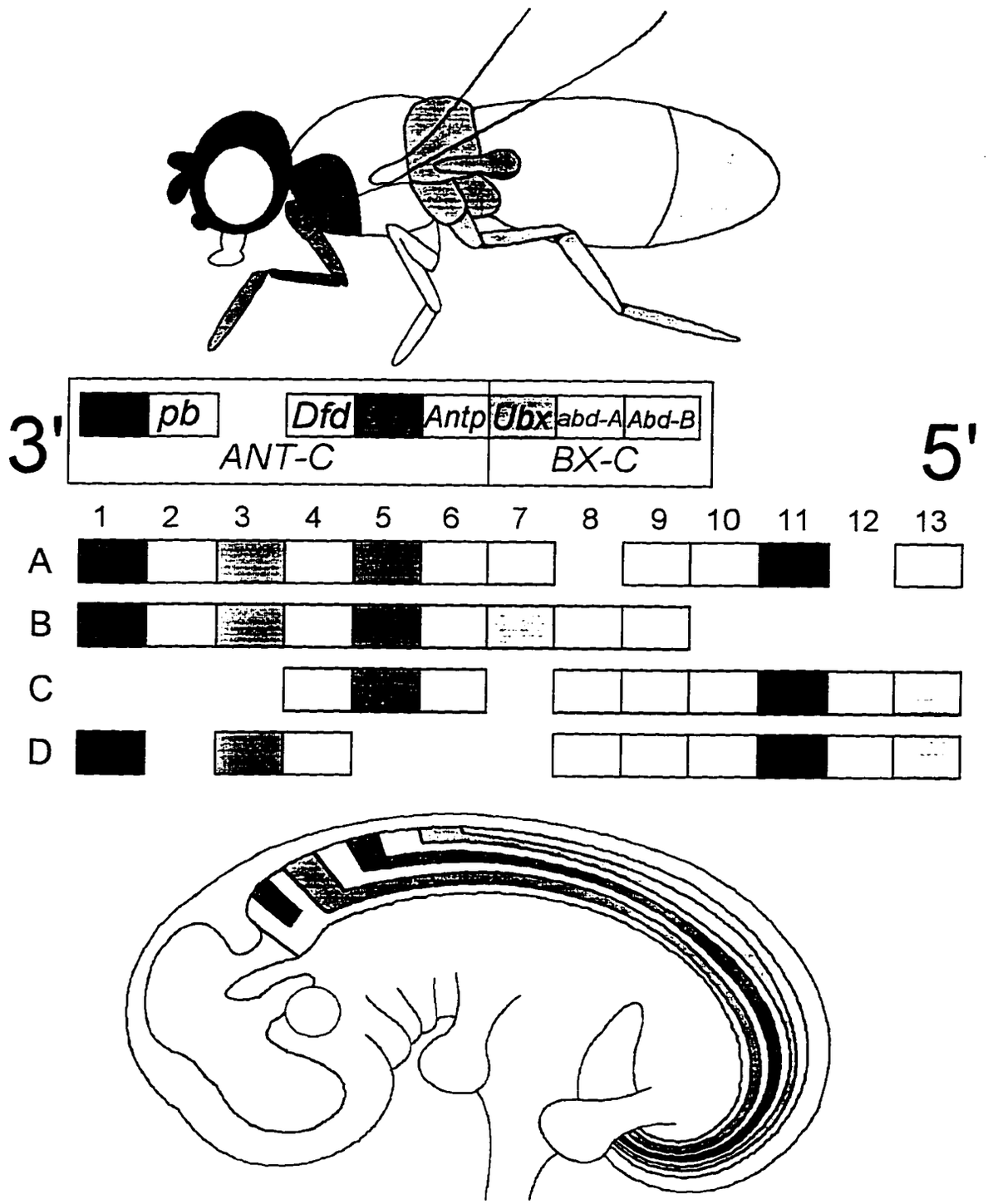
3'
pb
Dfd
Antp
Ubx
abd-A
Abd-B
ANT-C
BX-C
5'
1 2 3 4 5 6 7 8 9 10 11 12 13
A
B
C
D

chromosomes and the expression pattern (McGinnis and Krumlauf, 1992). The physical order of the *Hox* genes is the same as that of the *HOM-C* genes (figure 1-3), and like the fly, the *Hox* genes are expressed in an ascending order that starts at the 3' end of the complexes and continues to the 5' end (McGinnis and Krumlauf, 1992).

The role of the *Hox* genes has been studied mainly in the patterning of the vertebrate axial skeleton. However, *Hox* gene expression is seen in many different tissues during development (Hunt *et al.*, 1991). Since some of the *Hox* genes are expressed in regions where the inner ear develops, these patterning genes might play a role in the complex patterning of the inner ear structures.

1.5.1 *Hox* Genes and Inner Ear Development

Several *Hox* genes are expressed in rhombomeres 5 and 6 which are adjacent to the developing otic vesicle (Hunt *et al.*, 1991; Krumlauf, 1994). These are *Hoxa-2*, *Hoxa-3*, *Hoxb-2*, *Hoxb-3*, and *Hoxd-3* (Hunt *et al.*, 1991). As seen with the murine *kr* mutation, the lack of segmentation in this region resulted in defective otic vesicle development. Similarly, lack of patterning as a result of disrupting the *Hox* genes of this region might lead to similar defects in inner ear development, however, so far only two *Hox* genes have been reported to affect ear development.

Of these two *Hox* genes, the null mutation of *Hox-1.6* (now designated *Hoxa-1*) was the most disruptive to the ear (Lufkin *et al.*, 1991; Chisaka *et al.*, 1992). During early development the rhombomere failed to form discrete sections and remained smooth, a situation not unlike the *kr* mutation. Consequently the otocyst was small, under developed, and displaced rostrally towards the trigeminal ganglion (VII) and ventrally away from the neural tube towards the pharyngeal arches (Chisaka *et al.*, 1992). As the embryo further developed, the endolymphatic duct failed to form, no middle ear ossicles formed, both the cochlear and vestibular nerves were missing, and the external acoustic meatus was distorted (Chisaka *et al.*, 1992).

Whereas the mutation of *Hoxa-1* lead to gross morphological disturbances of the embryo, the disruption of *Hoxa-2* resulted in a homeotic transformation of certain skeletal elements of the head (Gendron-Maguire *et al.*, 1993; Rijli *et al.*, 1993). This included a duplication of the tympanic ring and disruptions of the middle ear structures, but the inner ear remained

unperturbed (Gendron-Maguire *et al.*, 1993; Rijli *et al.*, 1993). When *Hoxa-3* was disrupted, no ear defects were reported (Chisaka and Capecchi, 1991). Similarly, no reports of ear defects were described when *Hoxd-3* (Condie and Capecchi, 1994) was disrupted. These latter two *Hox* genes are expressed in either rhombomere 5 or 6. So what is going on?

There are three possible explanations. In the majority of these papers, the researchers focus on observing how the skeletal elements are perturbed and consequently they fail to report ear defects unless they are very dramatic. On the other hand, these genes, unlike *Hoxa-2* and *Hoxa-3*, might be specific for patterning the vertebrae and have nothing to do with ear development. Or, because of the overlapping expression domains of these genes, the result of mutating one gene may be hidden by the presence of another due to functional redundancy that exists amongst the *Hox* genes. As we discuss in the next section, there are other homeobox genes that are expressed in the head and do play a role in ear development.

1.5.2 Other Homeobox-Containing Genes and Inner Ear Development

There are many homeobox genes that do not belong to the *Antp* class and consequently are not considered to be *Hox* genes (Scott, 1992). Of the *Hox* genes, thirty-nine have been identified in mammals, however, over 170 different homeobox-containing genes have been cloned in vertebrates (Stein *et al.*, 1996). Many of these homeobox genes are expressed in regions where *Hox* gene expression is not seen. For example, in the central nervous system the most anterior expression of the *Hox* genes stops at the hindbrain-midbrain boundary (figure 1-3). Other homeobox genes, such as *paired-box* containing (*Pax*), *orthodenticle* (*Otx*), *empty spiracles* (*Emx*), and *Distal-less* (*Dlx*) genes are expressed beyond this anterior limit of the *Hox* genes and are involved in patterning the fore- and mid-brain regions (De Robertis, 1994). With regards to inner ear development, several of these homeobox genes have been demonstrated to be expressed during ear development. They include members from *pax, otx, nkx, SOHo, POU, msx,* and *dlx* gene families. So far, only the expression pattern of the majority of these genes has been reported. Their actual role in inner ear development has not been examined by gene disruption or antisense experiments.

Pax genes are a family of vertebrate genes related to *Drosophila* segmentation genes by virtue of a well conserved genetic element that codes for a protein motif called the paired box

(Dressler et al., 1988). As with the DNA binding properties of the homeodomain, the paired box is also capable of recognizing and binding to specific DNA sequences.

In the mouse several different *Pax* genes have been characterized. These include *Pax-1* (Balling *et al.*, 1988), *Pax-2* (Dressler *et al.*, 1990), *Pax-3* (Goulding *et al.*, 1991), and *Pax-6* (Hill *et al.*, 1991). Of these four genes, *Pax-2* transcripts are detected in the ventral wall of the developing otocyst from which the saccular and cochlear ducts will form (Dressler *et al.*, 1990). Recently this gene has been mutated (Torres *et al.*, 1996). In the *Pax-2* null mutant mice the developing cochlea fails to elongate into its characteristic spiral shape (Torres *et al.*, 1996). The abortive development of the cochlea may result in the absence of the cochlear ganglion, or alternatively, the cochlear ganglion requires *Pax-2* to regulate its development (Torres *et al.*, 1996).

Another family of homeobox-containing genes that are expressed in the developing auditory system, are members of the *Otx* class. *Otx* is composed of a family of vertebrate genes that are related by their sequence similarity to the *Drosophila orthodenticle* (*otd*) gene. As with the fly *otd* gene, *Otx* genes are detected in the developing head, and thus argues for an evolutionary conservation of function (Finkelstein and Boncinelli, 1994). *Otx* genes have been cloned in mouse (Simeone *et al.*, 1993), *Xenopus* (Kablar *et al.*, 1995), and zebrafish (Li *et al.*, 1994). In all three vertebrates, the expression of all *Otx* genes has been detected in the developing fore- and mid-brain. Furthermore, regardless of the species examined, the homologs of *Otx1* and *Otx2* are detected in the developing otic vesicle (Simeone *et al.*, 1993; Kablar *et al.*, 1995; and Li *et al.*, 1994). Later, the expression of these two genes becomes restricted to the epithelia of the auricular ducts of the sacculus and cochlea.

In the mouse, two groups, working independently, disrupted the *Otx2* gene and reported no defects in the inner ear even though both the eye and olfactory systems were abnormal, in addition to heavy deformations of the forebrain (Matsuo *et al.*, 1995; Ang *et al.*, 1996). When *Otx1* was disrupted, the lateral semicircular ducts of the inner ear were missing, but the other structures developed normally and thus it would appear that *otx* doesn't play a direct role in hair cell development (Acampora *et al.*, 1996).

As with the *Pax* and *Otx* genes, the *Nkx* genes are the vertebrate homologs of *Drosophila NK* genes because of their sequence similarities. In the mouse, *Nkx-5.1* and *Nkx-5.2* have been

described in the developing central nervous system (Rinkwitz-Brandt *et al.*, 1995). Unlike *Nkx-5.2*, transcripts of *Nkx-5.1* are detected in the early development of the otic placode (Rinkwitz-Brandt *et al.*, 1995). As the placode invaginates and forms an otic vesicle, its expression becomes restricted to the anterior and posterior margins of the dorsal side of the otic vesicle (Rinkwitz-Brandt *et al.*, 1995). However, the actual role of *Nkx-5.1* in the development of the otic placode has not been tested by disrupting its function, nor has it expression during later stages of development being described.

Unlike the *Pax*, *Otx*, and *Nkx* families, *POU* genes acquired their name by combining the first letter from the various transcription factors that they were initially identified in (i.e.: P = Pit-1 for pituitary-1; O = Oct-1 and Oct-2 for octamer-binding factors; and U = Unc-86 for uncoordinated-86)(De Robertis, 1994).

Recently two genes, *Brn-3.1* and *Brn-3.2*, belong to the *POU* family were disrupted in mice (Erkman *et al.*, 1996). *Brn-3.1* is specifically expressed in the cochlear and vestibular hair cells of the developing inner ear, but not in the surrounding support cells (Erkman *et al.*, 1996). Erkman and her coworkers (1996) found that when they disrupted the murine *Brn-3.1* gene the hair cells failed to terminally differentiate. As a result, the immature hair cells degenerated as well as the associated nerves, and the mice became deaf. Interestingly, the mouse *Brn-3.1* genomic locus corresponds to a human locus where an inherited form of late-onset degenerative deafness has been mapped (Leon *et al.*, 1992).

An additional homeobox-containing gene has been described to be express in the developing inner ear. *SOHo-1* (for sensory organ homeobox-1) was cloned from an embryonic chick retina library and is expressed in the otic pit, the otocyst, and later becomes restricted to regions that will form nonsensory tissues of the inner ear (Deitcher *et al.*, 1994). Although, *SOHo-1* is not expressed in the developing hair cells, it might be important with regard to hair cell regeneration, since it has been demonstrated that regenerated hair cells of the chick auditory epithelium (Navaratnam *et al.*, 1996) and axolotl neuromast organs (Jones and Corwin, 1993) come from the surrounding support cells. Perhaps, it may function to determine which cells of the developing sensory epithelium will become support cells, and cells that do not express it, at this stage, become hair cells.

So far, we have reviewed several genes that are expressed in the developing otic vesicle, and later, in the sensory epithelium and hair cells, yet we have not described genes that might play a role in the spatial arrangement of these hair cells. Two possible gene families that may play a role in patterning during ear development are *msx* and *dlx* homeobox genes. Members from both of these families are expressed during the formation and differentiation of the sensory hair cells of the zebrafish inner ear (Ekker *et al.*, 1992; Akimenko *et al.*, 1994).

1.6 The Role of *Dlx* and *Msx* Homeobox-containing Genes in Hair Cell Development

Both the muscle segment homeobox (*msh*) and the distal-less (*dll*) genes were first discovered in *Drosophila* (Fjose *et al.*, 1985; and, Cohen *et al.*, 1989 respectively). Subsequently, their homologs have been cloned from numerous vertebrate species where they are designated as *msx* and *dlx*, respectively.

The *dlx* family appears to have from 6 to 8 members (table 1-1). In tetrapods, they have identified 6 different *dlx* genes, whereas in the zebrafish a total of 8 *dlx* genes have been cloned (table 1-1). Similarly the *msx* family appears to have from 2 to 5 members depending on the organism examined (table 1-2). Genes from both families are involved in many different processes during development and are generally expressed in regions of epithelial-mesenchymal interactions (Jowett *et al.*, 1993; Davidson, 1995; Morasso *et al.*, 1995). The role of *dlx* has been studied mainly in the developing forebrain (Robinson *et al.*, 1991; Dollé *et al.*, 1992; Bulfone *et al.*, 1993; Papalopulu and Kintner, 1993; Akimenko *et al.*, 1994; Fang and Elinson, 1996; Nicolas *et al.*, 1996) and the limb (Beauchemin and Savard, 1992; Dollé *et al.*, 1992; Bulfone *et al.*, 1993; Ferrari *et al.*, 1995). However its expression has also been documented in the branchial arches (Robinson and Mahon, 1994; Qiu *et al.*, 1995), the olfactory placodes (Bulfone *et al.*, 1993), the otic placodes (Ekker *et al.*, 1992), the otocysts (Ekker *et al.*, 1992; Papalopulu and Kintner, 1993; Robinson and Mahon, 1994), the sensory hair cells (Ekker *et al.*, 1992), and the tooth buds (Dollé *et al.*, 1992; Robinson and Mahon, 1994). Similarly, *msx* expression has been well documented in different aspects of craniofacial development (Jowett *et al.*, 1993; Chen *et al.*, 1996) and in the developing limb (Robert *et al.*, 1991; Crews *et al.*, 1995). So far, the actual role of these genes in these processes is not well known, although, there is some evidence

Table 1-1. Vertebrate *dlx* genes. A total of eight zebrafish *dlx* genes have been cloned. Most of the mouse and human *dlx* genes have been cloned, and it appears that there are a total of six *dlx* genes in mammals. In *Xenopus* there has been two different *dlx-3* genes reported (*Xdll-2*; Papalopulu and Kintner, 1993; and Dirksen *et al.*, 1994). This situation is believed to have resulted from the duplication of the *Xenopus* genome. References for the sequences presented in this table are provide on p.p. 35 of the Materials and Methods section of chapter two.

	dlx-1	***dlx-2***	***dlx-3***	***dlx-4***	***dlx-5***	***dlx-6***	***dlx-7***	***dlx-8***
human	*DLX-1*	*DLX-2*	*DLX-3*		*DLX-5*	*DLX-6*	*DLX-7*	
mouse	*Dlx-1*	*Dlx-2*	*Dlx-3*		*Dlx-5*	*Dlx-6*	*Dlx-7*	
zebrafish	*dlx-1*	*dlx-2*	*dlx-3*	*dlx-4*	*dlx-5*	*dlx-6*	*dlx-7*	*dlx-8*
Xenopus		*Xdll-4*	*Xdll-2*$^{a+b}$		*Xdll-3*		*Xdll*	
newt			*NvHbox-4*				*NvHbox-5*	

Table 1-2. Vertebrate *msx* genes (adapted from Davidson, 1995). Notice that the zebrafish has 5 different *msx* genes whereas most vertebrates have 2. There may be additional *msx* genes in vertebrates other than zebrafish which have not yet been cloned. The column correspondance between the zebrafish *msx* genes and the other vertebrate *msx* genes does not indicate sequence homology. Sequencing data for this table was acquired from the following references: zebrafish *msh-A, msh-B, msh-E* (Akimenko *et al.*, 1994) *msh-C*, and *msh-D* (Ekker *et al.*, 1992); human *MSX-1* (Hewitt *et al.*, 1991), and *MSX-2* (Jabs *et al.*, 1993); mouse *Msx-1* (Robert *et al.*, 1989), and *Msx-2* (Monaghan *et al.*, 1991); *Xenopus msx-1* and *msx-2* (Su *et al.*, 1991); chick *Msx-1* (Coelho *et al.*, 1991) and *Msx-2* (Yokouchi *et al.*, 1991).

zebrafish	*msh-A*	*msh-B*	*msh-C*	*msh-D*	*msh-E*
	msx-1	***msx-2***	***msx-3***		
human	*MSX-1*	*MSX-2*			
mouse	*Msx-1*	*Msx-2*	*Msx-3*		
Xenopus	*msx-1*	*msx-2*			
chick	*Msx-1*	*Msx-2*			

to support the role of *msx* to maintain mesenchymal cells in an undifferentiated, proliferating state (Song *et al.*, 1992).

Members from both of these gene families are expressed during the development of the zebrafish inner ear (Ekker *et al.*, 1992; Akimenko *et al.*, 1994). In the mouse, only expression of *dlx-2* and *dlx-3* has been reported in the otocyst, and later in the epithelium of the utricle and semicircular canals (Robinson and Mahon, 1994). Similarly in *Xenopus*, transcripts of *Xdll-3* are detected in the developing otocyst (Papalopulu and Kintner, 1993). There has been no further reports of *msx* or *dlx* expression in the developing vertebrate inner ear; however, this could be an instance where researchers focused on other processes such as limb or craniofacial development and neglected to report or study expression in other areas.

In the zebrafish ear *dlx-3* transcripts are first detected in the ectoderm that will become the otic placode (Ekker *et al.*, 1992). Later in the otocyst, *dlx-3* expression becomes more restricted to the dorsal and posterior regions of the vesicle (Ekker *et al.*, 1992). Thereafter, as expression of *dlx-3* becomes further restricted, *msh-D* transcipts are detected along the dorsal side and travels from the anterior to the posterior region of the vesicle (Ekker *et al.*, 1992). As the vesicle begins to differentiate into the various complex structures of the inner ear, transcripts of *dlx-2*, *dlx-4*, *msh-C* and *msh-D* mRNA are detected in the precursor cells that will become the sensory hair cells (Ekker *et al.*, 1992; Akimenko *et al.*, 1994).

1.7 Introducing the Mexican Axolotl (*Ambystoma mexicanum*)

The Mexican axolotl (*Ambystoma mexicanum*) is a neotenous salamander whose native habitat is restricted to two lakes, lake Xhochimilco and lake Chalco, located near Mexico city. Unlike other salamander species, such as its close relative, *Ambystoma tigrinum*, it does not undergo metamorphorsis and consequently spends its entire lifecycle in the water. It is for this reason that it is termed neotenic, since it can reach sexual maturity while simultaneously existing in a 'juvenile' state.

In 1863, General Forey of the French Expeditionary Forces in Mexico shipped several axolotls to the National History Museum in Paris (Smith, 1989). Its hardiness and unusual lifecycle caused the axolotl to be quickly adopted as a laboratory research animal (Smith, 1989).

Moreover, the generosity of Auguste Duméril to supply other researchers with animals led to its early popularity (Smith, 1989).

The axolotl has many favorable features that made it popular as a research animal. It is very easy to breed and raise in the laboratory. It produces hundreds of eggs in a single spawning and can be induced to spawn again within two months. Its long lifecycle, greater than 10 years in the laboratory, ensured that just a few animals can continuously produce embryos.

Furthermore, developmental biologists have had a particularly close association with the axolotl for several excellent reasons. Its most attractive feature is the large size of the embryos (2 mm). This makes it easy to perform tissue manipulations such as transplanation and ablation experiments. In addition, tissue and organ cultures can easily be set-up. Moreover, the hardiness of these embryos toward surgical insult is high, and the developmental rate can be slowed down with cold without resulting in any adverse effects. Another attractive feature for developmental biologists is the large selection of colour and developmental mutations (Armstrong, 1985).

Although an enormous amount of research has been done on the different tissues interactions involved in development, the axolotl has not really caught the fancy of molecular embryologists. From their perspectives it suffers two drawbacks, large genome size and slow generation time. However because of the sheer volume of work that has been done during the course of axolotl organogenesis, it sets the groundwork for molecular biologists to fill in the picture by isolating the genes involved in these different processes. In addition, perhaps the most attractive reason for adopting the axolotl as a molecular research animal, is its incredible regenerative potential. This ability should be examined at the molecular level because of the medically related benefits that such research could yield.

1.8 The Lateral Line System of the Mexican Axolotl

In most aquatic amphibians and fishes the lateral line system is composed of two types of sensory tissue: mechanoreceptors and electroreceptors (Lannoo and Smith, 1989). The mechanoceptors are composed of neuromast organs which are either found within bony canals (most fishes) or located at the surface of the skin (most amphibians). The ampullary organs which constitute the electroreceptors have a similar placement depending on the animal

examined. Together both types of organs contribute to the make-up of the VIII cranial nerve complex (Lannoo and Smith, 1989).

In the axolotl, each neuromast organ is epidermally located and consists of a strip of hair cells which are protected by a gelatinous matrix (Lannoo and Smith, 1989; Smith *et al.*, 1990). The hair cells within these strips are organized in such a manner that they are very sensitive to water movement that travels parallel, along the length of the strip (Lannoo and Smith, 1989; Smith *et al.*, 1990). The 'hairs' of each hair cell consists of several stereocilia and a single, larger, kinocilium (Lannoo and Smith, 1989). Unlike the neuromast, the ampullary organ has not been as well characterized. It is an electroreceptor that is sensitive to the DC fields generated by animals and is probably used to distinguish between nonliving and living objects, especially in dark or muddy environments (Münz *et al.*, 1984).

The lateral line system develops from a series of placodes which form next to the otic placode (figure 1-4A). It is believed that there is a total of five placodes, two preotic placodes and three postotic placodes (Northcutt *et al.*, 1994). Out of the three postotic placodes, the posterior placode will form all of the three lines of the trunk (Northcutt *et al.*, 1994). In addition, unlike the other four placodes, the posterior placode **migrates** posteriorly depositing small clumps of itself that will form primary, and subsequently secondary, neuromast pairs (figure 1-4B and C) (Northcutt *et al.*, 1994). The migration of the posterior placode primordia is dependent on both the ectoderm and subjacent mesoderm, and seems to require a contact guidance mechanism for proper migration (Smith *et al.*, 1990). The other placodes form sensory ridges by an elongation process (Northcutt *et al.*, 1994).

When the lateral line system is completed, it is organized as three discrete lines in the head and trunk (figure 1-4D). In the head, two lines surround the eyes and are distinguished as the supraorbital and infraorbital lines, whereas a third line, the mandibular, travels along the bottom of the lower jaw (Lannoo and Smith, 1989). Unlike the lines of the head there are no ampullary organs present in the trunk lateral lines (Northcutt *et al.*, 1994). They are solely composed of neuromast organs and are designated as the dorsal, middle and ventral line (Lannoo and Smith, 1989).

Figure 1-4. Development of the lateral line placodes and their migration/elongation across the epidermis of the Mexican axolotl. (A) There are a total of five placodes which have formed by stage 35. (B) The placodes of the head form sensory ridges by an elongation process whereas the most caudal placode migrates depositing clumps of cells as it moves down the trunk. This elongation/migration process starts around stage 37. (C) By stage 41, most of the major organs and lateral line systems have been created. The creation of secondary ampullary organs and neuromasts occurs thereafter. (D) The completed lateral line system of the Mexican axolotl. The three lines of the head are the supraorbital (SO), infraorbital (IO), and mandibular (Ma) lines. On the trunk, the three lines are the dorsal (D), middle (M) and ventral (V) lines. Note that for the purpose of illustration, the lateral line systems are drawn as lines when in fact they develop as discrete 'stitches' (Adapted from Northcutt *et al.*, 1994; Lannoo and Smith, 1989).

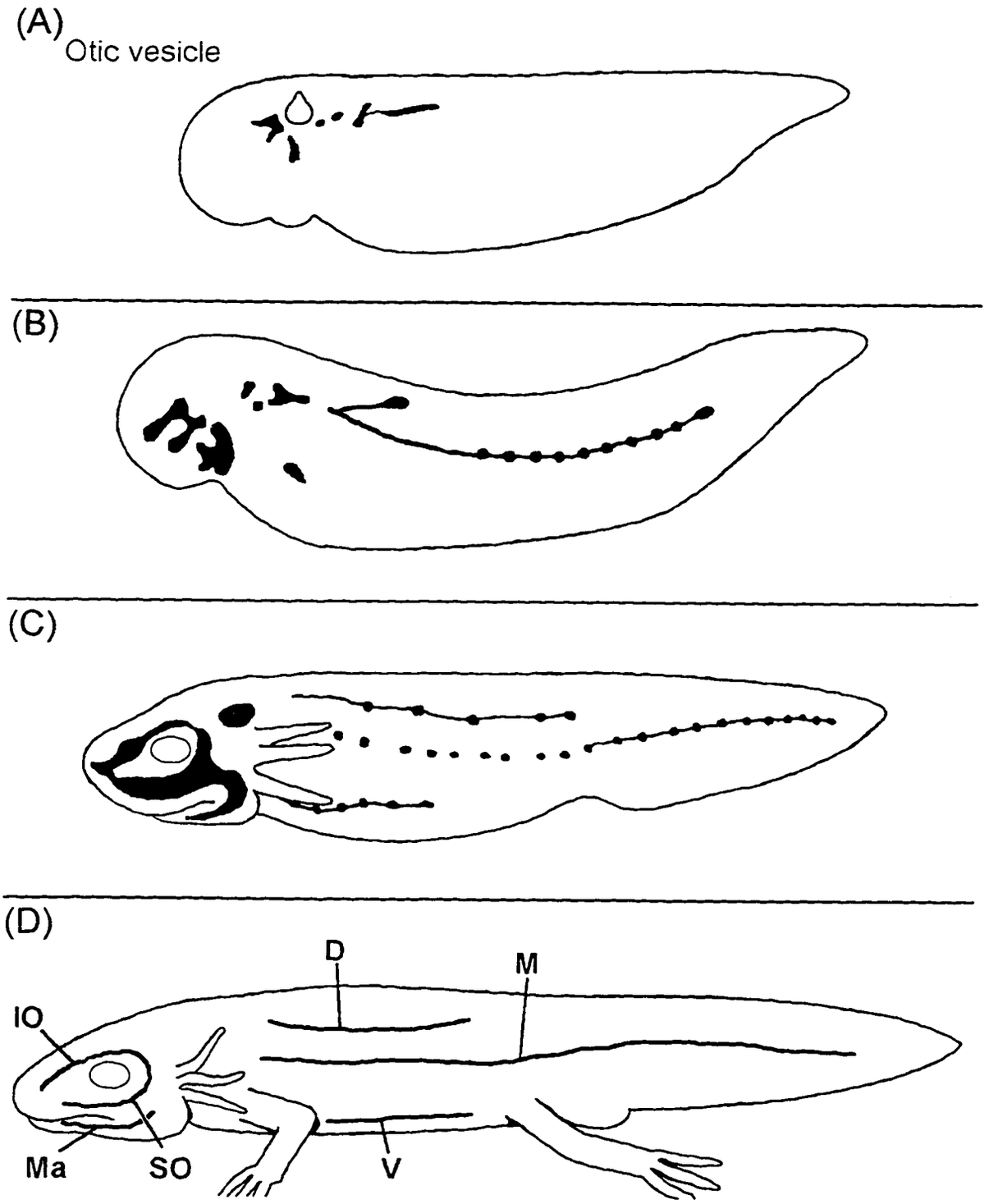
(A)
Otic vesicle
(B)
(C)
(D)
D
M
IO
Ma
SO
V

1.9 Objectives

Like the developing ear, the lateral line system starts with epidermal placodes, it forms organs (the neuromasts) which contain hair cells that are morphologically and functionally similar to the hair cells of the inner ear, it is innervated by the acoustic nerve complex (VIII), and there is evidence that the migratory cranial neural crest may play some role in the genesis of this organ system (Smith *et al.*, 1994). Consequently because of these numerous parallels, we believe that these similarities suggest that a conserved genetic pathway might be used during the morphogenesis of the neuromast organ. Thus we wish to test this proposal by examining if members of the *dlx* and *msx* gene families, which are expressed in the hair cells of the developing zebrafish inner ear, are also expressed in the hair cells of the developing neuromast organ of the Mexican axolotl. The first step in testing this proposal involves the cloning of these genes from the axolotl.

Chapter 2: Isolation of *dlx* and *msx* cDNA Sequences from the Mexican Axolotl

2.1 Introduction

The strategy to clone *dlx* and *msx* axolotl cDNA sequences would first involve using the polymerase chain reaction (PCR) to amplify the homeoboxes of these two gene families from genomic DNA or mRNA preparations. These homeoboxes would then be used as probes to screen a cDNA library for cDNA clones. Since members of both gene families are expressed in developing tissues during late neurulation, the cDNA library would be constructed from mRNA isolated from late neurula stage embryos.

The cloning of *msx* or *dlx* homeoboxes by using degenerate PCR primers that flank or lie within the homeoboxes of these genes is not new. Both Holland (1991), and Robinson and her coworkers (1991) took advantage of the fact that the homeoboxes of the *msx* and *dlx* families are very well conserved amongst its members and different species to design degenerate primers that either flanked or matched sequences within the homeobox.

Thus, Holland (1991) designed his 5' *msx* PCR primer to match the highly conserved amino acid sequence "TLRKH" which starts seven amino acids upstream of the *msx* homeodomain. Similarly, his 3' *msx* PCR primer was designed to match the highly conserved amino acid sequence "EAELEK" which is immediately downstream from the end of the *msx* homeodomain. By using these primers he was able to clone *msx* homeoboxes from mouse, zebrafish, and ascidian (Holland, 1991). This ability to design primers that can amplify *msx/msh* sequence from animals that are separated by great evolutionary distances (i.e.: mouse versus ascidian) demonstrates the high degree of sequence conservation of the *msx* homeoboxes.

Robinson and her coworkers (1991) used an identical strategy when they designed degenerate primers to match consensus sites amongst the different members of the *dlx* genes. Their 5' *dlx* PCR primer was designed to match the amino acid sequence "KPRTTY" which starts at the third amino acid position of the *dlx* homeodomain, and their 3' *dlx* PCR primer was designed to match the amino acid sequence "KIWFQN" which starts at the forty-sixth position of the homeodomain. These primers enabled this group to clone the *dlx-2* homeobox from the

mouse, which they then used to screen a mouse library for the full cDNA sequence (Robinson *et al.*, 1991).

By relying on the success of these previous experiments, two sets of degenerate PCR primers were used to clone the *msx* and *dlx* homeboxes from the axolotl (figure 2-1). These primers were modified slightly from the designs of Holland and Robinson *et al.* to accomodate new sequence information that has been made available since 1991. Basically they matched similarly conserved amino acid regions of the *msx* and *dlx* homeodomains. Thus, successful PCR using the degenerate *msx* primers should produce a 201 bp fragment, and with the degenerate *dlx* primers, we would expect a 156 bp PCR fragment when cDNA was used as the template. If genomic DNA is used in the *dlx* PCR experiment, the resulting products could be of varying sizes since the *dlx* homeobox contains an intron at a highly conserved position (132 bp from the start of the homeobox) which varies in length depending on which *dlx* homeobox is amplified. This problem can be avoided by using cDNA as the PCR template.

Figure 2-1. Sequence of PCR primers used to amplify the axolotl homeoboxes. (A) *msx* PCR primers used based on a modification of the PCR primers of Holland (1991). Notice that both oligos have restriction sites incorporated into their sequences to make the subcloning of the PCR products easier. (B) *dlx* PCR primers used to clone the axolotl *dlx* homeoboxes. The sequences of these primers were based on the design of an oligo pair used by Robinson, Wray and Mahon (1991) to clone the mouse *Dlx-2* homeobox. Degenerate nucleotide short-forms: **D** = A + G + T; **H** = A + C + T; **M** = A + C; **N** = all four nucleotides; **R** = A + G; **Y** = C + T.

A.

msx 5': 5'-ATGGATCC MCN CTN CGN AAR CAY AA-3'

msx 3': 5'-GGAATTC YTT YTC NAG YTC NGC YTC-3'

B.

dlx 5': 5'-GGAATTC AAR CCN MGN ACN ATH TA-3'

dlx 3': 5'-CGGGATCC RAA CCA DAT YTT NAC YTG-3'

2.2 Materials and Methods

2.2.1 Isolation of Axolotl Genomic DNA

Axolotl genomic DNA was prepared using a modified procedure as described by Akimenko (1993). Axolotl embryos were rinsed in phosphate buffered saline (PBS: 140 mM NaCl. 3 mM KCl. 6 mM Na_2HPO_4, and 1 mM KH_2PO_4, pH 7.4) before being quickly frozen in liquid nitrogen. While in the presence of liquid nitrogen. the frozen embryo pellet was ground into a fine powder. Once the embryos were pulverized into a powder, 5 ml of digestion buffer (10 mM Tris-HCl. 1% SDS. 5 mM EDTA. and 100 µg/ml of proteinase K) was added. This mixture was incubated at 37 °C for 5 hours. Every hour during the course of the incubation. the mixture was shaken by repeatedly inverting the tube from 6 to 10 times.

After the incubation. the digestion was extracted by combined it with an equal volume of phenol:chloroform:iso-amyl alcohol (50:48:2). This mixture was shaken for 5 minutes by repeatedly inverting the tube and then immediately centrifuged at 1400 rpm for 5 minutes (Sorvall centrifuge. model RT6000B). The aqueous phase was removed and extraction two more times. The final NaCl concentration of the aqueous phase was adjusted with 0.3 M NaCl and the genomic DNA was precipitated by adding 2.5 times volume of ice-cold 100% ethanol.

A glass hook was constructed out of a glass pasteur pipette and use to 'fish' out the precipitated DNA from the ethanol solvent. The precipitated DNA was transferred into an 1.5 mL eppendorf tube where it was allowed to dry on the bench top for 15 minutes before being resuspended in 1 ml of TE buffer (10 mM Tris-HCl, pH 8.0; 1 mM EDTA). To help resuspend the pellet. it was placed in a 37 °C water bath and every 15 minutes the tube was repeatedly inverted from 5 to 6 times. Once the pellet was dissolved, SDS was added at a final concentration of 0.2% and then the solution was extracted twice using an equal volume of phenol:chloroform:iso-amyl alcohol (50:48:2). A final extraction was performed using only chloroform:iso-amyl alcohol to remove any traces of phenol from the aqueous phase. The NaCl concentration of the aqueous phase was adjusted to 0.3 M NaCl and the DNA was precipitated by adding 2.5 times volume of ice-cold 100% ethanol. The DNA was then transferred to a new eppendorf tube. centrifuged for 10 minutes at 15000 rpm and then allowed to dry on the benchtop. The pellet was resuspended in 1 mL of TE buffer and stored at 4 °C.

The yield was determined by spectrophotometric measurements as detailed in Sambrook *et al.* (1989). Two optical density (OD) readings were taken at wavelengths of 260 nm and 280 nm. The former wavelength value was used to calculate the amount of DNA in the sample by relying on the standard value of 1 OD_{260} as corresponding to approximately 50 μg/ml of double-stranded DNA. The ratio between the $OD_{260}\backslash OD_{280}$ readings was used to estimate the purity of the nucleic acid obtained.

2.2.2 Isolation of Axolotl RNA

Total RNA was extracted from frozen embryonic pellets using a modification of the single-step guanidinium thiocyanate method (Ausubel *et al.*, 1995). Generally the modifications involved increasing the volumes of the reagents used during the extractions. Embryos for RNA extraction were collected in 14 ml tubes, rinsed twice with distilled water (to remove excess salts), quickly frozen in liquid nitrogen, and then stored at -70 °C.

During the extractions, the 14 ml tubes were placed on ice. 5 ml of denaturing solution (4M guanidium thiocyanate, 25 mM sodium citrate, pH 7.0; 0.5% sarcosyl; and 0.1M β-mercaptoethanol) was added to each tube, and the frozen pellets were immediately homogenized using telfon homogenizers. After the embryos were pulverized, 0.5 ml of 2 M sodium acetate (pH 4) was added, and tubes were inverted 5 to 6 times to mix the contents. Next, 5 ml of water saturated phenol was added and again the tubes were inverted 5 to 6 times to mix. 1 ml of chloroform-isoamyl alcohol, in a 49:1 ratio, was added, and each tube was shaken vigorously for 10 seconds and then placed on ice for 15 minutes.

Immediately before centrifugation, the entire content of each 14 ml tube was transferred into 30 ml glass centrifugation tubes (Corex centrifugation tubes, Corning). The aqueous and organic phases were separated by a centrifugation spin at 9,000 rpm for 20 minutes at 4 °C. The aqueous phase was removed and added to a clean 30 ml centrifugation tube, and the RNA was precipitated by adding 5 ml of isopropanol and then storing at -20 °C for two hours. The RNA was pelleted by centrifugation at 10,000 rpm for 15 minutes at 4 °C. The supernatant was discarded and the pellet was resuspended in 0.5 ml of denaturing solution before being transferred to a 1.5 ml eppendorf tube.

The RNA was reprecipitated by adding 0.5 ml of isopropanol and storing at -20 °C for 30 minutes. The RNA was pelleted by centrifugation for 15 minute at 10,000 rpm. The pellet was washed with 70% ethanol, vortex, and then left on the bench top for 10 minutes to allow the guanidium thiocyanate residues to wash out of the RNA. Again, the RNA was pelleted by a 5 minute centrifugation at 10,000 rpm, and the supernatant was discarded. The pellet was dried by vaccum and then 250 µl of DEPC (diethyl pyrocarbonate, BDH chemicals)-treated water and 750 µl of 4M LiCl (final concentration, 3M) were added to the pellet. The pellet was dissolved by repeated vortexing and pipetting. It was then stored at -20 °C overnight.

The next day the resuspended pellet was centrifuge at 10,000 rpm for 30 minutes in a 4 °C centrifuge. The pellet was washed with 70% ethanol, centrifuged briefly, and dried on the benchtop. The pellet was then redissolved in 60 µl of DEPC-treated water and stored at -70 °C. All RNA samples were quanitated by spectrophotometric measurements (using an OD_{260} value of 1 as equal to 40 µg/ml RNA yielded). Yields varied from 220 µg per 50 blastula stage embryos to 400 µg per 40 hatchling stage embryos.

2.2.3 PCR Primers and PCR Reaction conditions

The sequences of the degenerate PCR oligonucleotides are presented in figure 2-1. In general, standard PCRs were run with an annealing temperature varying between 50 °C to 58 °C. One cycle of a standard PCR involved a one minute 95 °C denaturing step followed by a one minute annealing step (at the appropriate temperature) and then a two minute extension step at 72 °C. Generally from 30 to 40 cycles were performed after an initial 2 minute soak at 95 °C prior to cycling.

Different templates were used, such as genomic DNA, cDNA made directly from mRNA, and aliquots of phage stock taken directly from the λZAP cDNA library.

2.2.4 Southern Blotting and Hybridization Conditions

For Southern analysis, agarose gels were shaken in a 0.4 N NaOH solution for 30 minutes before being set up for overnight transfer onto nylon membranes (PALL membranes, BioDyne). Transferring was done using 0.4 N NaOH as the transferring solution. Each gel was placed on top of a 3MM paper wick suspended over a tray of 0.4 N NaOH solution. A nylon membrane,

cut slightly smaller than the size of the gel, was placed on top of the gel, followed by several sheets of 3MM paper and paper towels that were cut smaller than the size of the membrane. After overnight transfer, the membrane was washed at room temperature for 15 minutes in neutralizing solution (0.2 M Tris-HCl, pH 7.5; 2X SSC), dried briefly on the benchtop, exposed to UV light for 2 minutes (Stratogene Stratolinker), and then washed at 65 °C in a stringency wash (0.1X SSC, 0.5% SDS) for one hour.

All Southerns and plaque lifts were prehybridized and hybridized in shaking waterbaths with temperatures ranging from 55 °C to 65 °C depending on the level of sequence homology to the probe. Blots and plaque lifts were prehybridized from 4 to 6 hours in prehybridization solution (6X SSC, 10X Denhardt's) and then hybridized overnight in hybridization solution (3.5X SSC, 5X Denhardt's, 0.5% SDS, 25 mM NaPO4, 2 mM EDTA, and 100 μg/ml of boiled, sheared salmon sperm DNA).

The probes used for Southern analysis and library screening were synthesis via the random priming method (Sambrook *et al.*, 1989) using [α-^{32}P]-dCTP (3000 Ci/mmol)(Amersham) as the radioactive nucleotide. Following synthesis of the radioactive probe, unincorporated nucleotides were removed using a sperminine tetrahydrochloride precipitation procedure. This involved adding 8 μl of sperminine tetrahydrochloride (10 mg/ml), 8 μl yeast tRNA (10 mg/ml), and 160 μl of dH_2O following probe synthesis. This mixture was then place on ice for 20 minutes before being centrifuge for 10 minutes at 14,000 rpm. The supernatant was discarded and the pellet was washed with 1X TE solution containing 1 mM sperminine tetrahydrochloride before being centrifuged again for 10 minutes at 14,000 rpm. This step was repeated two more times, each time removing the supernatant and washing the pellet with 1X TE containing 1 mM sperminine tetrahydrochloride. After the last wash, the pellet was resuspended in TE and boiled 5 minutes before adding to the hybridization solution.

The amount of α-P^{32} dCTP incorporated into the probe was approximated using an automated scintillation counter (BECKMAN, model LS 1701). As suggested by Ausubel *et al.* (1995) approximately 5 X 10^5 to 5 X 10^6 counts per minute (cpm) of probe was used per 15 ml of hybridization solution.

2.2.5 cDNA libraries

Two cDNA libraries were used in this project. The first library to be screened was a λZAP library made in the laboratory using the Stratagene cDNA library construction kit (Stratagene ZAP-cDNA Synthesis kit, catalog #200400; Stratagene Undigested Lambda ZAPII Cloning kit, catalog #236201). The second library was a λgt10 cDNA library kindly provided to us by Carl Séguin (Laval Université, Quebec City).

For the synthesis of the λZAP library, 5 μg of axolotl mRNA was used in the library's construction. The mRNA was isolated from total RNA using the Qiagen Oligotex-dT mRNA Mini Kit. Following mRNA isolation, poly-T primer/linkers were added to the mRNAs and first strand synthesis of the cDNAs was completed using Moloney Murine Leukemia reverse transcriptase (both linkers and enzymes were supplied in the Stratagene ZAP-cDNA Synthesis kit). Included within the sequence of the poly-T primer/linker was an *Xho*I restriction site. During second strand synthesis, methylcytosine was included in the nucleotide mix thus making cDNAs that were hemimethylated[2]. Following cDNA synthesis, *Eco*RI adapters were added to both ends of the cDNA molecules by blunt end ligation using T4 DNA ligase (supplied in the kit).

The cDNA molecules were then digested with both *Xho*I and *Eco*RI restriction enzymes (supplied in the kit). This generated cDNA molecules that had *Xho*I sites at their 3' ends and *Eco*RI sites at their 5' ends. Since the 5' and 3' ends of these fragments had different restriction sites, they could be ligated into the phage vector in only one orientation. Fragments were ligated into a λZAPII vector which had previously been digested with *Eco*RI-*Xho*I and treated with calf intestinal alkaline phosphatase to prevent their re-ligation (Stratagene Undigested Lambda ZAPII Cloning kit, catalog #236201).

The second library was also constructed using mRNA isolated from neurula staged embryos (Busse *et al.*, 1990). However, during the construction of this library the cDNA molecules contained *Eco*RI sites at both ends. Thus each cDNA molecule could be ligated in

[2] It was important to make the cDNA molecules hemimethylated so that internal restriction sites would be protected from digestion by either the *Xho*I or *Eco*RI restriction enzymes. Only these sites present at the ends of the cDNA molecules would be cut by these restriction enzymes.

either orientation into an *Eco*RI site of the polylinker that had previously been introduced into the λgt10 phage genome.

2.2.6 Library Screening

LE392 *Escherichia coli* (*E. coli*) cells (OD_{600} = 1.0), which were grown in 0.2% maltose and 10 mM $MgSO_4$ overnight, were infected with diluted phage from the amplified cDNA libraries and allowed to incubate 20 minutes at 37 °C. The infected bacteria were then plated with 6.5 ml of top agarose (temperature = 50 °C) onto 150 mm NZY plates at a calculated plaque forming unit (pfu) of 30,000 pfu's per plate. A total of 660,000 pfu's were screened. Plates were incubated at 37 °C for 7 to 8 hours until plaques were large but not confluent. Plates were stored at 4 °C overnight.

Plaque lifts were performed using nylon membranes (Hybond-N, Amersham). The following lifting protocol was used. The membrane was applied to the surface of each plate for 1 minute (2 minutes if a duplicate was made). Next, the membrane was placed, DNA side up, onto Whatmann's 3MM paper that was soaked in denaturant solution (0.5 M NaOH, 1.5 M NaCl). Each membrane was left in the denaturant solution for 7 minutes before being transferred to neutralizing solution (1.5 M NaCl, 0.5 M Tris-HCl, pH 7.2; 1 mM EDTA), which like the denaturant solution had been allowed to soak into Whatmann's 3MM paper. The membranes were left for 5 minutes on the neutralizing solution before being transferred to a wash solution (2X SSC, 1 mM EDTA). After 3 minutes in the wash solution, membranes were placed on dry paper towel and allowed to dry for 15 minutes. To fix the DNA onto the membranes, each membrane was placed into a Stratagene UV crosslinker, using the autolink setting (1200 kJ for 2 minutes).

As described in the Southern blotting section (2.2.4), plaque lifts were prehybridized and hybridized using the same conditions that were used for Southern Analysis.

Positive clones were subcloned into plasmid vectors using two methods. In the first method, PCR primers that match λgt10 sequences flanking the *Eco*RI insertion site were used to amplify the insert. These primers were provided by Dr. Peter Juranka (LOEB Institute of Medical Research, Ottawa) and worked using standard PCR conditions (as described in section 2.2.3) with an annealing temperature of 54 °C. The resulting PCR products were subcloned into

pCRII vectors using an Invitrogen pCRII Cloning kit. In cases where the λ primers failed to amplify the insert, phage DNA minipreps were performed as outlined by Grossberger (1987). The isolated phage DNA from the λgt10 cDNA library was cut with *Eco*RI to liberate the insert. These inserts were subcloned into pBS KS+ which had previously been linearized with *Eco*RI and treated with calf intestinal alkaline phosphatase.

2.2.7 Subcloning of cDNA Clones

Subclones of most of the cDNA clones were made so that these smaller fragments could be sequenced from both ends by manual sequencing (Sequenase 2.0, USB). Most of the subcloning involved using restriction sites that were present within the polylinker of the vector and the insert. Therefore, in addition to subcloning the restriction fragments, deletion clones could be created by simply religating together the vector less the excised restriction fragment.

pBS KS+ vectors were prepared by linearizing 1 μg of plasmid with the appropriate enzyme and then incubating with calf intestinal alkaline phosphatase at 37 °C for 1 hour. The enzyme was then heat inactivated at 75 °C for 15 minutes. Phenol:chloroform extractions were performed to remove the enzymes, and the linearized vector was precipitated from the aqueous phase by adjusting the salt concentration to 0.1 M with sodium acetate, adding 2X the volume of 100% ethanol, and storing at -20 °C for 30 minutes. The DNA was pelleted by centrifugation at 15.000 RPM for 15 minutes. The pellet was washed with 70% ethanol, and dried on the benchtop. The pellet was resuspended in 20 μl of 1X TE, thereby concentrating the plasmid to 50 ng/μl.

Deletion clones (i.e.: plasmids less their restriction fragment) and restriction fragments of the cDNA clones were band purified from agarose gels by using DEAE paper. This involved run the fragment of choice onto a piece of DEAE paper that had been inserted into the gel. To elute the DNA off of the paper, the paper was placed into an 1.5 ml eppendorf tube filled with 200 μl of elution solution (1 M NaCl, 10 mM arginine) and incubated at 68 °C for 20 minutes. The supernatant was collected into a second eppendorf, and the elution was repeated once more on the first eppendorf. The two supernatants were combined and extracted with an equal volume of phenol:chloroform:iso-amyl alcohol. To the aqueous phase, 2X its volume of 100% ethanol was added, and the DNA was precipitated at -70 °C for 20 minutes. The DNA was pelleted by

centrifugation at 14,000 rpm for 15 minutes. Then washed with 70% ethanol, centrifuged briefly, and allowed to dry on the benchtop for 15 minutes. The pellet was resuspended in 20 µl of TE buffer.

DEAE purified fragments were then ligated into the appropriate vector using a 3:1 ratio of insert to vector. All ligations were allowed to proceed overnight at 15 °C. The next day ligations were transformed into competent XL-1 Blue *E. coli* cells which were then plated onto LB plates containing ampillicin. Plates were incubated overnight at 37 °C. Ligation efficiencies were determined by comparing the number of transformants on the experimental plates (vector plus restriction fragment) against control plates (vector only). In most cases, several colonies from each plate were picked and grown in small volumes of LB media supplemented with ampicillin. The following day plasmids were isolated from these cultures and checked for the presence of inserts by digesting with the appropriate restriction enzyme.

2.2.8 Sequencing of Clones

The majority of the DNA sequencing was performed using the Sequenase sequencing kit, version 2 (USB). As instructed by the Sequenase manual, from 3 to 5 µg of plasmid DNA was used as the template in sequencing reactions that used [α-^{35}S]-dATP (1000 Ci/mmol)(Amersham) to label the sequenced fragments. In addition to the manual sequencing, sequencing was also performed using a Li-Cor automated sequencing machine (Model 4000L).

The identity of the clones was established by sequence comparison with known *msx* and *dlx* sequences. This was accomplished by submitting the sequencing data to BLAST searches (Altschul *et al.*, 1990). All sequence data was submitted at the nucleotide level using the BLASTn program, and at the protein level using the BLASTx program which automatically translates the query in all six reading frames.

2.2.9 Phylogenetic Analyses

Phylogenetic analyses were performed only on the homeobox/homeodomain regions of the *dlx* genes because we wanted to include the *dlx* PCR clones into the tree topologies. Since the PCR clones contained only the homeobox, their comparison against other sequences that

included the regions 5` and 3' to the homeobox would cause the MEGA software to crash.

Multiple alignments were performed using the CLUSTALV software package (Higgins and Sharp, 1989). Once the alignments were completed, the MEGA software was used to determine the relative frequencies of the 4 nucleotides (or of the 20 amino acids), and the number of transitional differences and transversional differences. These values in conjuction with guidelines provided with the MEGA documentation allowed us to select the most appropriate distance estimation formula (Kumar *et al.*, 1993). According to the guidelines provided with the MEGA documentation, and preliminary distance estimation values, the Jukes-Cantor distance estimation method was choosen for the nucleotide dataset (Jukes and Cantor, 1969). For the amino acid dataset, pairwise distances were calculated as percent similarities (p-values). Bootstrapped distance matrix trees were created using 1000 replicates and the randomly seeding option.

Sequence data for other organisms were obtained from the following references: *Drosophila Dll* (Cohen *et al.*, 1989); zebrafish *dlx-2*, *dlx-3*, and *dlx-4* (Akimenko *et al.*, 1994); newt *NvHBox-4* and *NvHBox-5* (Beauchemin and Savard, 1992); Xenopus *Xdll* (Asano *et al.*, 1992), *Xdll-2*[1] (Dirksen *et al.*, 1994), *Xdll-2*[2], *Xdll-3*, and *Xdll-4* (Papalopulu and Kintner, 1993);
chicken *Dlx-5* (Ferrari *et al.*, 1995); mouse *Dlx-1* (Price *et al.*, 1991), *Dlx-2* (Robinson *et al.*, 1991), *Dlx-3* (Robinson and Mahon, 1994), and *Dlx-7* (Nakamura *et al.*, 1996); and, human *DLX-1*, *DLX-5*, *DLX-6* (Simeone *et al.*, 1994), *DLX-2* (Selski *et al.*, 1993), and *DLX-7* (Nakamura *et al.*, 1996).

2.3 Results

Initially PCR was performed using the degenerate *msx* primers on axolotl genomic DNA, and later on, cDNA which was created from neurula staged mRNA. Although these PCR experiments produced fragments that were approximately the expected size, they failed to amplify *msx* homeoboxes as determined by Southern analysis. These primers were then tested on zebrafish *msh* clones to determine if the primers were defective. This experiment succeeded in amplifying the homeoboxes of the *mshB* and *mshD* genes, and thus the failure to amplify axolotl *msx* homeoboxes was not due to any flaw of the primer design or synthesis.

In the meantime, PCR using the *dlx* primers was also tried on both genomic DNA and cDNA. Again, as with the *msx* primers, this approach did not work. Although products of approximately the expected size were produced in some of these reactions, they failed to hybridize to a radioactively-labelled probe during Southern analysis. PCR was also tried using aliquots of the phage stock taken directly from the amplified λZAP cDNA library. This latter experiment worked and the results are presented in the following section.

2.3.1 Isolation of *dlx* Homeoboxes by PCR reactions

Several PCR experiments were tried with different *dlx* primers. In figure 2-2, each lane contains the amplified products of a PCR experiment that used different sets of *dlx* primers. Some of these primers were specifically designed to amplify *dlx* orthologs, such as *dlx-2* or *dlx-6* from zebrafish (lanes 3 and 4 respectively, figure 2-2). The results of PCR using the degenerate *dlx* primers are shown in lane 5 (figure 2-2).

PCR with degenerate *dlx* primers using aliquots of phage stock from the λZAP cDNA library produced four bands of various sizes (figure 2-2 (A), lane 5; labeled as (I), (ii), (iii), and (iv)). When the Southern blot of this gel was probed with the coding region of the zebrafish *dlx2* gene, a signal was visible in lane 5 on the autoradiograph after a 1 hour exposure (figure 2-2 (B)). The signals present in lane 3 were ignored since both the probe and the products in lane 3 contains *dlx-2* sequences. The products of lane 3, regardless of their actual identity, would have incorporated the *dlx-2* primer sequences and since the probe was constructed from zebrafish

Figure 2-2. Results of *dlx* PCR on aliquots of phage stock taken directly from the amplified axolotl λZAP cDNA library. (A) Photograph of the agarose gel on which aliquots from different PCR experiments were electrophoresis. Lane 1 contains a DNA standard (ϕx digested with *Hinc*II). Lane 2 contains the results of a PCR experiment that used *dlx* primers designed to match zebrafish *dlx* sequences. Lane 3 contains the results of a PCR experiment that used dlx primers designed to amplify the *dlx-2* homeobox from zebrafish. Lane 4 contains the results of a PCR experiment that used *dlx* primers designed to amplify the *dlx-6* homeobox from zebrafish. Lane 5 contains the results of the PCR experiment that used the degenerate primer pair as discussed in the introduction (2.1), and lane 6 contains a 735 bp fragment of the zebrafish *dlx-2* coding region (positive control for probe and hybridizing conditions during Southern analysis). Notice that in lane 5 there are a total of four products labelled as (i), (ii), (iii), and (iv). (B) Film of the Southern blot of the gel shown in (A) probed with a labelled zebrafish *dlx-2* fragment. The lane numbering corresponds to the same lanes as shown in (A). Notice that the probe hybridized to the products in lane 3. Hybridization in this lane was believed to be the result of hybridizing to the *dlx-2* PCR primers incorporated into these products and so these positives were avoided. In lane 5 there was a faint signal after only 1 hour exposure yet it did not match the intensity of the signal from lane 6 (positive control for probe). The signal in lane 5 either corresponded to band (iii) or (iv) on gel (A). Consequently, both of these bands were purified and subcloned into the pCRII cloning vector (Invitrogen) for sequencing.

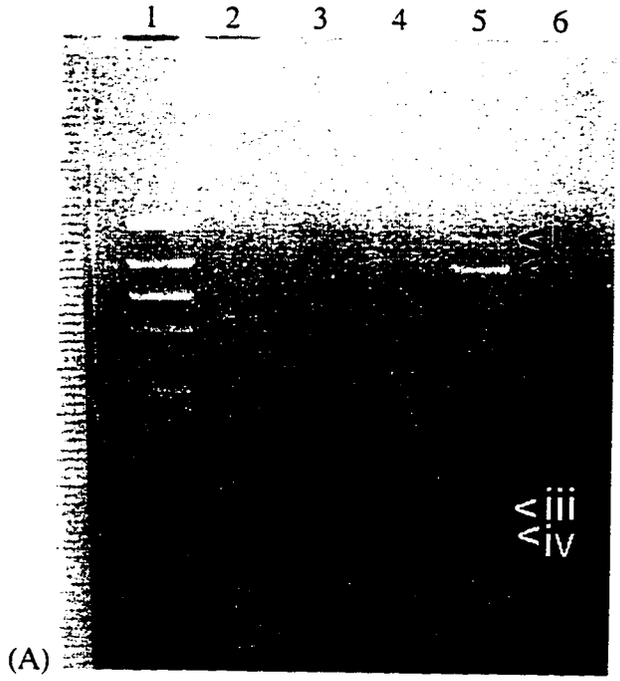

(A)

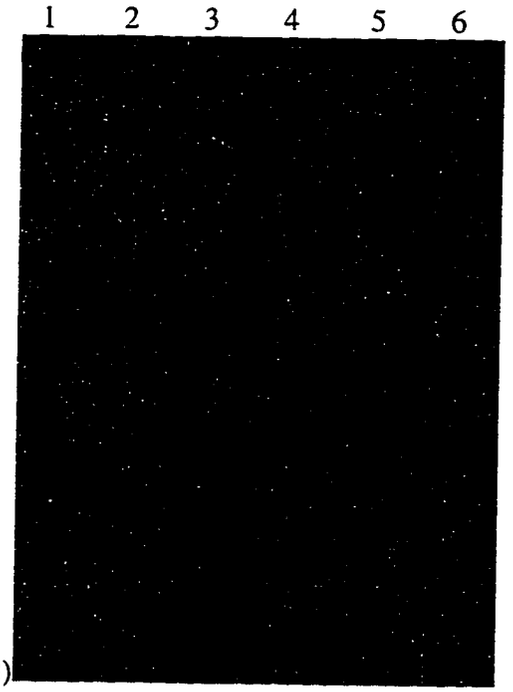

(B)

dlx-2 cDNA it should have hybridized to these sequences. In addition, the PCR products of lane 3 were not the predicted size (we expect a ~160 bp fragment); therefore, for these reasons the positive results of the Southern analysis for lane 3 were ignored.

In lane 5, the two larger fragments were clearly negative. However it was difficult to determine which of the two smaller fragments (approximately 180 bp, band labeled (iii) and 140 bp, band labeled (iv)) was hybridizing to the probe so both products were cloned into pCRII vectors (Invitrogen). Several colonies from each transformation were sequenced (Sequenase, USB) and their identities were determined by BLASTn searches.

Four of the colonies containing the larger fragment (iii) were identified as *dlx* homeoboxes. Their nucleotide sequences are shown in figure 2-3. These *dlx*-homeobox-containing PCR clones have been labelled as A, B, C, and D. Transformants containing the smaller PCR fragment were composed of λ phage sequences, and probably represent mispriming events with phage genomic sequences.

A summary of the results of a BLASTn search is presented in table 2-1. Clone A is most similar in sequence to the zebrafish *dlx-3* (91%) and the newt *NvHBox-4* (85%) homeoboxes. The homeobox of clone C is more similar to the homeobox of zebrafish *dlx-2* (83%), while the similarities of clones B and D varied between zebrafish *dlx-4* (89%), zebrafish *dlx-2* (68%), and zebrafish *dlx-1* (83%).

Since the amino acid sequences of the different *dlx* homeodomains are very well conserved amongst different vertebrates, it is possible to determine the identity of *dlx* homeoboxes based on the sequences of their translated products. In 1994, Simeone *et al* presented a composite figure of all of the known *dlx* homeodomains. Each ortholog could be characterized by amino acid substitutions that take place at highly conserved sites within the homeodomain. Therefore, when PCR clone A was translated and compared with an alignment of the different *dlx* homeodomains, it was found to have amino acid subsitutions at positions that are characteristic of *dlx-3* homeodomains (figure 2-4). These differences involve substitutions of tyrosine, alanines, lysine, and glutamine residues at conserved positions within the homeodomain, and are highlighted in bold in figure 2-4. The translations of clones B and C show that these fragments have an amino acid substitution of an alanine and a glutamine at

Figure 2-3. Alignment of the nucleotide sequences of the *dlx*-homeobox PCR fragments. Some sequences appeared to be incomplete since it was necessary to introduce gaps into their sequences. The double underline of the nucleotide sequence indicates the PCR primer sequences. Notice that within the 5' PCR primer there is an *Eco*RI site and within the 3' PCR primer there is a *Bam*HI site.

EcoRI

PCR A ggaattcaagccaagcacgatttta t cagttaccagctcgccgcgctccagcggc tt
PCR B ggaattcaagc actatttactccagtctccagctgcaggctctgaacaggcggtt
PCR C ggaattcaagcctaggactatttactccagtctccagctgcaggctctgaacaggcggtt
PCR D ggaattcaagcctaggacgatttactccagtgttcagctccaggctctgcaccacg t

PCR A ccagaaagcgcagtatctggcgctgccggagagagctgaactcgccgcacagctggggct
PCR B ccagcaaacccagtacttg ctctgccagagagagccgagctcgccgctagtcttgggct
PCR C ccagcaaacccagtatctggctctgcagaggagagccgagct gccgc actattgggct
PCR D ccagcagacccagtacctcgtgctgcccgaacgtgcagagctggccgtcaaactgggact

BamHI

PCR A cacacagacacaggtaaagatctggttcggatcccg
PCR B cacgcaaacacaagtgaaaatctggttcggatcccg
PCR C cacgcaaacacaggttaaaacttggttcggatcccg
PCR D gacgcaaacacaggttaaaatttggtttggatcccg

Table 2-1. Summary of the possible identities for the *dlx*-homeobox PCR products based on BLAST searches (Altschul *et al.*, 1990) of the National Institute of Health (NIH) databases. The nucleotide sequence of PCR clone A was most similar to the homeobox of *dlx-3*. Clone C resembles the homeobox of *dlx-2*. while clones B and D are similar to the homeoboxes of either *dlx-4*, *dlx-2* or *dlx-1*.

	BLASTn Similarities
PCR clone A	zebrafish *dlx-3* (91%), newt *NvHBox-4* (85%)
PCR clone B	zebrafish *dlx-4* (89%), zebrafish *dlx-2* (68%)
PCR clone C	zebrafish *dlx-2* (83%), *Xenopus Xdll* (77%)
PCR clone D	zebrafish *dlx-1* (83%), *Xenopus Xdll-3* (78%)

Figure 2-4. Comparison of the translated product of the *dlx*-homeobox PCR clones against the *Drosophila Dll* homeodomain (adapted from a figure used by Simeone *et al.*, 1994). The amino acid sequences are given in one letter code. Dashes below the *Drosophila Dll* homeodomain indicate amino acid agreement of the *dlx* PCR product to that of the fly's sequence. The bold lettering of the fly's *Dll* homeodomain indicates the region that spans the area amplified by the *dlx* primers. The first clone (A) appears to be *dlx-3* based on the presence of the tyrosine, alanines, lysine, and glutamines which are highlighted in bold. The next two clones (B and C) are most similar to the protein sequence of *dlx-1* based on the presence of the highlighted alanine and glutamine. The last clone (D) is similar to the homeodomains of either *dlx-1* or *dlx-6* due to the presence of an alanine and glutamine residue (found in both *dlx-1* and *dlx-6*), and the presence of a histidine residue (found only in *dlx-6*).

```
D11   MRKPRTIYSS LQLQQLNRRF QRTQYLALPE RAELAASLGL TQTQVKIWFQ NRRSKYKKMM
PCR A   --S--  - Y--AA-Q- - -KA------- ------Q--- ---------
PCR B   -  ----- ----A----- -Q---- --- ---------- ---------
PCR C   -------- -L--A----- -Q------QR --- - T--- ---------
PCR D   -------- V---A-HH   -Q----V--- -----VK--- ---------
```

positions observed in the homeodomain of *dlx-1* (figure 2-4). While the homeodomain of clone D resembled either *dlx-1* or *dlx-6* depending on the presence of an alanine and glutamine residue, found in both *dlx-1* and *dlx-6*, or the presence of a histidine residue, found only in *dlx-6*, at conserved sites (figure 2-4).

These *dlx*-homeobox PCR fragments were used to screen two cDNA libraries under conditions of reduced stringency so that other members of the *dlx* family might be uncovered.

2.3.2 The Results of cDNA Library Screening with the *dlx*-homeobox Fragments

Initially, the λZAP cDNA library was screened using a probe that included the entire coding sequence of the chicken *msx-1* gene (Benoit Robert, Pasteur Institute, Paris). Screening of this library was repeated several times, but failed to produce any positive clones that could be confirmed in a secondary screening. Carl Segiun generously supplied us with a λgt10 cDNA from which he and his coworkers had previously isolated the *Wnt-1* gene (Busse *et al.*, 1990).

When the λgt10 cDNA library was screened using a mixture of the four *dlx* homeoboxes we had cloned by PCR, more than thirty positives were identified in the primary screening. From the primary screening, twenty clones that produced 'strong' hybridization signals were picked for secondary screening. Ten of these twenty clones were still positive following the secondary screening.

Figure 2-5 (A) shows an autoradiograph of one of the lifts of a plate from the primary plating. There are 5 positive plaques on this plate labeled 18.1, 18.2, 18.3, 18.4, and 18.5. All five plaques were selected for secondary screening. From the five positives visible in figure 2-5 (A), cored samples 18.1, 18.2 (figure 2-5 (B)), and 18.5 (figure 2-5 (C)) produced positives in the secondary screening.

2.3.3 Subcloning of cDNA Inserts

As discussed in the Materials and Methods section, the inserts of these clones were subcloned into either pBS or pCRII vectors. The choice of plasmid vector depended on the ability of the PCR to amplify out the insert contained within the λgt10 vector.

Figure 2-5. Results of screening the λgt10 cDNA library using a mixture of the *dlx*-homeobox PCR clones and low stringency conditions. (A) Primary lift of plate number 18. On this plate 5 putative positives were picked for secondary screening ("*" denotes orientation marks for aligning the lift with the plate). (B) Cored sample numbered 18.2 produced positives in the secondary. Following subcloning and sequencing of this clone, it was identified as *msx-1* based on the results of a BLASTn search. (C) Cored sample numbered 18.5 also produced positives in the secondary. This clone was identified as *dlx-5*.

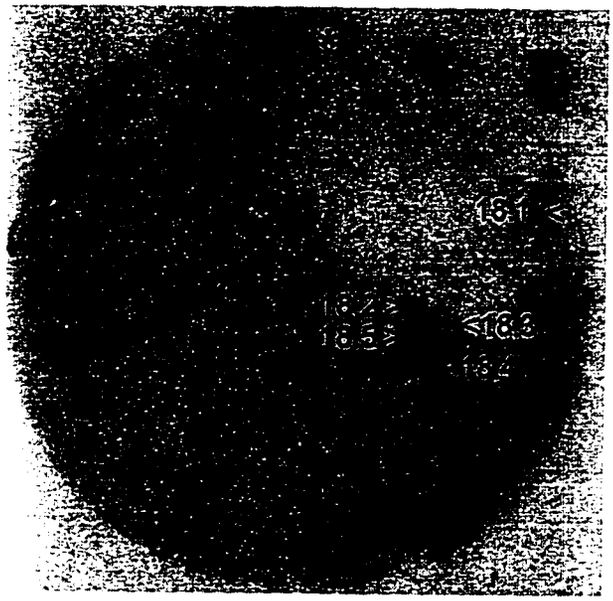

(A)

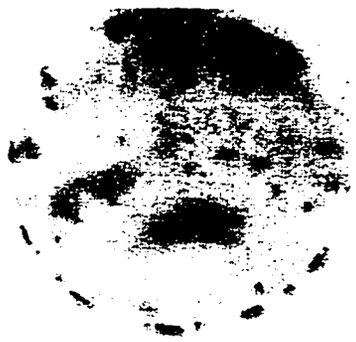

(B)

(C)

Figure 2-6. Amplification of the cDNA inserts performed on the positives picked from the secondary screening of the λgt10 library. (A) Gel of the PCR products. Lanes 1 through 10 contain the results of performing PCR on each of the purified clones. Lane 11 is a DNA standard, and lane 12 contains the zebrafish *dlx-2* fragment. Notice that not all samples produced products. Symbols: "<" = PCR product; "X" = spurious product produced in almost every lane; and "*" = primer dimers. (B) Southern blot of this gel. Notice that the products in lanes 1, 3, 4, 5, and 7 hybridized to the probe (mixture of the *dlx*-homeobox PCR clones). In addition, the probe bound to the zebrafish *dlx-2* cDNA fragment loaded into lane 12. Products in lanes 1, 3, 5, and 7 were successfully cloned into the pCRII cloning vector (Invitrogen). These products were later identified by sequence comparison as *msx-1*, *dlx-3*, *msx-1*, and *dlx-5* respectively.

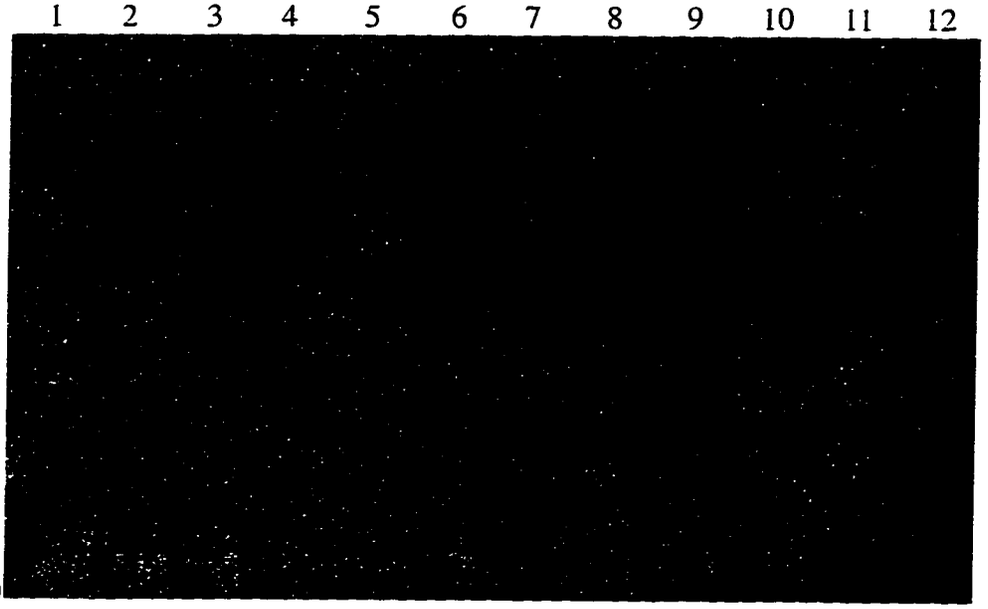

(A)

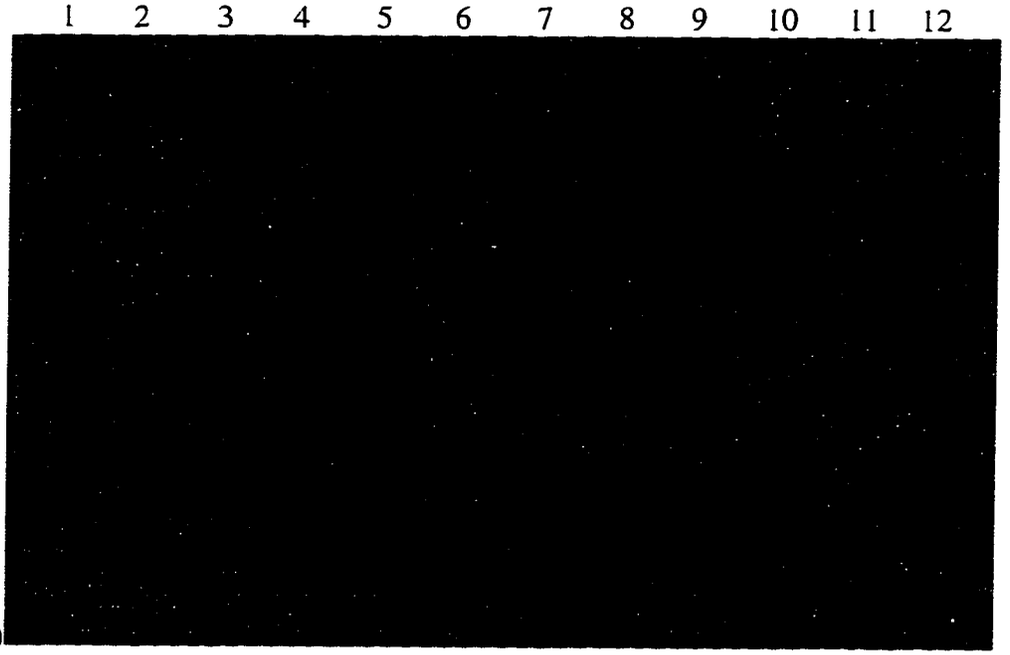

(B)

In the instances in which amplification of the cDNA insert was successful, the PCR produced individual bands (figure 2-6 (A), lanes 1, 3, 5, and 7). In addition, a spurious product of invariable size (marked by an "X" in lane 1, figure 2-6) was present in almost all reactions. Before band purification and subcloning of these products into pCRII vectors, the nature of these PCR fragments was tested by Southern analysis (figure 2-6 (B)). Southern analysis using a probe made from a mixture of the *dlx*-homeobox PCR fragments demonstrated that the PCR products in lanes 1, 3, 5, and 7 were sequences that contained homeoboxes.

In general, PCR succeeded in amplifying the cDNA insert for clones that were under 1800 bp in length (i.e.: *dlx-3*, *dlx-5*, *msx-2* and the smaller clone of *msx-1*). Anything larger failed to amplify. Consequently the phage containing the cDNA of interest had to be grown over night to produce enough phage particles so that the DNA could be extracted and digested with *Eco*RI to liberate the insert out of the phage DNA for subcloning. Figure 2-7 (A) shows a gel containing the products of *Eco*RI digestions on the remaining λgt11 clones that failed to have their inserts amplified by PCR. In this particular example not all digests yielded inserts (lanes 2, 4, 8, and 9) and consequently this approach had to be repeated for these clones. In the cases where *Eco*RI fragments were produced, the resulting bands were faint and are indicated by arrowheads adjacent to lanes (lanes 3, 5, 6, and 7; figure 2-7 (A)). As with the amplification of the cDNA inserts, the nature of these fragments was determined by Southern analysis. The results demonstrated that all *Eco*RI fragments contained homeoboxes when probed with the *dlx*-homeobox PCR fragments (figure 2-7 (B)). These fragments were subsequently band purified and subcloned into pBS KS+.

2.3.4 Sequence Data of the Axolotl *dlx* Clones

Once these clones were sequenced and the sequencing data was compared against sequences in the NIH databank (via BLASTn searches), we had cloned several axolotl homeobox genes: *dlx-3* (1 clone), *dlx-5* (1 clone), *dlx-7* (2 clones), *msx-1* (2 clones), *msx-2* (1 clone), *caudal* (2 clones), and a paired-box-like (*prd*) gene (1 clone).

Our axolotl *dlx-3* clone is 1269 nucleotides long (figure 2-8). Below the nucleotide sequence, the putative protein sequence is compared against the newt *NvHBox-4* (which is considered to be the *dlx-3* homolog in this species). The sequence of the newt *NvHBox-4*

Figure 2-7. *Eco*RI restriction digestion on λgt10 DNA from clones that failed to amplify their inserts during PCR. (A) Gel showing the results following *Eco*RI restriction digests on λgt10 DNA extracted from phage picked from the secondary. Only samples in lanes 3, 5, 6, and 7 contained inserts. These fragments are labelled a, b, c, and d respectively. In addition, an arrowhead points out these fragments since they are extremely faint. (B) Southern analysis of this gel using a probe made from a mixture of the *dlx*-homeobox PCR clones. Notice that all four samples hybridized to the probe. Following band purification and subcloning into pBS, these fragments were identified as *msx-2* (a), *caudal* (b), *dlx-7* (c), and *dlx-7* (d).

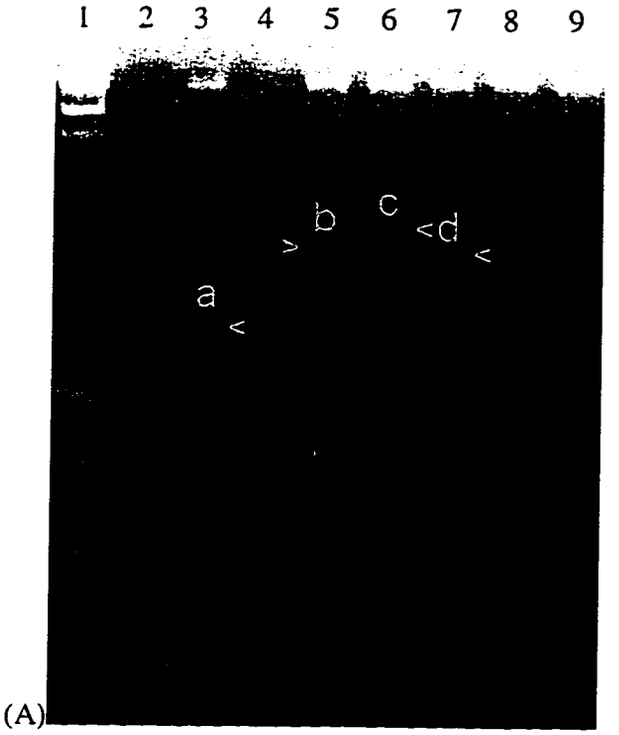

(A)

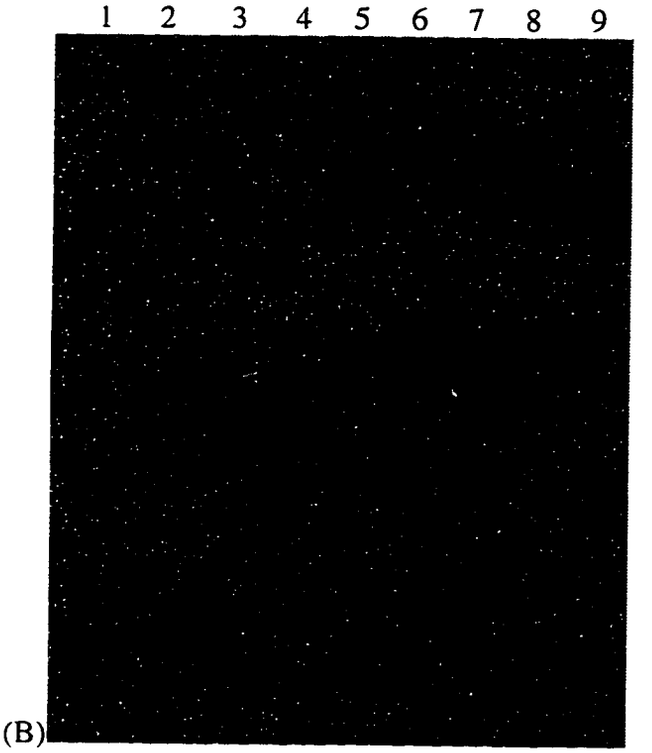

(B)

Figure 2-8. The axolotl *dlx-3* cDNA sequence. The *dlx-3* homeobox is highlighted in bold. Translation of its coding sequence is presented in uppercase, single letter code. Beneath this translation is the amino acid sequence of the newt *dlx-3* gene designated as *NvHBox-4* in the literature (Beauchemin and Savard, 1992). Conserved amino acid residues are indicated by a "•", and the termination amino acid is indicated by a "*".

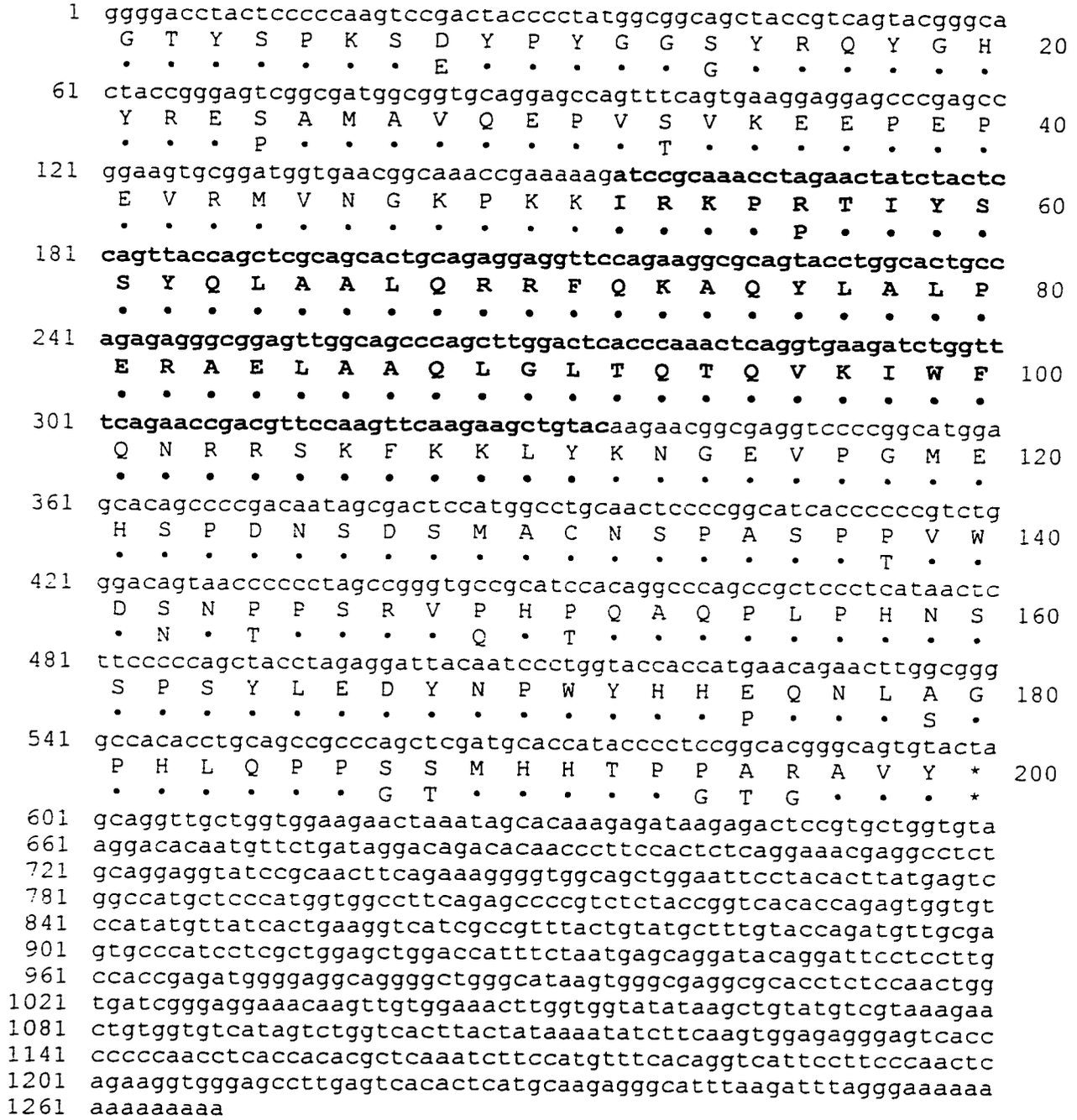
1 ggggacctactcccccaagtccgactaccctatggcggcagctaccgtcagtacgggca
G T Y S P K S D Y P Y G G S Y R Q Y G H 20
61 ctaccgggagtcggcgatggcggtgcaggagccagtttcagtgaaggaggagcccgagcc
Y R E S A M A V Q E P V S V K E E P E P 40
121 ggaagtgcggatggtgaacggcaaaccgaaaaagatccgcaaacctagaactatctactc
E V R M V N G K P K K I R K P R T I Y S 60
181 cagttaccagctcgcagcactgcagaggaggttccagaaggcgcagtacctggcactgcc
S Y Q L A A L Q R R F Q K A Q Y L A L P 80
241 agagagggcggagttggcagcccagcttggactcacccaaactcaggtgaagatctggtt
E R A E L A A Q L G L T Q T Q V K I W F 100
301 tcagaaccgacgttccaagttcaagaagctgtacaagaacggcgaggtccccggcatgga
Q N R R S K F K K L Y K N G E V P G M E 120
361 gcacagccccgacaatagcgactccatggcctgcaactccccggcatcacccccgtctg
H S P D N S D S M A C N S P A S P P V W 140
421 ggacagtaacccccctagccgggtgccgcatccacaggcccagccgctccctcataactc
D S N P P S R V P H P Q A Q P L P H N S 160
481 ttcccccagctacctagaggattacaatccctggtaccaccatgaacagaacttggcggg
S P S Y L E D Y N P W Y H H E Q N L A G 180
541 gccacacctgcagccgcccagctcgatgcaccataccctccggcacgggcagtgtacta
P H L Q P P S S M H H T P P A R A V Y * 200
601 gcaggttgctggtggaagaactaaatagcacaaagagataagagactccgtgctggtgta
661 aggacacaatgttctgataggacagacacaacccttccactctcaggaaacgaggcctct
721 gcaggaggtatccgcaacttcagaaaggggtggcagctggaattcctacacttatgagtc
781 ggccatgctcccatggtggccttcagagccccgtctctaccggtcacaccagagtggtgt
841 ccatatgttatcactgaaggtcatcgccgtttactgtatgctttgtaccagatgttgcga
901 gtgcccatcctcgctggagctggaccatttctaatgagcaggatacaggattcctccttg
961 ccaccgagatggggaggcaggggctgggcataagtgggcgaggcgcacctctccaactgg
1021 tgatcgggaggaaacaagttgtggaaacttggtggtatataagctgtatgtcgtaaagaa
1081 ctgtggtgtcatagtctggtcacttactataaaatatcttcaagtggagagggagtcacc
1141 cccccaacctcaccacacgctcaaatcttccatgtttcacaggtcattccttcccaactc
1201 agaaggtgggagccttgagtcacactcatgcaagagggcatttaagatttagggaaaaaa
1261 aaaaaaaaa

protein continues upstream beyond the sequence of the axolotl *dlx-3* and is not included in figure 2-8. Although there is an in-frame methionine residue at position 26, we do not believe this site to be the initation codon for two reasons. First, in the newt the *NvHBox-4* initiation codon is 71 residues upstream of the beginning of our *dlx-3* protein sequence. Since the newt is a cousin of the axolotl and therefore is separated by relatively short evolutionary distances, it is unlikely that the axolotl has a shorter *dlx-3* protein than the newt. Second, when the *dlx-3* sequences from numerous vertebrates are aligned (not shown), in all instances the methionine initiation residue and the length of the protein is highly conserved. Therefore, our axolotl *dlx-3* cDNA clone is probably a truncation of the full-length sequence. This conclusion is supported by the recent publication of the axolotl *dlx-3* clone by Mullen *et al.* (1996). Their sequence is identical to our own and contains the 5' region that is lacking in our clone. When Mullen *et al.*'s sequence is translated, it matches the length of the newt's *NvHBox-4* protein.

The axolotl *dlx-5* clone is 1193 bp long and its translated product is compared against the *Xenopus Xdll-3* protein which is considered to be the *Xenopus dlx-5* homolog (figure 2-9). Our axolotl *dlx-5* is probably truncated in the 5' region and is therefore missing part of the coding region. Although there are several in-frame methionines upstream of the homeodomain at amino acid positions 6 and 55, either one would produce a short *dlx-5* protein. In addition, the coding regions of both the *Xenopus* and chicken *dlx-5* genes continues further upstream beyond the axolotl *dlx-5* by 82 or 73 amino acid residues respectively. Therefore we believe that the sequence of axolotl *dlx-5* gene is incomplete, missing part of its coding region 5' to the homeodomain.

Two clones of the axolotl *dlx-7* gene were isolated from different plates during the primary screening. Sequencing revealed that they were identical in sequence and length and are therefore copies of one another. The axolotl *dlx-7* clone is 2100 bp[2] long, with the putative coding region encoding 245 or 241 amino acids depending on which methionine is the initiator codon (figure 2-10). Either start codon meet some of the sequence criteria of an initiator codon as described by Kozak's rule (Kozak, 1986). Both triplets are printed in bold and underlined in figure 2-10. The sequences of the first (ATCATGA) and the second (TCTATGG) initator codon are in-frame with a stop codon but are in poor agreement with the optimal sequence (Kozak's

[2] Part of the 3'UTR remains to be sequenced and therefore the exact size of this clone is not known.

Figure 2-9. The axolotl *dlx-5* cDNA sequence. Its homeobox is highlighted in bold. A possible polyadenylation site is underlined. The putative axolotl *dlx-5* protein is displayed in uppercase, one letter code, and it is compared against its *Xenopus* homolog (*Xdll-3*)(Papalopulu and Kintner, 1993). Conserved amino acid residues between the axolotl and *Xenopus* sequence are indicated by a "•", and the termination amino acid is indicated by a "*".

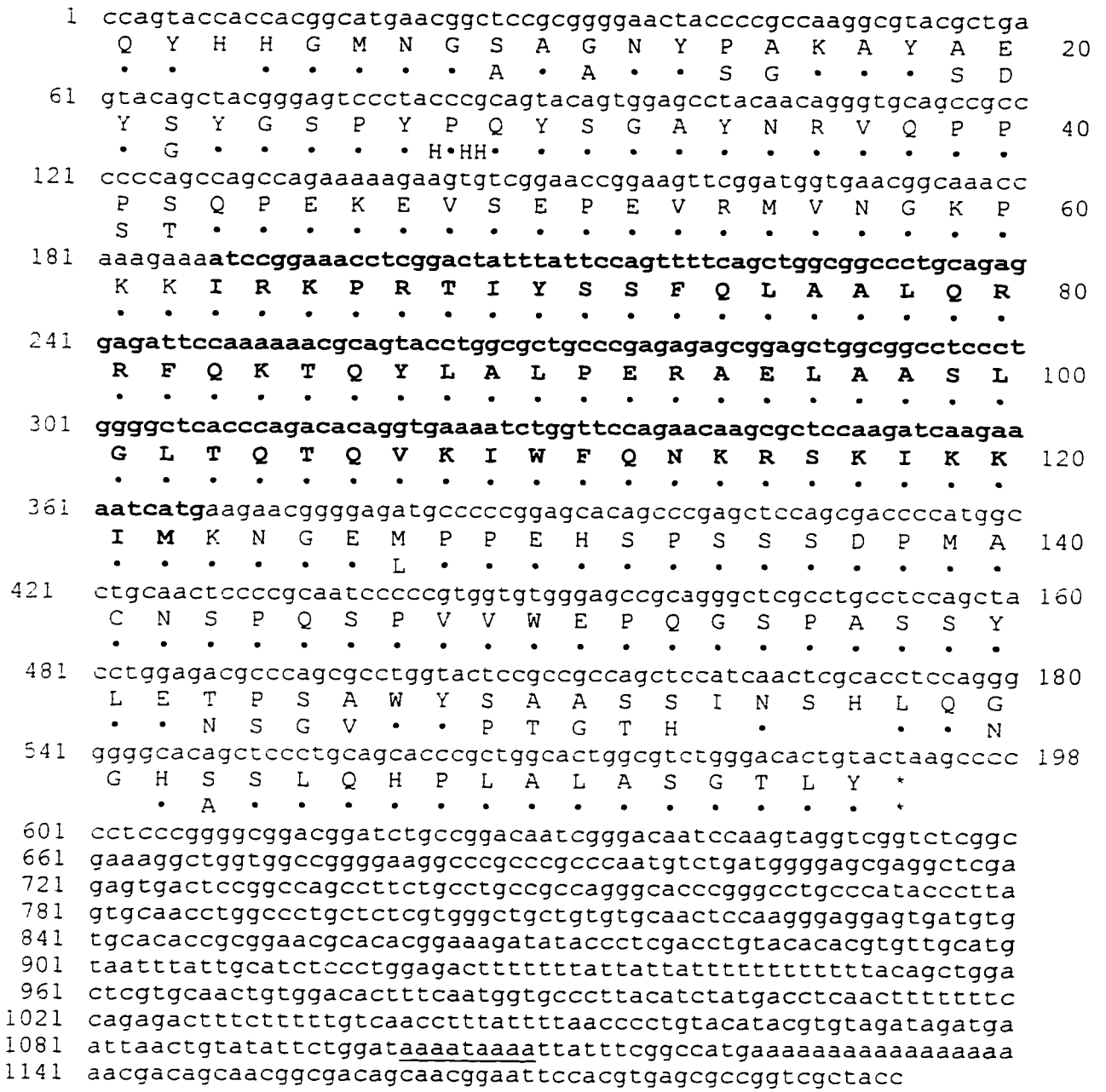
1 ccagtaccaccacggcatgaacggctccgcggggaactaccccgccaaggcgtacgctga
Q Y H H G M N G S A G N Y P A K A Y A E 20
• • • • • • • A • A • • S G • • • S D
61 gtacagctacgggagtccctacccgcagtacagtggagcctacaacagggtgcagccgcc
Y S Y G S P Y P Q Y S G A Y N R V Q P P 40
• G • • • • • H•HH• • • • • • • • • • •
121 ccccagccagccagaaaaagaagtgtcggaaccggaagttcggatggtgaacggcaaacc
P S Q P E K E V S E P E V R M V N G K P 60
S T • • • • • • • • • • • • • • • • • •
181 aaagaaaatccggaaacctcggactatttattccagttttcagctggcggccctgcagag
K K I R K P R T I Y S S F Q L A A L Q R 80
• • • • • • • • • • • • • • • • • • • •
241 gagattccaaaaaacgcagtacctggcgctgcccgagagagcggagctggcggcctccct
R F Q K T Q Y L A L P E R A E L A A S L 100
• • • • • • • • • • • • • • • • • • • •
301 ggggctcacccagacacaggtgaaaatctggttccagaacaagcgctccaagatcaagaa
G L T Q T Q V K I W F Q N K R S K I K K 120
• • • • • • • • • • • • • • • • • • • •
361 aatcatgaagaacggggagatgcccccggagcacagcccgagctccagcgaccccatggc
I M K N G E M P P E H S P S S S D P M A 140
• • • • • • • L • • • • • • • • • • • •
421 ctgcaactccccgcaatcccccgtggtgtgggagccgcagggctcgcctgcctccagcta 160
C N S P Q S P V V W E P Q G S P A S S Y
• • • • • • • • • • • • • • • • • • • •
481 cctggagacgcccagcgcctggtactccgccgccagctccatcaactcgcacctccaggg 180
L E T P S A W Y S A A S S I N S H L Q G
• • N S G V • • P T G T H • • • N
541 ggggcacagctccctgcagcacccgctggcactggcgtctgggacactgtactaagcccc 198
G H S S L Q H P L A L A S G T L Y *
• A • • • • • • • • • • • • • • • *
601 cctcccggggcggacggatctgccggacaatcgggacaatccaagtaggtcggtctcggc
661 gaaaggctggtggccggggaaggcccgcccgcccaatgtctgatggggagcgaggctcga
721 gagtgactccggccagccttctgcctgccgccagggcacccgggcctgcccataccctta
781 gtgcaacctggccctgctctcgtgggctgctgtgtgcaactccaagggaggagtgatgtg
841 tgcacaccgcggaacgcacacggaaagatataccctcgacctgtacacacgtgttgcatg
901 taatttattgcatctccctggagacttttttttattattatttttttttttacagctgga
961 ctcgtgcaactgtggacactttcaatggtgcccttacatctatgacctcaacttttttttc
1021 cagagactttctttttgtcaacctttatttttaacccctgtacatacgtgtagatagatga
1081 attaactgtatattctggataaaataaaattatttcggccatgaaaaaaaaaaaaaaaaa
1141 aacgacagcaacggcgacagcaacggaattccacgtgagcgccggtcgctacc

Figure 2-10. The axolotl *dlx-7* cDNA sequence. There exists two possible initiation codons which are underlined and highlighted in bold. We propose that the first putative initiation codon is the correct one since it maintains a translated product that is similar to its newt counterpart and it is in partial agreement with Kozak's rule regarding initiation codes (see text for further details). The translation of the axolotl *dlx-7* protein is depicted in uppercase, single letter code. Beneath it is the newt *NvHBox-5* protein (which is considered to be *dlx-7* by virtue of its sequence similarity to other vertebrates *dlx-7* genes)(Beauchemin and Savard, 1992). Conserved amino acid residues are indicated by a "•", and the termination amino acid is indicated by a "*".

```
   1 gttgctgtcgggctgcaggacgaggcaccggagcagagcgggccccatggagtccgctgg

                                                A  P  H  G  A  C  Q  T  S  G
  61 cccccacgcatcatgagcggttctatggccgagagcctgctgggctcagaccactccaaa
                     M  S  G  S  M  A  E  S  L  L  G  S  D  H  S  K   16
     T  L  R  S  .  .  .  .  .  .  .  .  .  .  .  .  .  .  .  .  .
 121 gccgcctttctggacttcgggccaggcagccgctcgccgcagagccactacccccctgcac
     A  A  F  L  D  F  G  P  F  S  R  S  P  Q  S  H  Y  P  L  H   36
     .  .  .  .  E  .  .  T  G  T  H  .  .  .  G  .  .  .  .  .
 181 ggcttccacaaccccgccgatgggccatacgggggctcgggctatggggcgacgaccctg
     G  F  H  N  P  A  D  G  P  Y  G  G  S  G  Y  G  A  T  T  L   56
     .  .  .  P  .  .  .  .  .  .  .  .  .  .  .  G  R  .  .
 241 ggttacccctacagccctcacggacacacgcagcaccatggcagtgcttacctgccctac
     G  Y  P  Y  S  P  H  G  H  T  Q  H  H  G  S  A  Y  L  P  Y   76
     .  .  .  .  .  .  .  .  .  .  P  .  .  .  A  .  P  .  .  .  .
 301 caccaggggcagcatggaggggtcttggacacgggagcagcagcctgcaggaggaggca
     H  Q  G  Q  H  G  G  G  L  G  H  G  S  S  S  L  Q  E  E  A   96
     .  .  .  .  .  .  .  .  S  .  .  .  .  G  .  R  .  D  .  D  T
 361 gacgtggacaaaaacacggtgatagaaaacagtgagatccgaatcaatggcaaaggcaaa
     D  V  D  K  N  T  V  I  E  N  S  E  I  R  I  N  G  K  G  K  116
     E  L  E  K  .  .  .  .  .  .  .  G  .  .  .  .  .  .  .  .  .
 421 aaaatccgcaaaccacgcaccatttactccagcgtgcagctgcaggccctgaaccaacgc
     K  I  R  K  P  R  T  I  Y  S  S  V  Q  L  Q  A  L  N  Q  R  136
     .  .  .  .  .  .  .  .  .  .  .  .  .  .  .  .  .  .  .  .  .
 481 ttccagcagacgcagtacctggcgctgcgggagagggcggacgtggcggcacacctcggc
     F  Q  Q  T  Q  Y  L  A  L  R  E  R  A  D  V  A  A  H  L  G  156
     .  .  .  .  .  .  .  .  .  .  P  .  .  .  E  L  .  .  .  .  .
 541 ctcactcaaacccaggtcaagatttggtttcagaacaaaaggtcaaagtacaagaaaatc
     L  T  Q  T  Q  V  K  I  W  F  Q  N  K  R  S  K  Y  K  K  I  176
     .  .  .  .  .  .  .  .  .  .  .  .  .  .  .  .  .  .  .  .  .
 601 atgaagcagggctccagtgtccaggaagggaccaacctccacacgtctgcttccatgtcg
     M  K  Q  G  S  S  V  Q  E  G  T  N  L  H  T  S  A  S  M  S  196
     .  .  .  .  .  .  .  I  .  .  .  E  H  .  .  S  .  .  .  .  .
 661 ccctgttcgcccaaaattctccctcactgggacagccccatgcagttaaaggggtccct
     P  C  S  P  K  I  L  P  H  W  D  S  P  M  Q  L  K  G  V  P  216
     .  .  .  .  N  .  P  .  .  .  .  .  .  .  G  T  .  .  G  .
 721 attggacatggcagctacatgaacaactatggggcctggtaccagcctcaccacccagac
     I  G  H  G  S  Y  M  N  N  Y  G  A  W  Y  Q  P  H  H  P  D  236
     .  .  .  .  .  .  I  .  .  .  .  P  .  .  .  .  .  .  Q  .
 781 agcatgccaaggccccaaatgatgtgatggtgccttcttggtaaacccaccagtcgtggc
     S  M  P  R  P  Q  M  M  *                                    244
     .  .  .  .  .  .  .  .  *
 841 ctggtcgtagccctgcctggcagacca (approximately 300 n.t. gap)
     cctcctgccaccgcagccatagaaacgttgatttctgatggataaggcacgcttgttgtc
     gtgtacctgcagcncttcctccctgggaggtaggcccctctgaaggcccacaagaagcaa
     gagagcagccctcatccgcccgcctgtttacaacgagttcaaaagcctcagggcgcagag
     gctcaccccggccctcaacacagaccttcaaaggggcagagtgtcttgttttctcttcag
     ttttaaaccatgaaagatgaacgttttcatggccggtgtgtggctgtccatctcgaactc
     atcactttgtgattaatttaacccgtttcctctgccttttaaggaggagttatttataa
     gaaaaatcattttgatattgtattgtatgtctttatataaaaagaggactgggcacgctg
     tagacttgcgtgcaactttgtttttatatttgtacagatgtatttcgtaggccacctatt
     gtatttttaaattctcacgtaggactggcccctaccaactttgtcatgaaattcgactg
     aggattcgaagccatattgcaggacccttccatgtcctagagtgggggtgaggggggcg
     gtcagggttgctgtccatccacaccactcttttcttccccgaataatccggttcgggtca
```

tattgcaaacaaaactgctccagaaaagaccggaatttgccagtatccttattttggttt
gatattgtgttatcctaaaggcgtttcaatgttgctagcctggttccaacatcataacca
aattaaaaatccaactgaactctccgacagcaacggaattcgatatcaagcttatcgata
ccgtcgacctcgaggggagccc

rule: ACCATGG). However, the first triplet is probably the actual start codon for the axolotl *dlx-7* coding sequence because when it is compared with the newt *NvHBox-5* amino acid sequence (considered *dlx-7* by sequence homology) the identical residues are conserved up to this site (figure 2-5). If we proceed further upstream, translation of the axolotl sequence is completely different than the newt's amino acid sequence. Thus, we argue based on the high level of conservation of amino acid sequence between the newt and the axolotl that the first methionine codon is the putative start site for translation.

2.3.5 Additional Axolotl Homeobox-Containing Genes were Cloned

Out of the ten positive clones from the secondary screening of the λgtll library we isolated clones for *msx-1*, *msx-2*, *caudal*, and a *prd*-like sequences when using the *dlx* homeobox fragments to screen the library. Here, we report the sequencing data for *msx-1*, *msx-2*, *caudal* and the *prd*-like cDNA clones.

Two clones of different lengths were isolated for the *msx-1* gene. The sequence and translation of the longer clone is presented in figure 2-11. This clone is 1845 nucleotides long and has an open reading frame that codes for a protein which is 284 amino acids long. The shorter clone is 1388 nucleotides long, and it is missing most of the coding region upstream of the homeodomain. The translation of the axolotl *msx-1* coding sequence is compared against the newt *msx-1* (figure 2-11). With the exception of a leucine subsituted in place of a phenylalanine in the axolotl homeodomain, the newt and axolotl homeodomain are identical. In the region upstream of the homeodomain, the amount of conservation between the newt and the axolotl is moderate at 61%, whereas in the shorter, region downstream of the homeodomain, the conservation is high at 94%.

The axolotl *msx-2* clone is 1369 nucleotides long (figure 2-12). The entire sequence appears to have numerous errors since it is difficult to find a single frame which codes for the correct protein sequence when compared to the *msx-2* protein sequences of other vertebrates. The mouse *msx-2* protein is compared against the coding region of the axolotl *msx-2*, yet there are many areas where it is difficult to determine the axolotl protein sequence. This problem is not easily resolved by the addition of a gap or the deletion of a nucleotide. Either approach does not yield a recognizable coding sequence with respect to other *msx-2* sequences. Both the highly

Figure 2-11. The axolotl *msx-1* cDNA sequence. Two clones of different lengths were isolated. This figure is the sequence of the longer clone. The axolotl initiation codon is highlighted in bold whereas a second possibility is double-underlined. The axolotl *msx-1* homeobox is highlighted in bold. A possible polyadenylation sequence is underlined. The axolotl *msx-1* protein is depicted in uppercase, single letter code with the newt *msx-1* amino acid coding sequence below it (Crews *et al.*, 1994). Conserved amino acid residues are indicated by a "•", and the termination amino acid is indicated by a "*".

```
   1 cgttgctgtcgctgatctgccctgtgtgatcctgctccccgtgccgcccggtcatccaca
  61 cgggaccagctctgcatggccccggtctatacatggcttctgtccagctcggagtgaag
                     M  A  P  G  L  Y  M  A  S  V  Q  L  G  V  K    15
                     .  .  .  .  .  .  .  .  .  .  .  .  .  .  .
 121 gccgaggagtcgcccgtcctaagcaagcagaggatgcagaccggcctgagctccggggcg
     A  E  E  S  P  V  L  S  K  Q  R  M  Q  T  G  L  S  S  G  A    35
     .  .  .  F  .  A  .  N  E  P  .  .  H  P  .  .  .  P  R  .
 181 gacgaggagccccagaaacccaagctgccggccatcctgccatttagcgtggaggccctc
     D  E  E  P  Q  K  P  K  L  P  A  I  L  P  F  S  V  E  A  L    55
     .  .  .  .  D  .  .  .  P  A  P  .  .  .  .  .  .  .  .  .
 241 atggctgaccgcaggccgacggtcagagaccgtgagcggtgcagccccgcggggacccag
     M  A  D  R  R  P  T  V  R  D  R  E  R  C  S  P  A  G  T  Q    75
     .  .  .  .  .  .  .  V  I  .  .  .  .  .  .  .  .  A  P  P
 301 ctgcccgggccctcgcaaaccagccccaggctagggggcacctctcaggaccggagccc
     L  P  G  P  S  Q  T  S  P  R  L  G  G  H  L  S  G  P  E  P    95
     .  .  .  .  .  .  .  .  .  .  K  M  L  .  P  E  .           .
 361 ctggatccgctctccatgaacagacactattccatgggtggcttactgcacttacaggaa
     L  D  P  L  S  M  N  R  H  Y  S  M  G  G  L  L  H  L  Q  E   115
     N  S  .  .  .  T  .  K  .  .  .  .  .  .  .  .  .  .  .  .
 421 gaggctcttgcgaagccggagagcccggacagccaggagaggaacccgtggatgcagagc
     E  A  L  A  K  P  E  S  P  D  S  Q  E  R  N  P  W  M  Q  S   135
     .  .  .  M  .  P  .  .  .  E  G  .  R  G  A  H  G  P  E
 481 cccaaattctccccaccctcagcaaggaggctgagcccaccggcctgcactctccggaag
     P  K  F  S  P  P  S  A  R  R  L  S  P  P  A  C  T  L  R  K   155
     .  .  R  .  .  .  .  .  .  .  .  .  .  .  .  .  .  .  .  .
 541 cacaagaccaaccggaagccgcggacgccgttcaccacgtcgcagctgctggccctggag
     H  K  T  N  R  K  P  R  T  P  F  T  T  S  Q  L  L  A  L  E   175
     .  .  .  .  .  .  .  .  .  .  .  .  .  .  .  .  .  .  .  .
 601 cggaagttccggcagaagcagtacctgtccatcgcggagcgcgccgagttctcgggctcc
     R  K  F  R  Q  K  Q  Y  L  S  I  A  E  R  A  E  F  S  G  S   195
     .  .  .  .  .  .  .  .  .  .  .  .  .  .  .  .  .  .  .  .
 661 ctcagcctgaccgagacgcaggtcaagatctggttccagaaccgccgcgccaaggccaag
     L  S  L  T  E  T  Q  V  K  I  W  F  Q  N  R  R  A  K  A  K   215
     .  .  F  .  .  .  .  .  .  .  .  .  .  .  .  .  .  .  .  .
 721 cggctgcaggaggccgagctggagaagctcaagatggccgccaagcccatgatgccgccg
     R  L  Q  E  A  E  L  E  K  L  K  M  A  A  K  P  M  M  P  P   235
     .  .  .  .  .  .  .  .  .  .  .  .  .  .  .  .  .  .  .  .
 781 gccttcggcatctccttccccctcggctctccagtgcacgcggcctccctgtacgggccc
     A  F  G  I  S  F  P  L  G  S  P  V  H  A  A  S  L  Y  G  P   255
     T  .  .  L  .  .  .  .  .  .  .  .  .  .  .  .  .  .  .  .
 841 tccggcccctccacagacccagcatgcccatgtcgcccatgggactgtacgccgctcac
     S  G  P  F  H  R  P  S  M  P  M  S  P  M  G  L  Y  A  A  H   275
     .  A  .  .  .  .  S  .  .  .  .  .  .  .  .  .  .  .  .  .
 901 atgggctacagcatgtaccacctgacataagggcgccgcagacccaccacagaccattca
     M  G  Y  S  M  Y  H  L  T  *                                  284
     V  .  .  .  .  .  .  .  .  *
 961 tgcagcacttttctgatgttgggccctgcccacgtctgccattggtggcactcaggcatg
1021 catgccaaccacgttggaaagaaccgagagcgtgattcggtggcaggaagagggggttg
1081 tgcatgcccattggctctcatcgcaatgaaggaacgctatgccaggcattgcacacctttt
1141 aacaagttgaacaaggacaatgttttgtgtcgtgaaggagcgcctcccacttctgaataa
1201 tagagagatggcatgtgtgcaccagcctgaaatacgccaggcgttttggattttcacagt
1261 gtgttcaacacctgtagagggaactgaaacatatttgtgagaagttcacgtttggacata
```

```
1321  cagttcctcacacgtggtttacagaaaagtccagcatttcagcagctcaacctggctcag
1381  caccattcaatacagaaagcccgacatcttgttgtatggccgcatgaattagttcacatc
1441  accgggaaatgtcatgagttctaagaagatgacttttttataaataaagcgctatcgaaaa
1501  tgctcctcaaaagtgccaccagacacacgtggaaaggcaacagaacttgtcaacgaatca
1561  ctgtgcttcactgtttcccttgcgtgtggatgttcctacactcgtcccttgggagcaggg
1621  gatccgtactatgtaatatactgtatatttgaaaaaaatattatcatttatattatagct
1681  atatttgttaaataaattaattttaagctaaaacaaaaaaaaaacgacaaacggaattcag
1741  tgagcgccgtcgctaccataccagttggctggtgtcaaaataataaccggcaggcctg
1801  tctaagccaattctgcagtatccatcacctgcggccgccgagcat
```

Figure 2-12. The axolotl *msx-2* cDNA sequence. Gaps had to be introduced into the sequence during translation so that it the protein sequence would be similar to its mouse homolog (Monaghan *et al.*, 1991). There are many areas where the introduction of a single gap does not translate the sequence into a recognizable amino acid sequence comparable to other vertebrate *msx-2* proteins. Consequently these areas are left untranslated. The homeobox is highlighted in bold. Partial translation of the axolotl sequence is presented in single letter, uppercase code whereas the entire mouse *msx-2* amino acid sequence is below it. Conserved amino acid residues between the axolotl and mouse sequence are indicated by a "•", and the termination amino acid is indicated by a "*".

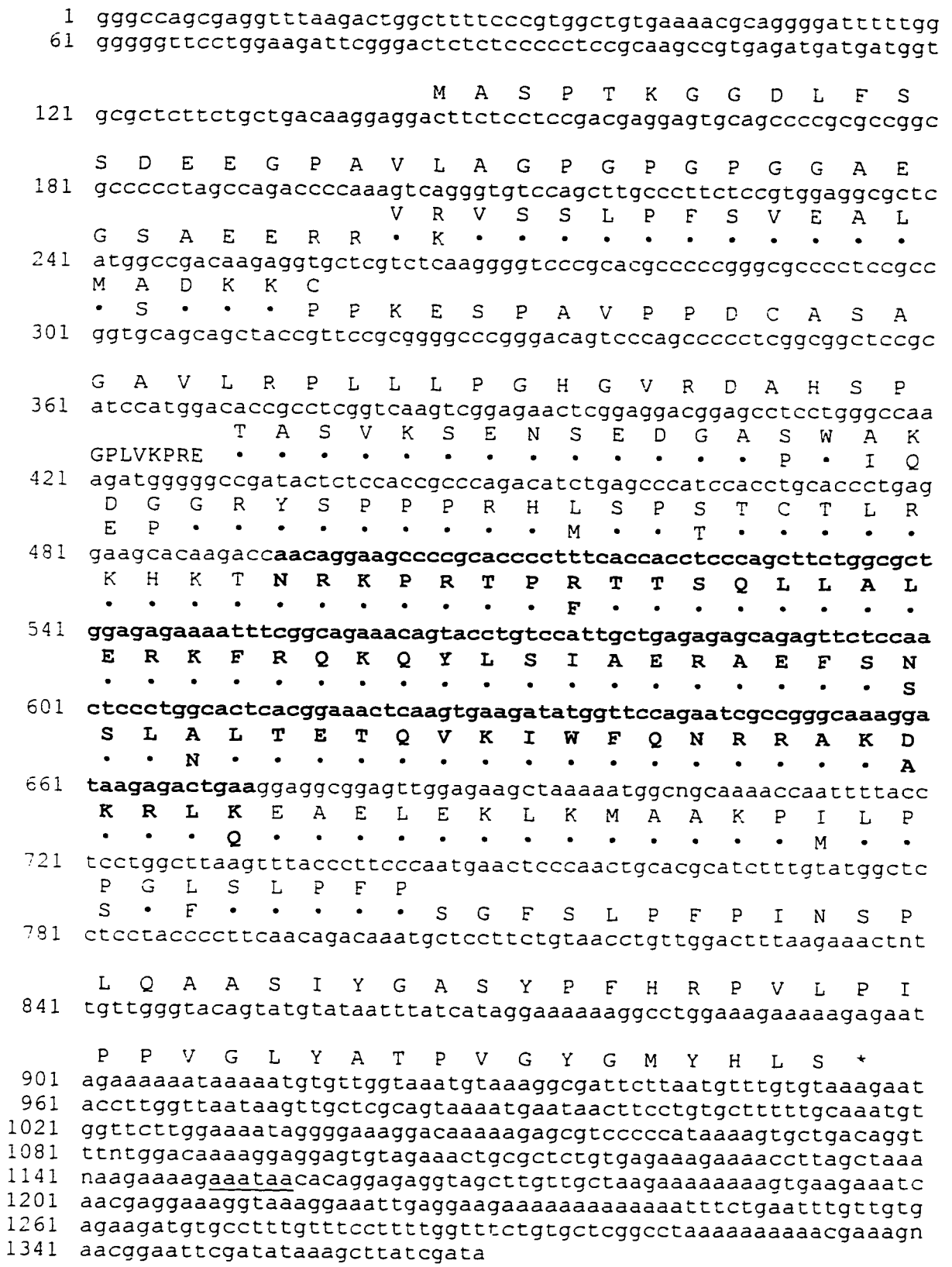

conserved decapeptide (LPFSVEALMS) and the *msx-2* homeodomain are clearly distinguishable, however, regions upstream and downstream of these areas are unrecognizable compared to *msx-2* proteins from other species. These differences cannot be explained due to evolutionary distances since comparisons of the *msx-2* protein sequences between vertebrates that are separated by large distances, such as chicken and mouse, reveal few dissimilarities.

The axolotl *caudal* cDNA clone is approximately 2000 nucleotides long and its putative protein sequence is compared against the chicken *caudal* protein (figure 2-13). There is an open reading frame that starts at nucleotide position 338, however, this would code for a very short protein that would place the homeodomain uncharacteristically close to the NH_2 terminus. Thus, based on its comparison with the chicken homolog, we believe that most of the coding region is present except for the region that includes the probable start codon.

Comparsion of the *caudal* homeodomains between axolotl and chicken reveals that they are well conserved (figure 2-13). However, each homeodomain contains an insert of an amino acid pair in a noncorresponding region of the homeodomains. The chicken *caudal* homeodomain has an insertion of a threonine-aspartic acid pair following the 8th amino acid residue of the homeodomain. Whereas the axolotl *caudal* homeodomain has an insertion of a lysine-glutamine pair after the 17th amino acid residue of the homeodomain. Both of these differences occur before the region of the homeodomain which codes for the third α helix which is the DNA recognition helix (Wright *et al.*, 1989). Since the coding of this third α helix region remains identical between these two vertebrates, the differences 5' of this area are probably attributed to the evolutionary time that separates these animals. The sequence upstream of the homeodomain is poorly conserved between these two species (41%), unlike the region downstream of the homeodomain which is moderately well conserved (63%).

The axolotl *prd*-like cDNA clone is approximately 2000 nucleotides long (figure 2-14). Its actual identity is difficult to establish. Different regions of its nucleotide sequence showed similarity to different gene families when they were sent on BLAST searches. Portions of its sequence showed similarities to the rat and mouse *Otx1*, the rat *Arix1* homeodomain, the zebrafish and *Xenopus pax-6* mRNA, and the mouse homeobox gene S8 mRNA. Since a region of this clone shared the highest degree of similarity with the mouse homeobox gene S8 homeodomain (Opstelten *et al.*, 1993; accession number g90640), it is compared against this

Figure 2-13. The axolotl *caudal* cDNA sequence. The entire homeobox is highlighted in bold. A possible polyadenylation sequence is underlined. The axolotl *caudal* protein is depicted in uppercase, single letter code. Its chicken *caudal* homolog is compared below it (Frumkin *et al.*, 1991). Conserved amino acid residues between the axolotl and chicken sequence are indicated by a "•", and the termination amino acid is indicated by a "*".

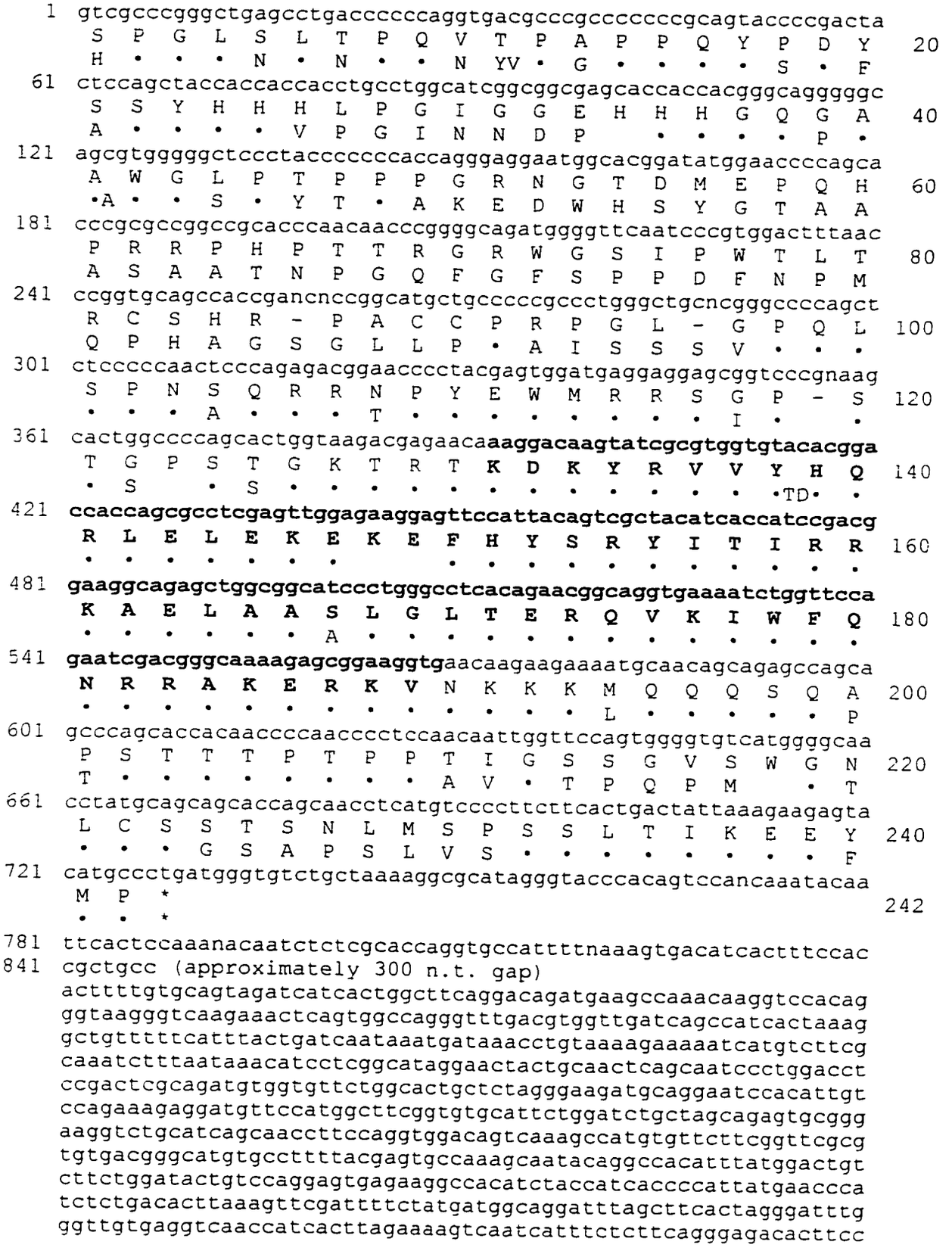

agaccacatccaattttgtattgttatcactttaaatcaccaaaaatctgaattgtcttt
acaaatgttactggggaaattgtaatggttcattgaaaacgtcaaacattgtgttatttt
tgcattgtatggttttgaaaaagcgataggattgtcacccctaagagtatcttcacccc
cggctgtacagataaactatacggaggtgcctcccataccatcaataaacaa

Figure 2-14. An axolotl *prd*-like cDNA sequence. Its putative translated product is compared against the mouse homeotic gene S8 (Opstelten *et al*., 1993; accession number g90640). The homeodomain regions of both of these proteins are similar; however, the areas upstream and downstream of this region are poorly conserved. Conserved amino acid residues are indicated by a "•". A possible polyadenylation sequence is underlined.

```
   1 gttgctgtcgcgcgaccgaagcagacgacacagcagccccaggtcccgcagctgggggggc
      L  L  S  R  D  R  S  R  R  H  S  S  P  R  S  R  S  W  G  A
  61 ctccgagatggagggcttcgaagagagcttcggcagcccccctccgaggaggcctgagcc
      S  E  M  E  G  F  E  E  S  F  G  S  P  P  P  R  R  P  E  P
 121 ccggcctgtcccctccagcgacggcaagggctcgaggaggacgcgcaagaagaagcaccg
      R  P  V  P  S  S  D  G  K  G  S  R  R  T  R  K  K  K  H  R
                        •  C  P  S  P  G  •  •  •  •  •  •  Q  •
 181 gcgcaaccgcaccaccttcaccagcttccagctgcaggagctggagcgcgccttcgagag
      R  N  R  T  T  F  T  S  F  Q  L  Q  E  L  E  R  A  F  E  R
      •  •  •  •  •  •  N  •  S  •  •  •  A  •  •  •  V  •  •  •
 241 atcccactacccggacgtgtacagccgcgaggagctggcgctcaaggtcaacctgcccga
      S  H  Y  P  D  V  Y  S  R  E  E  L  A  L  K  V  N  L  P  E
      T  •  •  •  •  A  F  V  •  •  •  •  •  R  R  •  •  •  S  •
 301 agtgcgcgtgcaggtctggttccagaacagaagagcgaaatggagaaggcaggagaagct
      V  R  V  Q  V  W  F  Q  N  R  R  A  K  W  R  R  Q  E  K  L
      A  •  •  •  •  •  •  •  •  •  •  •  •  F  •  •  N  •  R  A
 361 tgaggtcacctcaatgaagctgcaggaccaccaatcctatccttcaacaggtccccccag
      E  V  T  S  M  K  L  Q  N  H  Q  S  Y  P  S  T  G  P  P  S
      M  L  A  T  R  S  A  S  L  L  K  •  •  G  Q  E  A  A  I  E
 421 tccatccaccatgggtccgttgagtagcaacctctccctagagtcctggcttaacccgcc
      P  S  T  M  G  P  L  S  S  N  L  S  L  E  S  W  L  N  P  P
      Q  P  V  A  P  R  P  T  T  M  S  P  D  Y  •  •  P  A  S  S
 481 gttgcccagcagcgccccttacagaccctgccaggattcatgggctcaccacagaacct
      L  P  S  S  A  P  L  Q  T  L  P  G  F  M  G  S  P  Q  N  L
      S  •  •  •  S  V  P  P  Y  S  •  •  G  S  S  P  A  T  P  G
 541 tcccagtagctacaccccacctcccttcatgaactcaaccccatgtcccacaacctgca
      P  S  S  Y  T  P  P  P  F  M  N  S  T  P  M  S  H  N  L  Q
      V  N  M  A  N  S  I  A  S  L  R  L  K  A  K  E  F  S  •  H
 601 gcctatcggggccatgggaatgggctcctccaccataccagtgtggggcaattttatgga
      P  I  G  A  M  G  M  G  S  S  T  I  P  V  W  G  N  F  M  D
      H  S  Q  V  P  T  V  N
 661 caagttcccccct(approximately a 400 bp gap)
      K  F  P
tggcaacccatggcaatatatgactggcagctgtatgcaactgtggagcaaatgtatatg
ggggacacattgccaacgtggacacacggggcaatctatggcaaacagtggcagtaacct
gactccataggcccctttgacaagcaatggtcgataatggggctaacccgaaagggtaac
gcaagcccgggtgacagtgtagttaggcgggaactttcgcaaaccagggcaagaccgtca
tacgaaataagcaccagctaaagataaaaaaaagactccatctcgggacaaatttaagtt
taatcgatacacagacagcactgatctatgataattgtttagttctgtgtgtatttctca
tctgcgtttttgtgcaccactgtcttgttccgatatgatacttgctgttcatttattgat
gtatagttctacattatttatctgtgatgtttttgggttactctgcagtcaccaagagtc
cctctctttcggttcccagcattggtggcagactctgtaaaatgattctttttctttat
gtacctatctgatattatatcctgcaagtcttcattactggcaggactggtcatcaattt
ctttaaagttagcaaccatctatgaaatgcccagccaatcacgcgtcgcacagagagcaa
ccatctatgaaatgcccagccattcacgcgtcacacagagagcaaccatctatgaaatgc
ccagccaatcacgcgtgcacagagggcaccggaagtatgaatctgaaggacttttttaa
ttgtcagtattatttacttcttagatttatttttactttgtgaagccccaagtatttctac
taaatgtttaattcttaatatgattctcacattaggatttacgaactgattatttttcta
aataaagatccgtttaaaaatcaaaaaaaaaaaa
```

sequence in figure 2-14. The coding sequence of the mouse homeobox gene S8 is similar to that of the *Prx-2* protein of chicken (a paired box gene), and therefore this axolotl cDNA clone has been temporarily called a *prd*-like gene.

Outside of the putative *prd*-like homeodomain, the level of protein sequence similarity with the mouse is very poor and argues that this cDNA clone is not related to the mouse homeobox gene S8. However, similar pairwise comparisons against *Otx1*, *Arix1* and *pax-6* produced fewer sequence similarities. Therefore, it is quite possible that this cDNA clone represents a new unidentified homeobox gene, or more likely, as with the *msx-2* cDNA clone, there are sequencing errors that make the determination of its identity difficult. Consequently, the actual identity of this clone is not known. We can only speculate based on the presence of a homeobox and its similarity to *Otx*, *pax* and *prd*-like sequences that it is possibly a member of one of these families.

2.3.6 Phylogenetic Analysis of *dlx* Sequences

Phylogenetic trees were constructed for the *dlx* homeoboxes and their homeodomains to see if the resulting trees would support the evolutionary history of these genes as proposed by Stock *et al.* (1996). In addition to the axolotl *dlx* cDNA clones, the *dlx* PCR fragments were included in this analysis to see how they would fit into the overall topology of the trees.

Stock *et al.* (1996) produced trees whose topologies and bootstrap values support six groups of vertebrate *Dlx* genes with each group containing a single type of mammalian *Dlx* gene. Based on the topology of their trees, they suggested that the six groups divide into two major clades that are each monophyletic because of their linkage arrangements. One clade is composed of *Dlx2*, *Dlx3*, and *Dlx5*; whereas, the other clade contains *Dlx1*, *Dlx6*, and *Dlx7*. However, the relationships of the groups within each clade remained unclear because of the low bootstrap values and the different tree topologies that exist between the two trees that they discussed.

In figure 2-15, a tree constructed with *dlx* homeobox sequences and the Neighbor-Joining algorithm has a topology that partially supports the two clades proposed by Stock *et al* (1996). Members of *dlx-2*, *dlx-3*, and *dlx-5* group together into one clade while members from *dlx-1*, *dlx-6* and *dlx-7* could be grouped into a second clade, however, these three orthologous groups are placed in a consective branching pattern off of the first clade. In some cases, the phylogenetic

Figure 2-15. A Neighbor-Joining phylogenetic tree constructed using just the homeobox region of various *dlx* genes. The Jukes-Cantor distance estimation method was used to calculate the number of nucleotide differences between the *dlx* homeoboxes. The tree was bootstrapped using 1000 replicates and randomly seeding the sampling generator. Each '–' is approximately equal to the distance of 0.0042. All of these operations were performed using the MEGA software package (Kumar *et al.*, 1993).

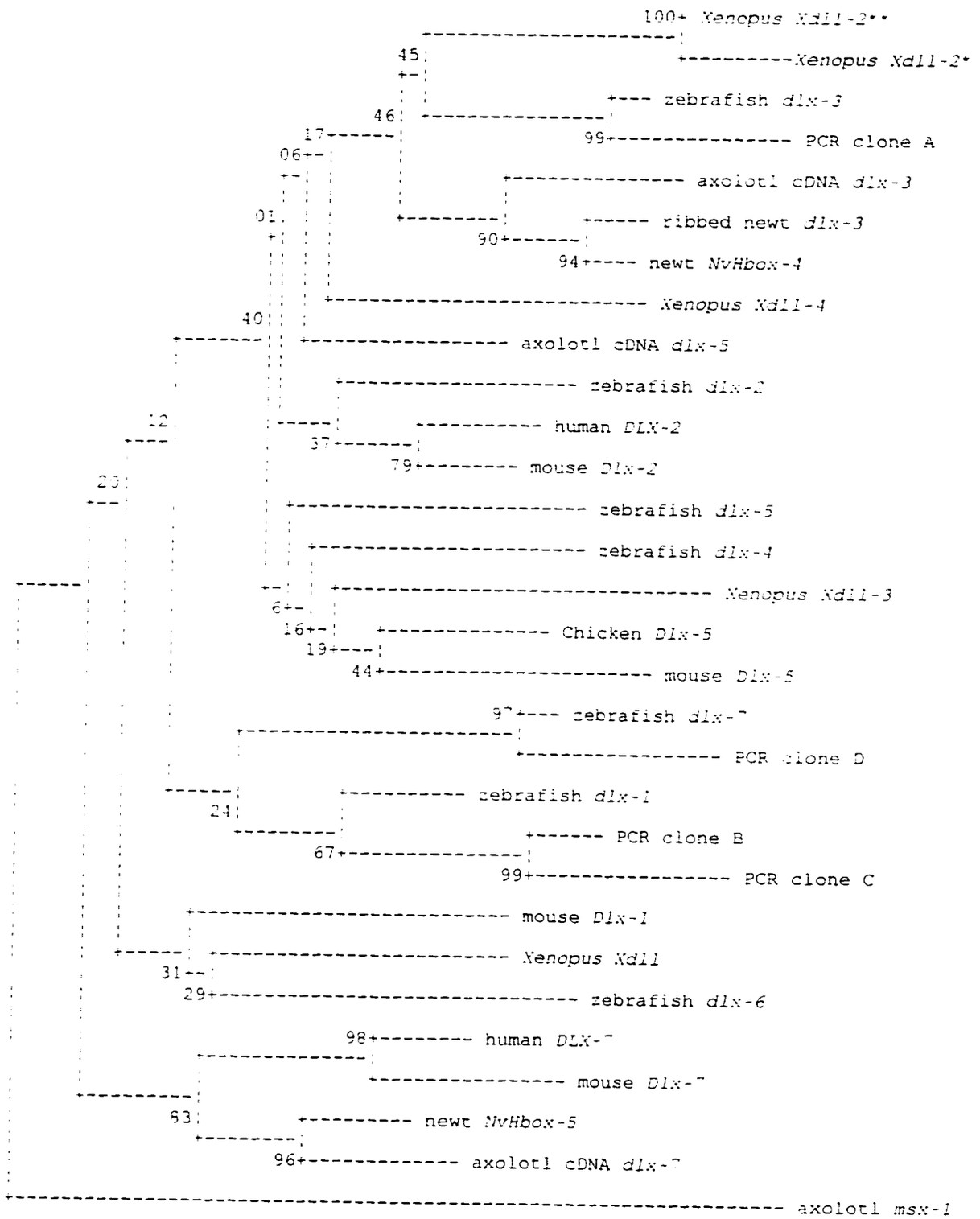
100+ Xenopus Xdll-2**
45
+---------Xenopus Xdll-2*
+--- zebrafish dlx-3
46
99+---------- PCR clone A
17+------
06+--
+---------- axolotl cDNA dlx-3
01
+------ ribbed newt dlx-3
90+------
94+----- newt NvHbox-4
+------------------------- Xenopus Xdll-4
40
+---------- axolotl cDNA dlx-5
+-------------------- zebrafish dlx-2
12
+----------- human DLX-2
37+-------
79+-------- mouse Dlx-2
20
+------------------------ zebrafish dlx-5
+---------------------- zebrafish dlx-4
+------------------------------- Xenopus Xdll-3
6+--
16+--
19+----
+--------------- Chicken Dlx-5
44+---------------------- mouse Dlx-5
97+--- zebrafish dlx-7
+----------------- PCR clone D
+---------- zebrafish dlx-1
24
+------- PCR clone B
67+----------
99+---------- PCR clone C
+--------------------------- mouse Dlx-1
+------------------------ Xenopus Xdll
31+--
29+------------------------------ zebrafish dlx-6
98+-------- human DLX-7
+---------- mouse Dlx-7
83
+--------- newt NvHbox-5
96+---------- axolotl cDNA dlx-7
+-- axolotl msx-1

relationships of the organisms is maintained. For example, in the case of *dlx-3*, the chicken and the mouse group together with *Xenopus* and then zebrafish branching off of this internal node.

Many of the immediate groupings that involve members within a homologous group are supported by high bootstrap values that vary from 94 to 100 (figure 2-15). However, beyond this area, the internal nodes have very low bootstraps. In particular the placement of the axolotl *dlx-5* homeobox as an outgroup to the *dlx-3* group, has a very low bootstrap at 06. Thus, its simultaneous placement outside of the *dlx-3* group and away from the *dlx-5* group is not supported.

In figure 2-15, all of the PCR fragments are grouped with zebrafish homeoboxes and not their orthologous axolotl homeoboxes. This may be the result of the fact that the PCR fragments, in general, do not correspond to the axolotl cDNA clones that were isolated. Consequently, they group with their homologous members in zebrafish.

Figure 2-16 depicts a tree constructed using the *dlx* homeodomains via the Neighbor-Joining algorithm. In this tree the two clades are clearly visible with one clade composed of members from *dlx-2*, *dlx-3*, and *dlx-5*; and the other clade encompassing members from *dlx-1*, *dlx-6* and *dlx-7*. Since there are few parsimony-informative sites because the sequences of the homeodomains within orthologous groups are identical, many of the nodes are 'collapsed'. For example, most of the *dlx-5* and *dlx-2* homeodomains don't have any branch lengths and exist essentially at the same nodal point.

In general, the bootstrap values are lower than those found on the tree constructed with the homeoboxes. In two of the three cases where there are no branch lengths separating the different species, the bootstrap values are low at 52 and 50 for the *dlx-5/dlx-2* and *dlx-1* groupings, respectively. However, the *dlx-3* grouping has a very high bootstrap of 95.

The translated products of the PCR fragments in this tree (figure 2-16) remain grouped within the same orthologous groups as shown in figure 2-15 except some of the relationships have changed. In figure 2-15, the PCR clone D is associated with the zebrafish *dlx-7* homeobox, whereas in the protein tree, it exists as a branch external to the newt *dlx-7* homeodomain. For PCR clones B and C, their intimate association in the DNA tree (bootstrap value of 99) is not maintained in the protein tree. Instead clone B is grouped along with several *dlx-1* homeodomains while clone C is placed on an external branch to this grouping. In this case, the

Figure 2-16. A Neighbor-Joining phylogenetic tree constructed using the *dlx* homeodomains from various species. Pairwise distances were calculated as percent similarities (p-values). Each "–" is approximately equal to the distance of 0.0019. As with the tree presented in figure 2-15, the tree was bootstrapped for 1000 replicates.

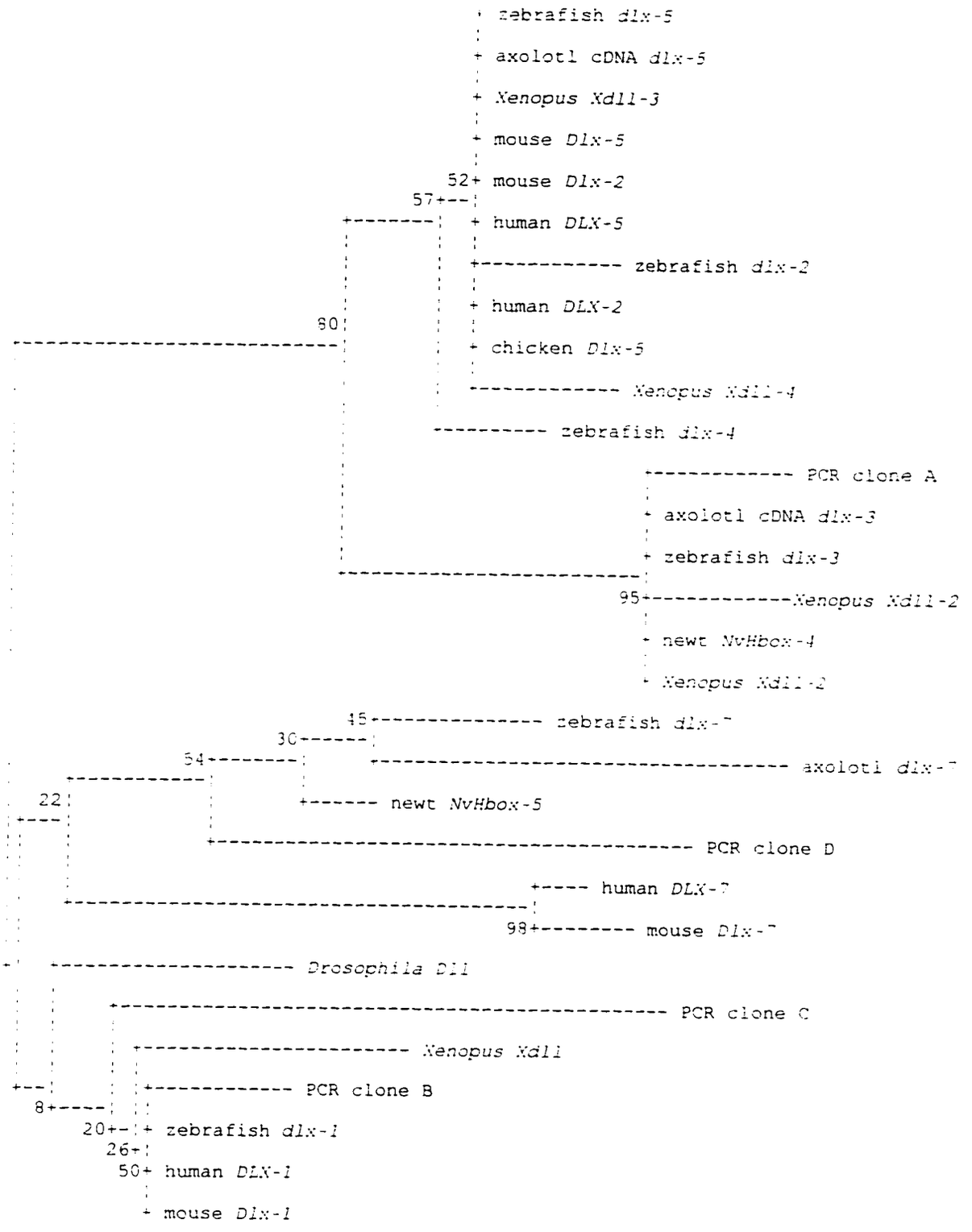
zebrafish dlx-5
axolotl cDNA dlx-5
Xenopus Xdll-3
mouse Dlx-5
52
mouse Dlx-2
57
human DLX-5
zebrafish dlx-2
human DLX-2
80
chicken Dlx-5
Xenopus Xdll-4
zebrafish dlx-4
PCR clone A
axolotl cDNA dlx-3
zebrafish dlx-3
95
Xenopus Xdll-2
newt NvHbox-4
Xenopus Xdll-2
45
zebrafish dlx-
30
54
axoloti dlx-
22
newt NvHbox-5
PCR clone D
human DLX-
98
mouse Dlx-
Drosophila Dll
PCR clone C
Xenopus Xdll
PCR clone B
8
20
zebrafish dlx-1
26
50
human DLX-1
mouse Dlx-1

branches are supported by very low bootstrap values (20 and 50). The placement of the PCR clone A remains essentially the same between the two trees. In general it is intimately associated with zebrafish *dlx-3*, and its association is supported by high bootstrap values of 99 for the DNA tree, and 95 for the protein tree.

2.4 Discussion

One challenge is to establish the actual identities of the *dlx* PCR fragments. This would have been easy had the corresponding cDNA clones had been isolated from the λgt10 cDNA library. In the following section, we discuss the results that demonstrate that the PCR clones are the sequences of axolotl *dlx-1*, *dlx-3*, and *dlx-6* homeoboxes.

2.4.1 The Probable Identities of the *dlx* homeobox PCR Fragments are *dlx-1*, *dlx-3*, and *dlx-6*

When the *dlx* homeobox fragments were compared at the nucleotide level against other homeoboxes in the National Institute of Health (NIH) databank, we found that clone A was most similar to *dlx-3*, clone C resembled the homeobox of *dlx-2*, and clones B and D resembled the homeoboxes of either *dlx-4*, *dlx-2*, or *dlx-1* (table 2-1). When these clones are translated and compared against a compilation of the homedomains of *dlx-1*, *dlx-2*, *dlx-3*, *dlx-4*, *dlx-5*, and *dlx-6* (figure 2-17), clone C still resembles the homeodomain of *dlx-3*, however, the translation of B and C indicated that both these fragments resembled the homeodomain of *dlx-1*, whereas clone D resembled the homeodomain of either *dlx-1* or *dlx-6* (figure 2-17).

When these PCR clones were included in the phylogenetic trees we saw that clone A grouped immediatedly with the zebrafish *dlx-3* homeobox (DNA tree; figure 2-15) or with the axolotl *dlx-3* homeodomain (protein tree; figure 2-16). Since clone A resembles *dlx-3* at both the nucleotide and protein level, and it is never associated with any other member of the *dlx* family, it is a *dlx-3* homeobox.

In the Neighbor-Joining trees, clones B and C either group together, with zebrafish *dlx-1* as an external branch (DNA tree; figure 2-15), or one of them groups with other *dlx-1* homeodomains while the other exists as an external branch to this group (protein tree; figure 2-16). In neither tree, do either of these two clones (B and C) group with *dlx-2* sequences. In addition, when they are compared against the homeoboxes of the *dlx* cDNA clones isolated from the library, we see that they share high nucleotide sequence similarity with the *dlx-3*, *dlx-5*, and *dlx-7* homeoboxes but share higher sequence homology between themselves (91%)(table 2-2). If we compare the two nucleotide sequences (figure 2-3), we see that there are a total of nine differences and three gaps out of 156 nucleotides. Out of these nine differences, six involve

Figure 2-17. Comparison of the deduced homeodomains of the *dlx* PCR clones and *dlx* cDNA clones to the *Drosophila Dll* and other vertebrate *Distal-less* (*Dlx*) homeodomains. Within each orthologous group there are 'diagnostic' amino acid residues that support membership within that group. For example, within the vertebrate *dlx-1* group, there is a highly conserved alanine and glutamine residue at amino acid positions 14 and 22 respectively. *Dlx* homeodomains from different vertebrates are indicated by a single letter where a = axolotl, m = mouse, *X* = *Xenopus*, and z = zebrafish.

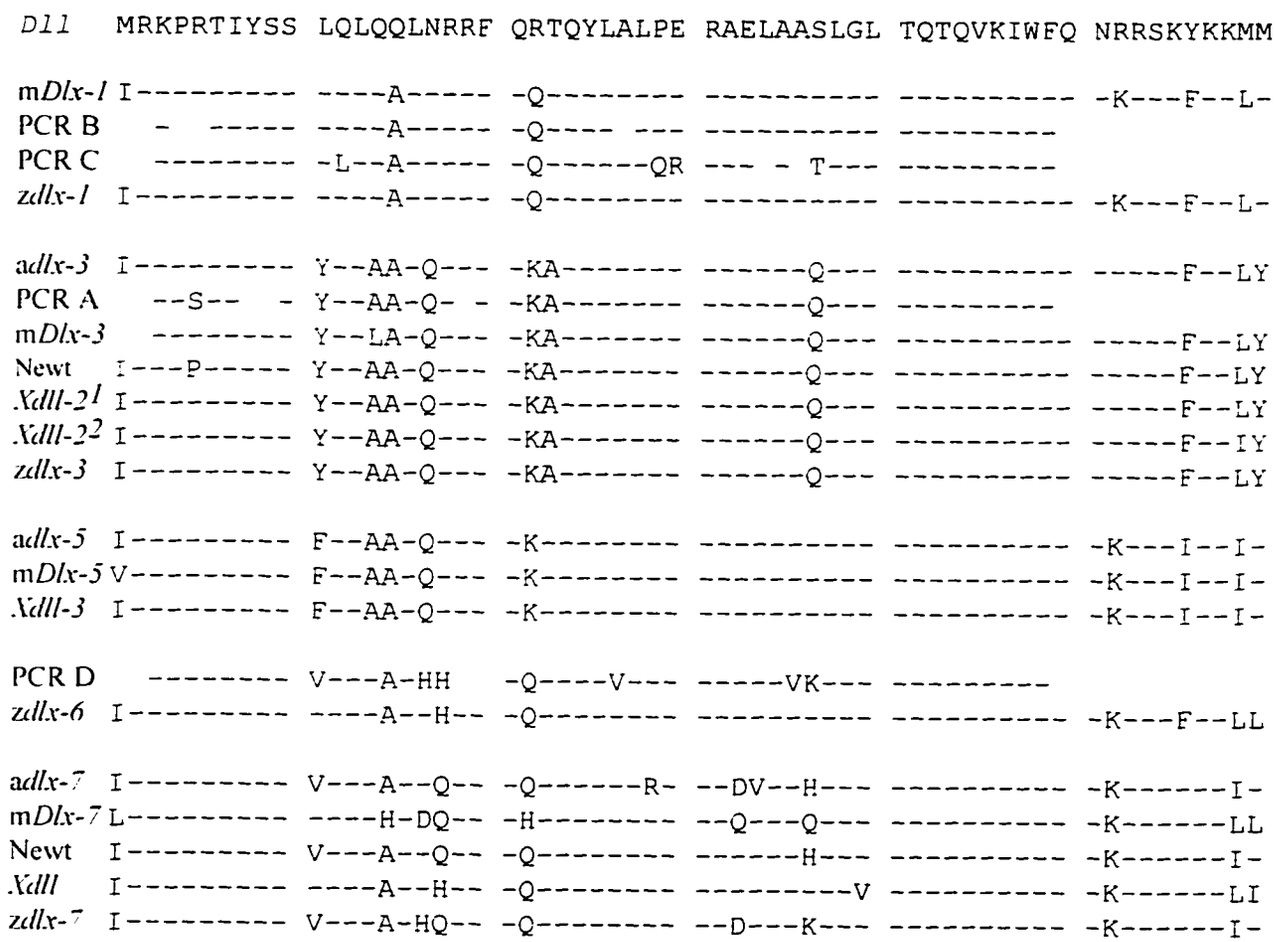
Dll MRKPRTIYSS LQLQQLNRRF QRTQYLALPE RAELAASLGL TQTQVKIWFQ NRRSKYKKMM
mDlx-1 I--------- ----A----- -Q-------- ---------- ---------- -K---F--L-
PCR B - ----- ----A----- -Q---- --- ---------- ---------
PCR C -------- -L--A----- -Q------QR --- - T--- ---------
zdlx-1 I--------- ----A----- -Q-------- ---------- ---------- -K---F--L-
adlx-3 I--------- Y--AA-Q--- -KA------- ------Q--- ---------- -----F--LY
PCR A --S-- - Y--AA-Q- - -KA------- ------Q--- ---------
mDlx-3 -------- Y--LA-Q--- -KA------- ------Q--- ---------- -----F--LY
Newt I---P----- Y--AA-Q--- -KA------- ------Q--- ---------- -----F--LY
Xdll-21 I--------- Y--AA-Q--- -KA------- ------Q--- ---------- -----F--LY
Xdll-22 I--------- Y--AA-Q--- -KA------- ------Q--- ---------- -----F--IY
zdlx-3 I--------- Y--AA-Q--- -KA------- ------Q--- ---------- -----F--LY
adlx-5 I--------- F--AA-Q--- -K-------- ---------- ---------- -K---I--I-
mDlx-5 V--------- F--AA-Q--- -K-------- ---------- ---------- -K---I--I-
Xdll-3 I--------- F--AA-Q--- -K-------- ---------- ---------- -K---I--I-
PCR D -------- V---A-HH -Q----V--- -----VK--- ---------
zdlx-6 I--------- ----A--H-- -Q-------- ---------- ---------- -K---F--LL
adlx-7 I--------- V---A--Q-- -Q------R- --DV--H--- ---------- -K------I-
mDlx-7 L--------- ----H-DQ-- -H-------- --Q---Q--- ---------- -K------LL
Newt I--------- V---A--Q-- -Q-------- ------H--- ---------- -K------I-
Xdll I--------- ----A--H-- -Q-------- ---------V ---------- -K------LI
zdlx-7 I--------- V---A-HQ-- -Q-------- --D---K--- ---------- -K------I-

Table 2-2. Percentage of nucleotide identity amongst the homeoboxes of the cloned PCR fragments and the axolotl cDNA clones isolated from the λgt10 library. Pairwise alignments were performed. Any gaps were not included in the calculation since they are non-informative sites. All values are rounded up.

	PCR B	PCR C	PCR D	*dlx-3*	*dlx-5*	*dlx-7*	*msx-1*	*msx-2*	*caudal*
PCR A	65	81	73	80	79	73	58	54	57
PCR B		91	79	76	79	72	64	67	57
PCR C			79	73	77	75	50	60	57
PCR D				71	73	76	46	61	53
dlx-3					78	74	66	64	57
dlx-5						76	69	63	60
dlx-7							64	66	55
msx-1								77	59
msx-2									60

either a reversal of sequences ('ct' versus 'tc') or a frame shift ('caga' versus 'agag'). The observed 9% difference between the nucleotide sequences of these two clones is probably due two factors: the low proof-reading capability of *Taq* polymerase during strand synthesis (Tindall and Kunkel, 1988) which would allow for the misincorporation of a base pair during PCR, and the presence of compressions on the sequencing film which could exaggerate the sequence difference between these two clones by making portions of the sequence illegible. Therefore, because of their high sequence similarity with one another, the fact that they are identified as *dlx-1* homeodomains when translated, and group with either *dlx-1* homeoboxes and *dlx-1* homeodomains during phylogenetic reconstruction, we believe that both these clones represent the axolotl *dlx-1* homeobox.

The last PCR clone, clone D, initially appeared to be most similar to the homeobox of *dlx-1* based on its nucleotide sequence (table 2-1). When it was translated into it putative homeodomain, it appeared to be similar to either *dlx-1* or *dlx-6*. However, in both phylogenetic trees, it groups consistently with *dlx-7* homeoboxes/homeodomains. In the DNA tree (figure 2-15) it groups with the zebrafish *dlx-7* homeobox away from the zebrafish *dlx-6* homeobox. Moreover, this topology is supported by a high bootstrap value of 97. When we do a pairwise comparison of it's nucleotide sequence against the axolotl *dlx-7* cDNA homeobox, we see that the level of sequence homology is 76% (table 2-2). Unfortunately the protein tree lacks any *dlx-6* homeodomains so that it was not possible to see if the translation of this PCR clone would paired it with any *dlx-6* homologs. In this second tree, it lies external to the *dlx-7* homologs and its node is supported by a low bootstrap value of 54 (figure 2-16). Since clone D shares 76% sequence similarity with the homeobox of the *dlx-7* cDNA sequence (and not 100% similarity as we would expect if it were a *dlx-7* homeobox sequence), and it has a substituted histidine residue at a position within the homeodomain which characterizes it as a *dlx-6* sequence (figure 2-4), we believe that its true identity is *dlx-6*. The reason for its association with *dlx-7* homologs in the DNA and protein trees probably reflects the poor representation of *dlx-6* sequences within these trees.

2.4.2 The Sequence Differences Between the *dlx-3* PCR Product and the *dlx-3* cDNA Clone is Due to Duplication of the Axolotl Genome and Therefore There Exists Two Copies of the *dlx-3* Gene in Mexican Axolotl

As discussed in the previous section, PCR clone A is a *dlx-3* homeobox. However, if we compare its sequence against the homeobox of the axolotl *dlx-3* cDNA clone, we see that they share 80% sequence identity at the nucleotide level (table 2-2). If we do a pairwise alignment of this PCR clone with the zebrafish *dlx-3* homeobox then the percentage of similarity climbs up to 95%. But because the percentage of similarity is not 100% with the zebrafish *dlx-3* homeobox, this *dlx-3* homeobox fragment is not the result of zebrafish DNA contamination. Moreover, if the fragment was the result of zebrafish contamination, then the other PCR fragments would likely also be zebrafish homeoboxes. Since none of these fragments share 100% identity with their zebrafish counterparts, the possibility of contamination from zebrafish sources is remote.

Therefore, the most probable explanation of why the sequence of the *dlx-3* PCR fragment is different than the homeobox of the *dlx-3* cDNA clone is that the axolotl, like *Xenopus*, has two *dlx-3* genes. In the case of the *Xenopus dlx-3* (*Xdll-2*) homologs, their two genes are more than 90% identical in their coding region and were created by a global duplication of the *Xenopus* genome resulting in tetraploidy (Kobel and DuPasquier, 1986). A similar possibility may exist for the axolotl but whether this is due to a complete or partial duplication of the axolotl genome is unknown.

When the translation of these two *dlx-3* homeoboxes are aligned (figure 2-18 (A)), we see that there is only one amino acid difference out of forty-four amino acids compared. However, when the alignment of the nucleotide sequences are examined, the are 28 sites that have different base pairs. This means that there is only 80% consensus between the two sequences (figure 2-18 (B)). These 28 differences cannot be explained as errors which occurred because of the *Taq* polymerase's low fidelity, in the case of the PCR clone, nor are they due to sequencing artefacts. More importantly, the majority of these differences occur in the third codon position which frequently is the site of synonymous substitutions that do not alter the amino acid residue for which they code. Consequently, because of the numerous difference between these two nucleotide sequences, we believe that we have cloned the homeoboxes of two separate axolotl

Figure 2-18. Sequence alignments of the axolotl PCR *dlx-3* clone against the homeodomain (A) and the homeobox (B) of the axolotl cDNA *dlx-3* clone. A star below each site indicates consensus. In the protein alignment there is only one difference (discounting the gaps). while in the nucleotide alignment there are 28 differences.

A. Protein Alignment

```
PCR             KPSTI--SYQLAALQR-FQKAQYLALPERAELAAQLGLTQTQVKIWF
cDNA            KPRTIYSSYQLAALQRRFQKAQYLALPERAELAAQLGLTQTQVKIWF
                ** **  ********* ********************************
```

B. DNA Alignment

```
PCR             AAGCCAAGCACGATTTAT--CAGTTACCAGCTCGCCGCGCTCCAGCGGC-
cDNA            AAACCTAGAACTATCTACTCCAGTTACCAGCTCGCAGCACTGCAGAGGAG
                ** ** ** ** ** **   *************** ** ** *** **

PCR             -TTCCAGAAAGCGCAGTATCTGGCGCTGCCGGAGAGAGCTGAACTCGCCG
cDNA            GTTCCAGAAGGCGCAGTACCTGGCACTGCCAGAGAGGGCGGAGTTGGCAG
                 ******** ******** ***** ***** ***** ** **  * ** *

PCR             CACAGCTGGGGCTCACACAGACACAGGTAAAGATCTGGTTC
cDNA            CCCAGCTTGGACTCACCCAAACTCAGGTGAAGATCTGGTTT
                * ***** ** ***** ** ** ***** ***********
```

dlx-3 genes. Further work may also reveal that other members of the *dlx* family have more than one actively transcribed copy within the axolotl genome.

If these two axolotl *dlx-3* genes have evolved in a similar fashion to their *Xenopus* homologs then we would expect these genes to be either expressed in different tissues or at different times during embryogenesis. In *Xenopus*, one *dlx-3* gene is expressed during late neurulation (Papalopulu and Kintner, 1993) while the second member is expressed during eariler stages in the embryonic ectoderm (Dirksen *et al.*, 1994). Theoretically, a similar possibility exists for the two copies of *dlx-3* in the axolotl. In fact, considering that the newt and *Xenopus* each have detectable transcripts of *dlx-3* in their embryonic ectoderm and adult epidermis, we can be sure that one of the axolotl *dlx-3* homologs will have a similar expression pattern.

Thus so far, we have isolated three different PCR homeoboxes (*dlx-1*, *dlx-3*^{a}, and *dlx-6*) and an additional three *dlx* cDNA sequences (*dlx-3*^{b}, *dlx-5*, and *dlx-7*) from two axolotl cDNA libraries. Both libraries were constructed from neurula stage embryos. Therefore, we can conclude that at this stage all six genes are being actively transcribed. In the case of the two axolotl *dlx-3* genes, this is identical to the results reported for *Xenopus*, where researchers found both copies of the *Xenopus dlx-3* gene being actively transcribed during neurulation (Papalopulu and Kintner, 1993; and Dirksen et al., 1994). Furthermore the cloning of other homeobox genes from the λgt10 cDNA library, indicates that both *msx-1* and *msx-2* as well as *caudal* are being actively transcribed.

2.4.3 The Isolation of Additional homeoboxes cDNAs Other Than the *dlx* Clones is due to the Low Stringency Conditions Used During Screening

When we screened the λgt10 library with our *dlx* homeoboxes, we isolated *msx* clones, in addition to *caudal* and *prd*-like genes. This result is neither unusual nor novel since in 1991 Akimenko and co-workers isolated zebrafish *dlx* genes when they screened a library with a *msx* probe. We accomplished the same result except in reverse by using *dlx* sequences to isolate *msx* sequences. If we compare the level of nucleotide similarity between the *dlx* homeobox fragments used to screen the library and the homeoboxes of the *msx* and *caudal* clones, we find that it varies between 67 to 46 percent (table 2-2), respectively, depending on which PCR fragments are

being compared to each cDNA clone. This high to moderate level of nucleotide conservation coupled with the low stringency with which the library was screened would explain why these additional clones were isolated besides the *dlx* cDNA clones.

2.4.4 The Initiator Codon of the Published Axolotl *msx-1* cDNA Sequence is Probably Incorrect

The sequence of the axolotl *msx-1* cDNA has been submitted to genbank by Koshiba *et al.* (accession number D82577). In their *msx-1* sequence they indicate a different start site from the start site that we have indicated in figure 2-11. Koshiba *et al.* initiator codon is indicated by a double-underline whereas our initiator codon is highlighted in bold in figure 2-11. Both start codons are in-frame with a downstream stop codon, however the Koshiba *et al.* methionine lies immediately downstream of a conserved decapeptide which is found in all *msx* proteins. In addition, the comparison of the newt *msx-1* protein with the axolotl translation would support the claim that the methionine further upstream is the correct initiator because of the high level of protein sequence conservation between these two species in this region. Therefore, we propose that the methionine which we have indicated in bold in figure 2-11 represents the correct initiator.

2.4.3 Conclusions

Although we have not yet demonstrated the expression of the *dlx* and *msx* genes in the axolotl lateral line system, we have completed the first step of our proposal by isolating different members from these two gene families. In addition, we have cloned cDNA sequences of two previously unreported homeobox-genes in the Mexican axolotl: *caudal* and a *prd*-like gene. We have presented evidence that two different copies of the *dlx-3* gene exist in the axolotl due to duplication of its genome. Moreover, in addition to the cDNA clones of *dlx-3*, *dlx-5*, and *dlx-7*, we have cloned the putative homeobox portions of the axolotl *dlx-1* and *dlx-6* genes. This collections of homeoboxes includes almost three-quarters of the vertebrate *dlx* homeoboxes. Since *msx* sequences have been reported in the zebrafish inner ear (Ekker *et al.*, 1992) we have also isolated cDNA clones of the axolotl *msx-1* and *msx-2* genes.

References

Acampora, D., Mazan, S., Avantaggiato, V., Barone, P., Tuorto, F., Lallemand, Y., Brlet, P., and Simeone, A., 1996. Epilepsy and brain abnormalities in mice lacking the *Otx1* gene. *Nature Genet.* **14**, 218-222.

Akam, M., 1987. The molecular basis for metameric pattern in the *Drosophila* embryo. *Development* **101**, 1-22.

Akimenko, M.-A., 1993 . "Preparation of genomic DNA for Southern analysis" in The Zebrafish Book (ed. Monte Westerfield). University of Oregon Press. p.p. 9.11

Akimenko, M.-A., Ekker, M., Wegner, J., Lin, W., and Westerfield, M., 1994. Combinatorial expression of three zebrafish genes related to *Distal-less*: part of a homeobox gene code for the head. *J. Neuro.* **14**, 3475-3486.

Altschul, S., Gish, W., Miller, W., Myers, E., and Lipman, D., 1990. Basic local alignment search tool. *J. Mol. Biol.* **215**, 403-410.

Alvarez, I. S., and Navascues, J., 1990. Shaping, invagination, and closure of the chick embryo otic vesicle: scanning electron microscope and quantitative study. *Anat. Rec.* **228**, 315-326.

Ang, S.-L., Jin, O., Rhinn, M., Daigle, N., Stevenson, L., and Rossant, J., 1996. A targeted mouse *Otx2* mutation leads to severe defects in gastrulation and formation of axial mesoderm and to deletion of rostral brain. *Development* **122**, 243-252.

Asano, M., Emori, Y., Saigo, K., and Shiokawa, K., 1992. Isolation and characterization of a *Xenopus* cDNA which encodes a homeodomain highly homologous to Drosophila *Distal-less*. *J. Biol. Chem.* **267**, 5044-5047.

Ard, M. D., Morest, D. K., and Hauger, S. H., 1985. Trophic interactions between the cochleovestibular ganglion of the chick embryo and its synaptic targets in culture. *Neuroscience* **16**, 151-170.

Armstrong, J. B., 1985. The axolotl mutants. *Dev. Genet.* **6**, 1-25.

Ausubel, F. M., Brent, R., Kingston, R. E., Moore, D. D., Seidman, J.G., Smith, J. A., and Struhl, K., 1995. Current Protocols in Molecular Biology. John Wiley and Sons Inc.,

Balling, R., Deutsch, U., and Gruss, P., 1988. *undulated*, a mutation affecting the development of the mouse skeleton, has a point mutation in the paired box of *Pax-1*. *Cell* **55**, 531-535.

Beauchemin, M., and Savard, P., 1992. Two *Distal-less* related homeobox-containing genes expressed in regeneration blastemas of the newt. *Dev. Biol.* **154**, 55-65.

Bradley, D. J., Towle, H. C., and Young, W.S. III., 1994. α and β thyroid hormone receptor (TR) gene expression during auditory neurogenesis: evidence for TR isoform-specific transcriptional regulation *in vivo*. *Proc. Natl. Acad. Sci. USA* **91**, 439-443.

Bulfone, A., Kim, H.-J., Puelles, L., Porteus, M., Grippo, J., and Rubenstein, L., 1993. The mouse *Dlx-2* (*Tes-1*) gene is expressed in spatially restricted domains of the forebrain, face and limbs in midgestation mouse embryos. *Mech. Dev.* **40**, 129-140.

Busse, U., Guay, J., and Seguin, C., 1990. Nucleotide sequence of a cDNA encoding *Wnt-1* of the Mexican axolotl *Ambystoma mexicanum*. *Nucl. Acids Res.* **18**, 7439.

Chen, Y., Bei, M., Woo, I., Satokata, I., and Maas, R., 1996. *Msx1* controls inductive signaling in mammalian tooth morphogenesis. *Development* **122**, 3035-3044.

Chisaka, O., and Capecchi, M. R., 1991. Regionally restricted developmental defects resulting from targeted disruption of the mouse homeobox gene *hox-1.5*. *Nature* **350**, 473-479.

Chisaka, O., Musci, T. S., and Capecchi, M. R. 1992. Developmental defects of the ear, cranial nerve and hindbrain resulting from targeted disruption of the mouse homeobox gene *Hox-1.6*. *Nature* **355**, 516-520.

Coelho, C. N., Sumoy, L., Kosher, R. A., and Upholt, W. B., 1991. *Ghox-7*: a chicken homeobox-containing gene expressed in a fashion consistent with a role in patterning events during embryonic chick limb development. *Differentiation* **49**, 85-92.

Cohen, S. M., Bönner, G., Küttner, F., Jürgens, G., and Jäckle, H., 1989. *Distal-less* encodes a homoeodomain protein required for limb development in *Drosophila*. *Nature* **338**: 432-434.

Collazo, A., Fraser, S. E., and Mabee, P. M., 1994. A dual embryonic origin for vertebrate mechanoreceptors. *Science* **264**, 426-430.

Condie, B. G., and Capecchi, M.R., 1994. Mice with targeted disruptions in the paralogous genes *hoxa-3* and *hoxd-3* reveal synergistic interactions. *Nature* **370**, 304-306.

Cordes, S. P., and Barsh, G. S., 1994. The mouse segmentation gene *kr* encodes a novel basic domain-leucine zipper transcription factor. *Cell* **79**, 1025-1034.

Corey, D. P., and Breakefield, X. O., 1994. Transcription factors in inner ear development. *Proc. Natl. Acad. Sci. USA* **91**, 433-436.

Corwin, J. T., and Cotanche, D. A., 1988. Regeneration of sensory hair cells after acoutic trauma. *Science* **240**, 1772-1774.

Crews, L., Gates, P. B., Brown, R., Joliot, A., Foley, C., Brockes, J.P., and Gann, A. A. F., 1995. Expression and activity of the newt *Msx-1* gene in relation to limb regeneration. *Proc. R. Soc. Lond. B* **250**, 161-171.

Davidson, D., 1995. The function and evolution of *Msx* genes: pointers and paradoxes. *TIG* **11**, 405-411.

De Robertis, E. M., 1994. "The Homeobox in Cell Differentiation and Evoluton" in Guidebook to the Homeobox Genes (Ed. Denis Duboule). Oxford University Press.

Deitcher, D. L., Fekete, D. M., and Cepko, C. L., 1994. Asymmetric expression of a novel homeobox gene in vertebrate sensory organs. *J. Neuro.* **14**, 486-498.

Deol, M. S., 1964. The origin of the abnormalities of the inner ear in *kriesler* mice. *J. Embryol. Exp. Morph.* **12**, 475-490.

Deol, M.S., 1966. Influence of the neural tube on the differentiation of the inner ear on the mammalian embryo. *Nature* **209**, 219-220.

Dirksen, M.L., Morasso, M. I., Sargent, T. D., and Jamrich, M., 1994. Differential expression of a *Distal-less* homeobox gene *Xdll-2* in ectodermal cell lineages. *Mech. Dev.* **46**, 63-70.

Dollé, P., Price, M., and Duboule, D., 1992. Expression of the murine *Dlx-1* homeobox gene during facial, ocular and limb development. *Differentiation* **49**, 93-99.

Dollé, P., Ruberte, E., Leroy, P., Morriss-Kay, G., and Chambon, P., 1990. Retinoic acid receptors and cellular retinoic binding protiens. I. A systematic study of their differential pattern of transcription in the developing central nervous system. *Development* **110**, 1133-1151.

Dressler, G. R., Deutsch, U., Balling, R., Simon, D., Guenet, J. L. and Gruss, P., 1988. Murine genes with homology to *Drosophila* segmentation genes. *Development* **104 (Suppl.)**, 181-186.

Dressler, G. R., Deutsch, U., Chowdhury, K., Nornes, H. O., and Gruss, P., 1990. *Pax2*, a new murine paired-box-containing gene and its expression in the developing excretory system. *Development* **109**, 787-795.

Durston, A. J., Timmermans, J. P. M., Hage, W. J., Hendriks, H. F. J., De Vries, N. J., Heideveld, M. and Nieuwkoop, P. D., 1989. Retinoic acid causes an anteroposterior transformation in the developing central nervous system. *Nature* **340**, 140-144.

Ekker, M., Akimenko, M.-A., Bremiller, R., and Westerfield, M., 1992. Regional expression of three homeobox transcripts in the inner ear of zebrafish embryos. *Neuron* **9**, 27-35.

Epstein, D. J., Vekemans, M., and Gros, P.. 1991. *Splotch* (*Sp*^{2H}), a mutation affecting development of the mouse neural tube, shows a deletion within the paired homeodomain of *Pax-3*. *Cell* **67**, 767-774.

Erkman, L., McEvilly, R. J., Luo, L., Ryan, A. K., Hooshmand, F., O'Connell, S. M., Keithley, E. M., Rapaport, D. H., Ryan, A. F., and Rosenfeld, M. G.. 1996. Role of transcription factors *Brn-3.1* and *Brn-3.2* in auditory and visual system development. *Nature* **381**, 603-606.

Fang, H., and Elinson, R. P.. 1996. Patterns of distal-less gene expression and inductive interactions in the head of the direct developing frog *Eleutherodactylus coqui*. *Dev. Biol.* **179**, 160-172.

Ferrari, D., Sumoy, L., Gannon, J., Sun, H., Brown, A. M. C., Upholt, W. B., and Kosher, R. A.. 1995. The expression pattern of the *Distal-less* homeobox-containing gene *Dlx-5* in the developing chick limb bud suggests its involvement in apical ectodermal ridge activity, pattern formation, and cartilage differentiation. *Mech. Dev.* **52**, 257-264.

Finkelstein, R., and Boncinelli, E.. 1994. From fly head to mammalian forebrain: the story of *otd* and *Otx*. *Trends Genet.* **10**, 310-315.

Fjose, A., McGinnis, W. J., and Gehring, W. J.. 1985. Isolation of a homoeo box-containing gene from the engrailed region of Drosophila and the spatial distribution of its transcripts. *Nature* **313**, 284-289.

Forge, A., Li, L., Corwin, J.T., and Nevill, G.. 1993. Ultrastructural evidence for hair cell regeneration in the mammalian inner ear. *Science* **259**, 1616-1619.

Foy, C., Newton, V., and Welleslwy, D.. 1990. Assignment of the locus for Waardenbug syndrome type I to human chromosome 2q37 and possible homology to the *Splotch* mouse. *Am. J. Hum. Genet.* **46**, 1017-1023.

Friedman, R. A., and Ryan, A. F.. 1992. Transgenic mice: current applications to the study of the auditory and vestibular systems. *Otolaryng. Clinics of NA* **25**, 1017-1025.

Fritzsch, B., and Wahnschaffe, U.. 1987. Electron microscopical evidence for common inner ear and lateral line efferents in urodeles. *Neurosci. Lett.* **81**, 48-52.

Frumkin, A., Rangini, Z., Ben-Yehuda, A., Gruenbaum, Y., and Fainsod, A.. 1991. A chicken caudal homologue, *Chox-cad*, is expressed in the epiblast with posterior localization and in the early endodermal lineage. *Development* **112**, 207-219.

Gendron-Maguire, M., Mallo, M., Zhang, M., and Gridley, T.. 1993. *Hoxa-2* mutant mice exhibit homeotic transformation of skeletal elements derived from cranial neural crest. *Cell* **75**, 1317-1331.

Gibson, F., Walsh, J., Mburu, P., Varela, A., Brown, K. A., Antonio, M., Beisel, K.W., Steel, K. P., and Brown, S. D. M.. 1995. A type VII myosin encoded by the mouse deafness gene *shaker-1*. *Nature* **374**, 62-64.

Goulding, M. d., Chalepakis, G., Deutsch, U., Erselius, J. R., and Gruss, P.. 1991. *Pax-3*, a novel murine DNA binding protein expressed during early neurogenesis. *EMBO J.* **10**, 1135-1147.

Grossberger, D.. 1987. Minipreps of DNA from bacteriophage lambda. *Nucl. Acids Res.* **15** (16), 6737.

Harrison, R. G. . 1924. Experiments on the development of the internal ear. *Science* **59**, 448.

Harrison, R. G.. 1935. Factors concerned in the development of the ear in *Amblystoma punctatum*. *Anat. Rec.* **64** (suppl. 1), 38-39.

Hendriks, D. M., and Toerien, M. J.. 1973. Experimental endolymphatic hydrops. *S. Afr. Med. J.* **47**, 2294-2298.

Hewitt, J., Clark, L., Ivens, A., and Williamson, R.. 1991. Structure and sequence of the human homeobox gene *Hox7*. *Genomics* **11**, 670-678.

Higgins, D. G., and Sharp, P. M.. 1989. Fast and sensitive multiple sequence alignments on a microcomputer. *CABIOS* **5**, 151-153.

Hill, R. E., Favor, J., Hogan, B. L. M., Ton, C. C. T., Saunders, G. F., Hanson, I. M., Prosser, J., Jordan, T., Hastie, N. D., and Van Heyningen, V.. 1991. Mouse *Small eye* results from mutations in a paired-like homeobox-containing gene. *Nature* **354**, 522-525.

Holland, P.W.H.. 1991. Cloning and evolutionary analysis of *msh*-like homeobox genes from mouse, zebrafish, and ascidian. *Gene* **98**, 253-257.

Hunt, P., Gulisano, M., Cook, M., Sham, M.-H., Faiella, A., Wilkinson, D., Boncinelli, E., and Krumlauf, R.. 1991. A distinct *Hox* code for the branchial region of the vertebrate head. *Nature* **353**, 861-864.

Jabs, E. W., Muller, U., Li, X., Ma, L., Luo, W., Haworth, I.S., Klisak, I., Sparkes, R., Warman, M.L., and Mulliken, J.B.. 1993. A mutation in the homeodomain of the human *MSX2* gene in a family affected with autosomal dominant craniosynostosis. *Cell* **75**, 443-450.

Jones, J. E., and Corwin, J. T.. 1993. Replacement of lateral line sensory organs during tail regeneration in salamanders: identification of progenitor cells and analysis of leukocyte activity. *J. Neuro.* **13**, 1022-1034.

Joly, J.-S., Maury, M., Joly, C., Duprey, P., Boulekbache, H., and Condamine, H.. 1992. Expression of a zebrafish caudal homeobox gene correlates with the establishment of posterior cell lineages at gastrulation. *Differentiation* **50**, 75-87.

Jowett, A. K., Vainio, S., Ferguson, M. W. J., Sharpe, P. T., and Thesleff, I.. 1993. Epithelial-mesenchymal interactions are required for *msx1* and *msx2* gene expression in the developing murine molar tooth. *Development* **117**, 461-470.

Jukes, T. H. and Cantor, C.R.. 1969. "Evolution of protein molecules" in Mammalian Protein Metabolism (Ed. H. N. Munro). Academic Press, New York.

Kablar, B., Vignali, R., Menotti, L., Pannese, M., Andreazzoli, M., Polo, C., Giribaldi, M. G., Boncinelli, E., and Barsacchi, G.. 1996. *Xotx* genes in the developing brain of *Xenopus laevis*. *Mech. Dev.* **55**, 145-158.

Kalthoff, K. 1996. Analysis of Biological Development. Toronto: McGraw-Hill, Inc..

Kappen, C., Schugart, K., and Ruddle, F.. 1989. Two steps in the evolution of *Antennapedia*-class vertebrate homeobox genes. *Proc. Natl. Acad. Sci. USA* **86**, 5459-5463.

Kelley, M. W., Xu, X.-M., Wagner, M. A., Warchol, M. E., and Corwin, J. T.. 1993. The developing organ of Corti contains retinoic acid and forms supernumerary hair cells in response to exogeneous retinoic acid in culture. *Development* **119**, 1041-1055.

Kessel, M.. 1992. Respecification of vertebral identities by retinoic acid. *Development* **115**, 487-501.

Kozak, M.. 1986. Point mutations define a sequence flanking the AUG initiator codon that modulates translation by eukaryotic ribosomes. *Cell* **44**, 283-292.

Krumlauf, R.. 1994. *Hox* genes in vertebrate development. *Cell* **78**, 191-201.

Kumar, S., Tamura, K., and Nei, M.. 1993. MEGA: Molecular Evolutionary Genetics Analysis, version 1.01. Pennsylvania: Pennsylvania State University.

Lannoo, M. J., and Smith, S. C.. 1989. "The Lateral Line System" in Developmental Biology of the Axolotl (eds. J.B. Armstrong and G. M. Malacinski)

Lefebvre, P.P., Malgrange, B., Staecker, M., Moonen, G., and Van de Water, T. R.. 1993. Retinoic acid stimulates regeneration of mammalian auditory hair cells. *Science* **260**, 692-695.

Leon, P.E., Raventos, H., Lynch, E., Morrow, J. and King, M.-C.. 1992. The gene for an inherited form of deafness maps to chromosome 5q31. *Proc. Natl. Acad. Sci. U.S.A.* **89**, 5181-5184.

Leon, Y., Sanchez, J. A., Miner, C., Ariza-McNaughton, L., Represa, J. J., and Giraldez, F., 1995. Developmental regulation of *fos*-protein during proliferative growth of the otic vesicle and its relation to differentiation induced by retinoic acid. *Dev. Biol.* **167**, 75-86.

Lewis, E. B., 1978. A gene complex controlling segmentation in *Drosophila*. *Nature* **276**, 565-571.

Li, Y., Allende, M. L., Finkelstein, R., and Weinberg, E. S., 1994. Expression of two zebrafish *orthodenticle*-related genes in the embryonic brain. *Mech. Dev.* **48**, 229-244.

Lufkin, T., Dierich, A., Lemeur, M., Mark, M. and Chambon, P., 1991. Disruption of the *hox-1.6* homeobox gene results in defects in a region corresponding to its rostral domain of expression. *Cell* **66**, 1105-1120.

Lumsden, A., and Keynes, R., 1989. Segmental patterns of neuronal development in the chick hindbrain. *Nature* **337**, 424-428.

Mallo, M., and Gridley, T., 1996. Development of the mammalian ear: coordinate regulation of formation of the tympanic ring and the external acoustic meatus. *Development* **122**, 173-179.

Mansour, S. L., Goddard, J. M., and Capecchi, M. R., 1993. Mice homozygous for a targeted disruption of the proto-oncogene *int-2* have developmental defects in the tail and inner ear. *Development* **117**, 13-28.

Matsuo, I., Kuratani, S., Kimura, C., Takeda, N., and Aizawa, S., 1995. Mouse *Otx2* functions in the formation and patterning of the rostral head. *Genes & Dev.* **9**, 2646-2658.

McGinnis, W., and Krumlauf, R., 1992. Homeobox genes and axial patterning. *Cell* **68**, 283-302.

Mitchell, L. G., Mutchmor, J. A., and Dolphin, W. D., 1988. Zoology. Don Mills: Benjanin/Cummings Publishing Company.

Monaghan, A. P., Davidson, D. R., Sime, C., Graham, E., Baldock, R., Bhattacharya, S. S., and Hill, R. E., 1991. The *Msh*-like homoebox genes define domains in the developing vertebrate eye. *Development* **112**, 1053-1061.

Moore, K.L., and Persaud, T. V. N., 1993. The Developing Human: Clinically Oriented Embryology (fifth ed.). Philadelphia: W.B. Saunders Company.

Morasso, M. I., Mahon, K. A., and Sargent, T. D., 1995. A *Xenopus Distal-less* gene in transgenic mice: conserved regulation in distal limb epidermis and other sites of epithelial-mesenchymal interaction. *Proc. Natl. Acad. Sci. USA* **92**, 3968-3972.

Mullen, L., Bryant, S., Torok, M., Blumberg, B., and Gardiner, D.. 1996. Nerve dependency of regeneration: the role of Distal-less and FGF signalling in amphibian limb regeneration. *Development* **122**, 3487-3497.

Münz, H., Claas, B., and Fritzsch, B.. 1984. Electroreceptive and mechanoreceptive units in the lateral line of the axolotl *Ambystoma mexicanum*. *J. Comp. Physiol. A*. **154**, 33-44.

Nakamura, S., Stock, D. W., Wydner, K. L., Bollekens, J. A., Takeshita, K., Nagai, B.M., Chiba, S., Kitamura, T., Freeland, T. M., Zhao, Z. Y., Minowada, J., Lawrence, J. B., Weiss, K. M., and Ruddle, F. H.. 1996. Genomic analysis of a new mammalian *Distal-less* gene: *Dlx-7*. *Genomics* **38**. 314-324.

Navaratnam, D. S., Su, H. S., Scott, S.-P., and Oberholtzer, J. C.. 1996. Proliferation in the auditory receptor epithelium mediated by a cyclic AMP-dependent signaling pathway. *Nature Medicine* **2**, 1136-1139.

Nicolas, S., Massacrier, A., Caubit, X., Cau, P., and LeParco, Y.. 1996. A *Distal-less* like gene is induced in the regenerating central nervous system of the urodele *Pleurodeles waltl*. *Mech. Dev.*

Northcutt, R. G., Brandle, K., and Fritzsch, B.. 1995. Electroreceptors and mechanosensory lateral line organs arise from a single placodes in axolotls. *Dev. Biol.* **168**: 358-373.

Northcutt, R. G., Catania, K. C., and Criley, B. B.. 1994. Development of lateral line organs in the axolotl. *J. of Comp. Neuro.* **340**:480-514.

Otting, G., Qian, Y. Q., Billeter, M., Muller, M., Affolter, M., Gehring, W. J., and Wuthrich, K..; 1990. Protein-DNA contacts in the structure of a homeodomain-DNA complex determined by nuclear magnetic resonance spectroscopy in solution. *EMBO J.*, **9**, 3085-3092.

Papalopulu, N., and Kintner, C.. 1993. *Xenopus Distal-less* related homeobox genes are expressed in the developing forebrain and are induced by planar signals. *Development* **117**, 961-975.

Pickles, J. O., and Corey, D. P.. 1992. Mechanoelectrical transduction by hair cells. *Trends in Neuro.* **15,** 254-259.

Price, M., Lemaistre, M., Pischetola, M., Di Lauro, R., and Duboule, D.. 1991. A mouse gene related to *Distal-less* shows a restricted expression in the developing forebrain. *Nature* **351**, 748-751.

Qian, Y. Q., Billeter, M., Otting, G., Muller, M., Gehring, W. J., and Wuthrich, K.. 1989. The structure of the *Antennapedia* homeodomain determined by NMR spectroscopy in solution: comparison with prokaryotic repressors. *Cell* **59**, 573-580.

Qiu, M., Bulfone, A., Martinez, S., Meneses, J., Shimamura, K., Pedersen, R., and Rubenstein, J.. 1995. Null mutation of *Dlx-2* results in abnormal morphogenesis of proximal first and second branchial arch derivatives and abnormal differentiation in the forebrain. *Genes & Dev.* **9**, 2523-2538.

Represa, J., Leon, Y., Miner, C., and Giraldez, F.. 1991. The *int-2* proto-oncogene is responsible for induction of the inner ear. *Nature* **353**, 561-563.

Represa, J., Sanchez, J. A., Miner, C., Lewis, J., and Giraldez, F.. 1990. Retinoic acid modulation of the early development of the inner ear is associated with the control of *c-fos* expression. *Development* **110**, 1081-1090.

Rijli, F. M., Mark, M., Lakkaraju, S., Dierich, A., Dolle, P., and Chambon, P.. 1993. A homeotic transformation is generated in the rostral branchial portion of the head by disruption of *Hoxa-2*, which acts as a selector gene. *Cell* **75**, 1333-1349.

Rinkwitz-Brandt, S., Justus, M., Oldenettel, I., Arnold, H.-H., and Bober, E.. 1995. Distinct temporal expression of mouse *Nkx-5.1* and *Nkx-5.2* homeobox genes during brain and ear development. *Mech. Dev.* **52**, 371-381.

Roberson, D. W., and Rubel, E. W.. 1994. Cell division in the gerbil cochlea after acoutic trama. *Amer. J. Otolaryngol.* **15**, 28-34.

Robert, B., Lyons, G., Simandl, B. K., Kuroiwa, A., and Buckingham, M.. 1991. The apical ectodermal ridge regulates *Hox-7* and *Hox-8* gene expression in developing chick limb buds. *Genes & Dev.* **5**, 2363-2374.

Robert, B., Sassoon, D., Jacq, B., Gehring, W., and Buckingham, M.. 1989. *Hox-7*, a mouse homeobox gene with a novel pattern of expression during embryogenesis. *EMBO J.* **8**, 91-100.

Robinson, G. W., and Mahon, K. A.. 1994. Differential and overlapping expression domains of *Dlx-2* and *Dlx-3* suggest distinct roles for *Distal-less* homeobox genes in craniofacial development. *Mech. Dev.* **48**, 199-215.

Robinson, G. W., Wray, S., and Mahon, K. A.. 1991. Spatially restricted expression of a member of a new family of murine *Distal-less* homeobox genes in the developing forebrain. *New Biologist* **3**, 1-8.

Roth, G., Dicke, U., and Nishikawa, K.. 1992. How do ontogeny, morphology, and physiology of sensory systems constrain and direct the evolution of amphibians? *Amer. Naturalist*, **139**, S105-S124.

Ruberte, E., Friedrich, V., Morriss-Kay, G. and Chambon, P.. 1992. Differential distribution patterns of CRABP I and CRABP II transcripts during mouse embryogenesis. *Development* **115**, 973-989.

Ruiz I Altaba, A., and Jessell, T.M.. 1991. Retinoic acid modifies the pattern of cell differentiation in the central nervous system of neurula stage *Xenopus* embryos. *Development* **112**, 945-958.

Ryals, B. M., and Rubel, E. W.. 1988. Hair cell regeneration after acoustic trauma in adult *Coturnix* quail. *Science* **240**, 1774-1776.

Sambrook, J., Fritsch, E. F., and Maniatis, T.. 1989. Molecular Cloning: A Laboratory Manual (2nd Edition). Cold Spring Harbor Laboratory Press.

Scott, M. P.. 1992. Vertebrate homeobox gene nomenclature. *Cell* **71**, 1-20.

Selski, D., Thomas, N., Coleman, P.D. and Rogers, K.E.. 1993. The human brain homeogene, *DLX-2*; cDNA sequence and alignment with the murine homologue. *Gene* **132**, 301-303.

Simeone, A., Acampora, D., Pannese, M., D'Esposito, M., Stornaiuolo, A., Gulisano, M., Mallamaci, A., Kastury, K., Druck, T., Huebner, K., and Boncinelli, E.. 1994. Cloning and characterization of two members of the vertebrate *Dlx* gene family. *Proc. Natl. Acad. Sci. USA* **91**, 2250-2254.

Simeone, A., Acampora, D., Mallamaci, A., Stornaiuolo, A., D'Apice, M.R., Nigro, V., and Boncinelli, E.. 1993. A vertebrate gene related to orthodenticle contains a homeodomain of the bicoid class and demarcates anterior neuroectoderm in the gastrulating mouse embryo. *EMBO J.* **12**, 2735-2747.

Smith, H. M.. 1989. "Discovery of the Axolotl and its Early History in Biological Research" in Developmental Biology of the Axolotl (eds. J.B. Armstrong and G.M. Malacinski).

Smith, S. C., Graveson, A. C., and Hall, B. K.. 1994. Evidence for a developmental and evolutionary link between placodal ectoderm and neural crest. *J. Exp. Zool.* **270**, 292-301.

Smith, S. C., Lannoo, M. J., and Armstrong, J. B.. 1990. Development of the mechanoreceptive lateral line system in the axolotl: placode specification, guidance of migration, and the origin of neuromast polarity. *Anat. Embryol.* **182**, 171-180.

Sokolowski, B. H. A., Stahl, L. M., and Fuchs, P. A.. 1993. Morphological and physiological development of vestibular hair cells in the organ-cultured otocyst of the chick. *Dev. Biol.* **155**, 134-146.

Song, K., Wang, Y., and Sassoon, D.. 1992. Expression of *Hox-7.1* in myoblasts inhibits terminal differentiation and induces cell transformation. *Nature* **360**, 477-481.

Stein, S., Fritsch, R., Lemaire, L., and Kessel, M.. 1996. Checklist: Vertebrate homeobox genes. *Mech. Dev.* **55**, 91-108.

Stock, D. W., Ellies, D. L., Zhao, Z., Ekker, M., Ruddle, F. H., and Weiss, K. M., 1996. The evolution of the vertebrate Dlx gene family. *Proc. Natl. Acad. Sci. USA* **93**, 10858-10863.

Stone, L. S., 1931. Induction of the ear by the medulla and its relation to experiments on the lateralis system in amphibia. *Science* **74**, 577.

Su, M.-W., Suzuki, H., Solursh, M., and Ramirez, F., 1991. Progressively restricted expression of a new homeobox-containing gene during *Xenopus laevis* embryogenesis. *Development* **111**, 1179-1187.

Thaller, C., and Eichele, G., 1987. Identification and spatial distribution of retinoids in the developing chick limb bud. *Nature* **327**, 625-628.

Tickle, C., Alberts, B., Wolpert, L., and Lee, J., 1982. Local application of retinoic acid to the limb bud mimics the action of the polarizing region. *Nature* **296**, 564-566.

Torres, M., Gomez-Pardo, E., and Gruss, P., 1996. *Pax2* contributes to inner ear patterning and optic nerve trajectory. *Development* **122**, 3381-3391.

Uziel, A., Babrion, J., Ohresser, M. and Legrand, C., 1981. Effects of hypothyroidism on the sturctural development of the organ of Corti in the rat. *Acta Otolaryngol.* **92**, 469-480.

Waddington, C. H., 1937. The determination of the auditory placode in the chick. *J. Exp. Biol.* **14**, 232-239.

Warchol, M. E., Lambert, P. R., Goldstein, B. J., Forge, A., and Corwin, J. T., 1993. Regenerative proliferation in inner ear sensory epithelia from adult guinea pigs and humans. *Science* **259**, 1619-1622.

Wilkinson, D. G., Peters, G., Dickson, C., and McMahon, A. P., 1988. Expression of the FGF-related proto-oncogene *int-2* during gastrulation and neurulation in the mouse. *EMBO J.* **7**, 691-695.

Yamashita, H. and Oesterle, E. C., 1995. Induction of cell proliferation in mammalian inner-ear sensory epithelia by transforming growth factor α and epidermal growth factor. *Proc. Natl. Acad. Sci. USA* **92**: 3152-3155.

Zhao, G.-Q., Zhao, S., Zhou, X., Eberspaecher, H., Solursh, M., and de Crombrugghe, B., 1994. *rDlx*, a novel *distal-less*-like homeoprotein is expressed in developing cartilages and discrete neuronal tissues. *Dev. Biol.* **164**, 37-51.